SYNTHESIS AND ISOMORPHOUS SUBSTITUTION REACTIONS OF SOME HYDROXYAPATITES

BY

GODWIN O. INIKORI,

B.Sc. (Hons) NSUKKA, M.Sc, P.G.D.E. {ABU)

A Thesis Submitted to the Post-Graduate School,
Ahmadu Bello University, Zaria

In Partial Fulfilment of the Requirements for the
Degree of Doctor of Philosophy in Chemistry

Department of Chemistry
Faculty of Science
Ahmadu Bello University,
Zaria, Nigeria

December, 1992

DECLARATION

I hereby declare that this thesis has been written by me and that it is a record of my own research. It has not been presented in any previous application for a higher degree.

All sources of information are specifically acknowledged by means of references.



GODWIN O. INIKORI

December, 1992

CERTIFICATION

This dissertation entitled "**SYNTHESIS AND ISOMORPHOUS SUBSTITUTION REACTIONS OF SOME HYDROXYAPATITES**" by **GODWIN O. INIKORI** meets the regulations governing the award of the degree of Doctor of Philosophy of Ahmadu Bello University, and is approved for its contribution to knowledge and literary presentation.

Prof. S.A. Thomas
B.Sc. (Hons), D. Phil.
Chairman, Supervisory Committee

Date

Dr. J.F. Iyun
B.Sc. (Hons), Ph.D
Member, Supervisory Committee

25/11/93.
Date

Prof. A.I. Onuchukwu
B.Sc. (Hons), M.Sc., Ph.D
External Examiner

25/11/93
Date

Prof. S.A. Thomas
B.Sc. (Hons), D. Phil.
Head, Department of Chemistry

Date

Prof. Dalhatu Muhammed
B.A. (Hons), Ph.D
Dean, Post-Graduate School

15/5/96
Date

DEDICATION

To my parents,

Late **Ejerharha Inikori**

and

Madam **Omovie Inikori**

for their care and love.

ACKNOWLEDGEMENTS

With gratitude to God, I wish to sincerely thank:

i. Prof. S.A. Thomas for supervising this work and whose encouragement, material in-put and untiring efforts made this work a reality;

ii. Dr. J.F. Iyun, for his interest, guidance and assistance;

iii. Prof. J.Y. Olayemi who was the Head of Chemistry Department during the experimental part of this programme and Prof. S.A. Thomas the present Head of Department for granting me the opportunity to carry out this work in the department;

iv. Dr. G.F. Harrison for his assistance and useful suggestions;

v. Dr. G.A. Ayoko for his interest, inspiration and assistance;

vi. the Soil Science Department for granting me permission to use their AAS, and Mr. Lawal who is always ready to assist in the operation of the instrument;

vii. Mr. Adi Atoshi of the NNPC who made it possible for me to use their AAS;

viii the management and staff of Food and Drugs Administration Laboratory Kaduna, for granting me permission to use their infra-red absorption spectrophotometer;

ix. Mr. David Barak who carried out the X-ray analyses;

x. Mr. Victor Ajibola for his immense contributions;

xi. all the technical staff of the Department particularly, Mrs. Iyun, Messrs, A.F. Smith, Sylvester Ichaver, and Clement Atayi for their assistance;

xii Mrs. Roseline Kassar for her assistance throughout the experimental stage of this work;

xiii Messrs. Timothy Areo and Daniel Adaji for their assistance;

xiv. Mallam Abu Yusufu for his assistance in the typing and printing of this work; and

xv. my wife, Theresa, for her patience and support throughout the tenure of the programme.

ABSTRACT

Cation exchange reactions in calcium, strontium and lead hydroxy apatites have been carried out by the method of co-precipitation in aqueous ammonia and acidic media. Solid state synthesis was applied in some cases. Products of the substitution reactions were analysed by atomic absorption spectrometry, infra-red and ultraviolet/visible spectrophotometry and in some cases by X-ray powder diffractometry.

Magnesium formed solid solutions of calcium-magnesium hydroxyapatite in the entire composition range at pH 12. Solid solutions of calcium-zinc hydroxyapatite in the whole series were also obtained in both basic (pH = 10.5) and acidic (pH 5.0 -6.0) media. It is the first time that the formation of calcium-zinc hydroxyapatite solid solutions in the entire range is being reported. Calcium-lead hydroxyapatites in the entire series were obtained by solid state synthesis at 900°C. Formation of solid solutions between Mg^{2+} and Ca^{2-} appears to be dependent on the pH of the precipitating medium. Replacement of Ca^{2+} by Mg^{2+} in the apatite lattice resulted in enhancement of peak intensity and sharpening of X-ray powder diffraction peaks. Expansion of lattice parameters was observed when Pb^{2+} substituted Ca^{2+} in hydroxyapatite. Infra-red frequencies for the OH and $P0_4$ groups were shifted to lower values in calcium-magnesium, calcium-lead and calcium-zinc 4 with increasing replacement of Ca^{2+} .

Cadmium replaced lead in lead hydroxyapatite (PbHA) in the whole series in basic (pH = 10.5) and acidic media (pH 5.0 - 6.0). Replacement of Pb^{2+} by Cd^{2+} in the PbHA caused the absorption frequencies for the OH stretching mode to shift to lower values while those for the PO_4 group shifted to higher values as the Cd^{2+} content increased. X-ray powder diffraction peaks for cadmium-lead hydroxyapatites are sharpened with increasing concentration of cadmium.

Solid solutions of barium-lead hydroxyapatite were obtained only in the range of barium concentration from 0 to 40% in aqueous medium. Amorphous precipitates were obtained for reactions beyond 40 atom % barium. Solid solutions of barium-lead hydroxyapatite were however obtained for the whole composition range by solid state reaction between PbHA and barium hydroxyapatite (BaHA) at 900^0C Replacement of Pb^2+ by Ba2+ in PbHA caused the infra-red frequencies for the OH group to shift to lower values while that for the PO_4. group shifted to higher values with increasing barium content. Broadening of X-ray powder diffraction peaks with increasing barium concentration was observed.

Solid solutions of strontium-cadmium, strontium-lead and strontium-zinc hydroxyapatite were also obtained in the entire composition range in basic and acidic media. Cd^{2+} and Zn^{2+} showed similar behaviour towards strontium hydroxyapatite (SrHA) probably due to similarities in their chemistries. Infra-red frequencies for the PO_4 vibrational

modes and OH stretching modes for strontium-cadmium, strontium-lead and strontium-zinc hydroxyapatites were shifted to lower values with increasing replacement of Sr^{2+} in each case. The OH librational frequencies are shifted to higher values in strontium-cadmium and strontium-zinc hydroxyapatite solid solutions but to lower values in strontium-lead hydroxyapatite with increasing replacement of strontium.

The above results indicate that the pH of the mediating medium, the method of preparation; and the size of the substituting cation affect cationic isomorphous substitution in the apatite systems. In addition, crystallinity of apatitic solid solutions appear to increase with increasing replacement of a larger cation with a smaller cation. Crystallinity however decreases with increasing replacement of a smaller cation by a larger one in an apatite.

A modified method for a high yield preparation of PbHA from the basic salt, $Pb_60_5(N0_3)_2$ has been devised. Relative intensities and d-spacings for the prepared PbHA samples are in agreement with standard values provided by the Joint Committee on Powder Diffraction Standards.

TABLE OF CONTENTS

Title		Page
Title Page		i
Declaration		ii
Certification		iii
Dedication		iv
Acknowledgements		v
Abstract		vii
Table of Contents		x
List of Tables		xvi
List of Figures		xxiii
List of Appendices		xxvi
Abbreviations and Symbols		xxvii
CHAPTER ONE:		
INTRODUCTION		1
1.0	Some Calcium Phosphate Systems	1
1.1	Apatites	1
1.1.1	Calcium Hydroxyapatite Formation	6
1.1.2	Octacium Phosphate (OCP)	7
1.1.3	Whitlockite, β-Tricalcium Phosphate (TCP)	7
1.1.4	Struvite	8
1.2	Research Objectives	9

CHAPTER TWO

REVIEW OF LITERATURE 11

2.1 Substitution in Apatite Systems 11

2.1.1 Effects of Anion Substitutions on the Formation and Stability of Apatite. 12

2.1.2 Effects of Cation Substitutions on the Formation and Stability of Apatite. 16

2.1.2.1 Magnesium Substitution 18

2.1.2.2. Strontium Substitution 19

2.1.2.3 Lead Substitution 22

2.1.2.4 Barium Substitution 24

2.1.2.5 Tin Substitution 25

2.1.2.6 Substitution by Other Cations. 26

2.1.3 Factors Affecting Cation Substitution in Hydroxyapatite 27

2.1.4 Methods for Investigating Cation Substitutions in Apatite Systems 30

2.1.4.1 Infra-red Absorption Spectroscopy 31

2.1.4.2 X-ray Analysis 40

2.1.4.3 Atomic Absorption Specttroscopy (AAS) 46

2.1.4.4. UV-Visible Spectroscopy 50

CHAPTER THREE

ISOMORPHOUS SUBSTITUTIONS IN CALCIUM HYDROXYAPATITE BY MAGNESIUM, ZINC AND LEAD 54

3.1 Introduction 54

3.2 Experimental 59

3.2.1	Preparation of Calcium Hydroxyapatite	59
3.2.2	Preparation of Magnesium Hydroxyapatite	60
3.2.3	Preparation of Calcium-magnesium Hydroxyapatite	60
3.2.4	Preparation of Zinc Hydroxyapatite	61
3.2.5	Preparation of Calcium-zinc Hydroxyapatite	61
3.2.6	Preparation of Lead Hydroxyapatite	61
3.2.7	Preparation of Lead-Calcium Hydroxyapatite by Solid Process	62
3.2.8	Chemical Analyses of Samples	62
3.2.8.1	Colorimetric Determination of Phosphorus Content of Apatite Samples	62
3.2.8.2	Determination of Ca, Mg, Zn, and Pb Content of Apatite Samples by Atomic Absorption Spectrometry	65
3.2.8.3	Infra-red Absorption Analysis	69
3.1.9	X-ray Powder Diffraction Analysis	69
3.3	Results	70
3.4	Discussion	87

CHAPTER FOUR

ISOMORPHOUS SUBSTITUTIONS IN LEAD HYDROXYAPATITE BY CADMIUM AND BARIUM 94

4.1	Introduction	94
4.2	Experimental	95
4.2.1	Preparation of Lead Hydroxyapatite (PbHA)	95

4.2.2	Preparation of Cadmium Hydroxyapatite (CdHA)	95
4.2.3	Preparation of Barium Hydroxyapatite	96
4.2.4	Preparation of Lead-cadmium Hydroxyapatite	96
4.2.5	Preparation of Lead-Barium Hydroxyapatite	97
4.2.6	Preparation of Barium Hydroxyapatite by Solid State Reaction	97
4.2.7	Preparation of Barium Hydroxyapatite by Solid State Reaction	97
4.2.8	Chemical Analyses of Cadmium and Barium Substituted Lead Hydroxyapatite	98
4.2.8.1	Colorimetric Determination of Phosphorus Content	98
4.2.8.2	Determination of Lead, Cadmium and Barium Contents of Prepared Samples by Atomic Absorption Spectrometry	98
4.2.8.3	Infra-red Absorption Analysis	100
4.2.9	X-ray Powder Diffraction Analysis	100
4.3	Results	100
4.4	Discussion	114

CHAPTER FIVE

ISOMORPHOUS SUBSTITUTION IN STRONTIUM HYDROXYAPATITE BY CADMIUM, ZINC AND LEAD 119

5.1	Introduction	119
5.2	Experimental	120

5.2.1	Preparation of Strontium Hydroxyapatite	120
5.2.2	Preparation of Cadmium Hydroxyapatite	120
5.2.3	Preparation of Strontium-cadmium Hydroxyapatite	121
5.2.4	Preparation of Zinc Hydroxyapatite	121
5.2.5	Preparation of Strontium-zinc Hydroxyapatite	121
5.2.6	Preparation of Lead Hydroxyapatite	122
5.2.7	Preparation of Strontium-lead Hydroxyapatite	122
5.2.8	Chemical Analyses of Cadmium, Zinc and Lead Substituted Strontium Hydroxyapatite	122
5.2.8.1	Colorimetric Determination of Phosphorus Content	122
5.2.8.2	Determination of Cadmium, Lead and Strontium and Zinc Contents of Prepared by Samples	123
5.2.8.3	Infra-red Absorption Analysis	125
5.3	Results	125
5.4	Discussion	140

CHAPTER SIX

A MODIFIED METHOD OF PREPARATION OF LEAD HYDROXYAPATITE FROM AQUEOUS SOLUTION 144

6.1	Introduction	144
6.2	Experimental	145

6.2.1	Preparation of the Basic Salt, $Pb_6O_5(NO_3)_2$	145
6.2.2	Preparation of Lead Hydroxyapatite from the Basic Salt, $Pb_6O_5(NO_3)_2$	145
6.2.3	Chemical Analyses of Lead Hydroxyapatite	147
6.2.3.1	Colorimetric Determination of Phosphorus Content of Lead Hydroxyapatite	147
6.2.3.3	Infra-red Absorption Analysis	147
6.2.4	X-ray Powder Diffraction Analysis	147
6.2.5	Results and Discussion	147

CHAPTER SEVEN

SUMMARY, CONCLUSION AND RECOMMENDATIONS		152
7.1	Summary	152
7.2	Conclusion	157
7.3	Recommencations	161
	REFERENCES	162
	APPENDICES	173

LIST OF TABLES

Title		Page
2.1	Radii of Some Ions	28
2.2	Vibrations of the Phosphate Ions in Substances having the Apatites Structure	35
3.1	Calcium, Magnesium and Phosphorus Contents (weight percent) of Calcium-magnesium solid solutions precipitated from Aqueous Ammonia Solution (pH - 12) and their Infra-red Frequencies.	73
3.2	Expected and Observed Calcium, Magnesium and Phosphorus Contents (weight Percent) of Calcium-magnesium Hydroxyapatite precipitated from (pH = 12) Based on the Molecular Formula $Ca_{10-x}Mg_x(PO_4)_6(OH)_2$	73
3.3	Some Literature Reports on the Interaction of Magensium with Calcium hydroxyapatite in Aqueous Medium	77
3.4	Calcium, Zinc and Phosphorus Contents (weight percent) of Calcium-zinc Hydroxyapatatie solid Solutions Precipitated from aqueous ammonia solution (pH = 10.5) and their infra-red Frequencies	77

3.5 Expected and Observed Calcium, Zinc and Phosphorus contents (weight percent) of calcium-zinc hydroxyapatite solid solutions precipitated from aqueous ammonia (pH = 10.5` $Ca_{10-x}Zn_x(PO_4)_6(OH)_2$ 78

3.6 Calcium, Z ›horus Contents (weight p -inc Hydroxya medium

3.7 Expect Phosp zinc Med Ca 82

3.8 C t and 82

3. ›ercent) of Leau, ›ium- Lead hydroxyapati… State reaction at 900°C Bases on t… ılar Formular $Ca_{10-x}Zn_x(PO_4)_6(OH)_2$ 85

3.10 Lattice Constants of Lead-Calcium Hydroxyapatite Solid Solutions Synthesised by Solid State reaction 85

4.1 Lead, Cadmium and Phosphorus contents (weight/percent) of Lead-Cadmium hydroxyapatite solid solutions precipitated from basic medium (pH = 10.5) and their infra-red frequencies. 100

4.2 Lead, Cadmium and Phosphorus Contents (weight percent) of Lead-Cadmium hydroxyapatite solid solutions precipitated from acidic medium (pH = 5-6) and their infra-red frequencies. 104

4.3 Expected [e] and Observed [o] concentrations of Lead, cadmium and Phosphorus in lead-cadmium hydroxyapatite solid solutions precipitated from Aqueous Ammonia Solution. (pH = 10.5) based on the molecular formula, $Pb_{10-x}Cd_x(PO_4)_6(OH)_2$. 107

4.4 Expected [e] and Observed [o] contents (weight percent) of lead, cadmium and phosphorus in lead-cadmium hydroxyapatite solid solutions precipitated from acidic medium (pH = 5-6) based on the molecular formula, $Pb_{10-x}Cd_x(PO_4)_6(OH)_2$. 107

4.5 Lead, barium and phosphorus contents (weight percent) of Lead-Barium hydroxyapatite precipitated from Aqueous Ammonia Solution (pH =10.5) and their infra-red frequencies. 108

4.6 Barium, lead and phosphorus contents (weight percent) of Lead-Barium hydroxyapatite precipitated from acidic medium (pH = 5-6) and their infra-red frequencies. 108

4.7 Expected [e] and Observed [o] contents (weight percent) barium, of lead, and phosphorus in lead-barium hydroxyapatite solid solutions precipitated from Aqueous Ammonia (pH 10.5) based on the molecular formula, $Pb_{10-x}Ba_x(PO_4)_6(OH)_2$. 109

4.8 Expected [e] and Observed [o] contents (weight percent) of barium, lead and phosphorus in lead-barium hydroxyapatite solid solutions precipitated from Acidic medium based on the molecular formula, $Pb_{10-x}Ba_x(PO_4)_6(OH)_2$. 109

4.9 Lead, barium and phosphorus contents (weight percent) of lead-barium hydroxyapatite solid solutions prepared by solid state reaction at 900°C and their infra-red frequencies. 110

4.10 Expected [e] and Observed [o] contents (weight percent) of lead-barium hydroxyapatite solid solutions prepared by solid state reaction at 900°C values based on the molecular formula, $Pb_{10-x}Ba_x(PO_4)_6(OH)_2$. 110

5.1 Cadmium, strontium and Phosphorus contents of Strontium-Cadmium hydroxyapatite solid solutions precipitated from Aqueous Ammonia Solution (pH = 10.5) and their infra-red frequencies. 128

5.2 Expected [e] and Observed [o] contents (weight percent) of cadmium, strontium and Phosphorus in strontium-cadmium hydroxyapatite solid solutions precipitated from Basic medium (pH = 10.5) based on the molecular formula, $Sr^{10-x}Cd_x(PO_4)_6(OH)_2$. 128

5.3 Cadmium, strontium and Phosphorus contents (weight percent) of Strontium-Cadmium hydroxyapatite solid solutions precipitated from Acidic (pH 5-6) medium and their infra-red frequencies. 130

5.4 Expected [e] and Observed [o] contents (weight percent) of cadmium, strontium and phosphorus in strontium-cadmium hydroxyapatite solid solutions precipitated from Acidic medium (pH = 5-6) based on the molecular formula, $Sr_{10-x}Cd_x(PO_4)_6(OH)_2$. 130

5.5 Lead, strontium and Phosphorus contents (weight percent) of Strontium-lead hydroxyapatite solid solutions precipitated from Aqueous Ammonia Solution (pH 10.5) and their infra-red frequencies. 132

5.6 Expected [e] and Observed [o] contents (weight percent) of lead, strontium and phosphorus in strontium-lead hydroxyapatite solid solutions precipitated from Aqueous Ammonia Solution (pH 10.5) based on the molecular formula, $Sr_{10-x}Cd_x(PO_4)_6(OH)_2$. 132

5.7 Lead, strontium and Phosphorus contents (weight percent) of strontium-lead hydroxyapatite solid solutions precipitated from Acidic medium (pH 5-6) and their infra-red frequencies. 134

5.8 Expected [e] and Observed [o] contents (weight percent) of lead, strontium and phosphorus in strontium-lead hydroxyapatite solid solutions precipitated from mild Acidic medium based on the molecular formula, $Sr_{10-x}Cd_x(PO_4)_6(OH)_2$. 134

5.9 Strontium, zinc and Phosphorus contents (weight percent) of Strontium-zinc hydroxyapatite solid solutions precipitated from Aqueous Ammonia Solution (pH 10.5) and their infra-red frequencies. 136

5.10 Expected [e] and Observed [o] contents (weight percent) of strontium, zinc and phosphorus in strontium-zinc hydroxyapatite solid solutions precipitated from Aqueous Ammonia Solution (pH = 10.5) based on the molecular formula, $Sr_{10-x}Zn_x(PO_4)_6(OH)_2$. 136

5.11 Strontium, zinc and Phosphorus contents (weight percent) of Strontium-zinc hydroxyapatite solid solutions precipitated from Acidic Medium and their their infra-red frequencies. 138

5.12 Expected [e] and Observed [o] strontium, zinc and phosphorus contents (weight percent) of strontium-zinc hydroxyapatite solid solutions precipitated from Acidic medium (pH = 5-6) based on the molecular formula, $Sr_{10-x}Zn_x(PO_4)_6(OH)_2$. 138

6.1 Expected and Observed Lead and Phosphorus Contents of Lead Hydroxyapatite Prepared by the Modified Method and its Infra-red Frequencies 150

6.2 Observed Molecular Formula and Mole-atom Ratio of Lead Hydroxyapatite Prepared by the Modified Method. 150

LIST OF FIGURES

Figure	Title	Page
3.1	Infra-red Frequencies of Ca-Mg Hydroxy-apatite Solid Solutions Against Atom % Magnesium	74
3.2	X-ray Powder Diffraction Paterns for Ca-Mg Hydroxyapatite	75
3.3	X- ray Powder Diffraction Patterns for Magnesium Hydroxyapatite	76
3.4	Infra-red Frequencies of Ca-Zn Hydroxy-apatite against atom % Zinc (Basic Medium)	79
3.5	Infra-red Frequencies of Ca-Zn Hydroxyapatite against atom % Zinc (Acidic Medium)	80
3.6	Infra-red Spectra for Ca-Zn Hydroxyapatite	81
3.7	Infra-red Frequencies of Ca-Pb Hydroxyapatite against atom % Lead (Solid State Synthesis)	83
3.8	Infra-red Spectra for Ca-Pb Hydroxyapatite Solid Solutions (Solid State Synthesis)	84
3.9	Lattice Parameters for Ca-Pb Hydroxyapatite against atom % Lead (Solid State Synthesis)	86
4.1	Infra-red Frequencies of Pb-Cd Hydroxyapatite Solid Solutions against atom % cadmium (Basic Medium)	105
4.2	Infra-red Frequencies of Pb-Cd Hydroxyapatite Solid Solutions against atom % cadmium (Acidic Medium)	106

4.3	Infra-red Frequencies of Pb-Ba Hydroxyapatite Solid Solutions against atom % Barium (Solid State Synthesis)	111
4.4	X- ray Powder Diffraction Patterns for Pb-Cd Hydroxyapatite Solid Solutions (Basic Medium)	112
4.5	X- ray Powder Diffraction Patterns for Pb-Ba Hydroxyapatite Solid Solutions (Basic Medium)	113
5.1	Infra-red Frequencies for Sr-Cd Hydroxyapatites Against atom % Cadmium (Basic Medium)	129
5.2	Infra-red Frequencies for Sr-Cd Hydroxyapatites Against atom % Cadmium (Acidic Medium)	131
5.3	Infra-red Frequencies for Sr-Pb Hydroxyapatites Against atom % Lead (Basic Medium)	133
5.4	Infra-red Frequencies for Sr-Pb Hydroxyapatites Against atom % Lead (Acidic Medium)	135
5.5	Infra-red Frequencies for Sr-Zn Hydroxyapatites Against atom % Lead (Basic Medium)	137
5.6	Infra-red Frequencies for Sr-Zn Hydroxyapatites Against atom % Zinc (Acidic Medium)	139

6.1 Comparison of X-ray Powder Diffraction Patterns for Lead Hydroxyapatite 151

LIST OF APPENDICES

Appendix	Title	Page
I:	X-ray Powder Diffraction Data for Calcium-Lead Hydroxyapatite Solid Solutions	173
II:	X-ray Powder Diffraction Data for Lead-cadmium Hydroxyapatite Solid Solutions	175
III:	X-ray Powder diffraction data for Barium Substituted lead hydroxyapatite (Basic Medium pH = 10.5)	176
IV	X-ray Powder Diffraction Data for Lead Hydroxyapatite, $Pb_{10}(PO_4)_6(OH)_2$, prepared by the modified method.	179
V	Joint Committee on Powder Diffraction Standards (1974) for Lead Hydroxyapatite, $Pb_5(PO_4)_3OH$.	181

ABBREVIATIONS AND SYMBOLS

AAS:	Atomic Absorption Spectrometry
BDH:	British Drug House Limited
cm:	Centimeter
M:	Molarity
g:	Grame
θ:	theta
l:	litre
EDTA:	Ethylenediaminetetraacetic acid disodium
IR:	Infra-red frequencies

CHAPTER ONE

INTRODUCTION

1.0 SOME CALCIUM PHOSPHATE SYSTEMS

1.1 APATITES

The apatites constitute a class of minerals having the general formula, $M_5(PO_4)_3X$ or $M_{10}(PO_4)_6X_2$ (M = metal ion; X = OH, halogen, etc). Its most important member calcium hydroxyapatite, $Ca_5(PO_4)_3(OH)$, has biological, geological and economic significance. It constitutes the principal inorganic phases of teeth and bones. It is the most abundant mineral in human tissue and one of the few crystals formed in vivo (Van Wazer, 1961, Eanes, 1979, Sowerby and Emeleus, 1975). Calcium hydroxyapatite, (CaHA) is also found in nature as the mineral hydroxyapatite which is similar to that found in biological apatites. Biological apatite is however known to be associated with many other elements in both small and large amounts. For this and similar reasons, biological apatites are referred to as impure hydroxyapatites (Bigi et al., 1984).

Some of the impurities associated with biological apatites include Sr^{2+}, Ba^{2+}, Mg^{2+}, K^{+}, Pb^{2+}, Zn^{2+} Fe^{2+}, Cd^{2+} and other cationic trace elements which are able to replace calcium either wholly or partly in the hydroxyapatite lattice; others include CO_3^{2-}, HPO_4^{3-}, $P_2O_7^{4-}$ capable of substituting for the PO_4^{3-} ion and finally, Cl^{-}, F^{-}, H_2O and CO_3^{2-} which do replace the OH group in the hydroxyapatite (Baud and Very, 1975, Baud,

Bangs and Very, 1977, Legeros et al., 1980).

The biological apatites are microcrystalline (compared to the macro dimensions of mineral apatites), of variable composition and therefore heterogeneous even within each category and even within each calcified tissue (enamel, dentine, bone). Some of the problems associated with biological apatites (McConnel, 1973), include:

i) non-stoichiometry, e.g. the Ca/P ratio of biological apatites range from 1.54 to 1.73 compared to 1.67 for pure calcium hydroxyapatite;

ii) co-existence or pre-existence of possible precursors, e.g., calcium phosphate decahydrate, octacalcium phosphate, tricalcium phosphate, amorphous calcium phosphate, and possibly others.

The biological apatites are however similar in one respect: they all contain the carbonate ion in different amounts usually as a substituent for phosphate in the apatite structure. Generally, they differ in crystallite sizes, shapes, and their physico-chemical (susceptibility to acid dissolution) and thermal stabilities. For instance, apatite crystallites of enamel are much larger than those of dentine or bone; apatites from pathological tissue calcifications (e.g. salivary stones, dental calculi) show greater crystallinity than those of bone and dentine but less than those of enamel except in the case of enamel pearls in which the crystallinity of the apatite is more similar to that of the enamel (Brown et al., 1962;

Eanes, 1979; Elliot, 1973).

Consequent upon these problems associated with biological apatites, many studies on biological apatites (Baravelli, et al., 1984) have been carried out indirectly by studying synthetic apatites prepared from aqueous and non-aqueous systems. The direct extrapolation of results from such studies to biological apatites is however not possible some of the time (Legeros and Legeros, 1980).

Other calcium phosphates [brushite or calcium hydrogen phosphate dihydrate, $CaHPO_4.2H_2O$; Octacalcium phosphate, $Ca_8H_2(PO_4).5H_2O$; whitlockite or tricalcium phosphate, $Ca_3(PO_4)_2$; calcium pyrophosphate dihydrate (mono- and triclinic forms), $Ca_2P_2O_7$; amorphous calcium phosphate, ACP]; and Magnesium phosphates [struvite, $MgNH_4PO_4.6H_2O$; newberlite, $MgNHPO_4.3H_2O$; amorphous magnesium phosphate, ACMP], have been identified in association with apatite phase. In the presence of low concentrations of $P_2O_7^{4-}$, the growth of $CaHPO_4.2H_2O$ crystals are suppressed and their morphology highly modified but at higher concentrations, amorphous calcium phosphate forms. The presence of Mg^{2+} encourages the formation of β-tricalcium phosphate from aqueous solution (Baravelli et al., 1984). For this reason, its presence in biological systems is always associated with magnesium.

Many phosphate minerals with an apatite structure are also formed magmatically or hydrothermally. The economic importance of this group of mineral is related to the

fossil deposits they form which serves as a good source for fluorine, calcium, uranium and the rare earth metals.

The ideal apatite structure possesses a hexagonal space group.($P6_3/m$) although it can be described in terms of a monoclinic cell ($P2_1/b$) which is often distorted by isomorphous substitution (Young, Sudarsanan and Mackie, 1968). The cell contains six nearly tetrahedral PO_4^{3-} ions in three crystallographically non-equivalent but chemically distinguishable positions, ten bivalent cations, M^{2+}, in two chemically different environments, $M^{2+}(I)_4$ and $M^{2+}(II)_6$ and two monovalent anions which are located in columns along the principal axis.

It is only the X ions that occupies the crystal axis while the high close-order symmetry of the neighbouring positive and negative centres gives an almost uniform electrical field along it,with very shallow potential wells. Isomorphous substitution takes place easily along these columns, which can almost be seen as atomic-scale tunnels by which ions move very easily. While the hydroxide and fluoride ions are the most commonly found X ions that form hydroxyapatite and fluorapatite respectively, the chloride and the bromide are able to substitute wholly or partly for them. In addition, many natural and synthetic apatites have significant quantities of these sites occupied by oxide, peroxide or carbonate ions.

The relatively unpolarisable alkaline earth metals,

Ca^{2+}, Sr^{2+} and Ba^{2+} or the moderately polarisable metals such as Mn^{2+}, Cd^{2+}, Pb^{2+} and Zn^{2+} and other cationic trace elements are able to occupy the cation sites (Sowerby and Emeleus, 1975). Limited isomorphous substitution is well known for a wide range of cations, including sodium, many transition elements and some lanthanides (Legeros et al., 1980).

Occupancy of the tetrahedral site is limited to phosphate, arsenate, vanadate and small quantities of carbonate and silicate. Arsenate completely or partly replaces phosphate in either hydroxyapatite or fluorapatite in a continuous range of solid solutions.

On the whole, the chemistry of hydroxyapatite is greatly complicated by its ability to form interlayered mixtures with octacalcium phosphate, OCP; on the other hand, this structural relationship provides a rational basis for understanding physiologically important phenomena (Brown, Schroeder and Ferris, 1979) such as:

i. a mechanism for prevention of dental caries by fluoride in drinking water;

ii. the cause of ribbon like and platy morphologies of biological apatitic crystallites;

iii the unusual variability in the stoichiometry of apatite precipitates;

iv. a possible mechanism for incorporation of impurities and defects into dental enamels;

v. a mechanism of growth of biological apatites and

vi. a rationale why teeth enamel vary in their caries susceptibility.

1.1.1 Calcium Hydroxyapatite Formation

The precipitates of calcium phosphate from aqueous solutions at moderate temperature is initially amorphous and deficient in calcium with a Ca: P ratio of 1.45 (Nancolla, 1971 in Sowerby and Emeleus, 1975). The crystalline hydroxyapatite is formed from this amorphous phase in two stages (Eanes and Posner, 1970). The first stage leads to the formation of colloidal hydroxyapatite particles. This usually takes place quite rapidly because the amorphous phase has a higher energy and is more soluble than the hydroxyapatite. As soon as the amorphous phase disappears, hydroxyapatite starts growing although at a slower rate.

The presence of threshold agents such as sodium pyrophosphate prevents the transformation of the amorphous phase into crystalline hydroxyapatite. For example, a solution at pH of 7.4 and 25°C containing 10^{-2}M $CaCl_2$ and NaH_2PO_4 forms crystalline hydroxyapatite within 45 minutes but when $(NaHO_3P)_2$ cCl_2 or $(NaHO_3P)_2$ $C(OH)CH_3$ was added at the 10^{-3} M level, only amorphous gels were formed (Francis, 1969).

At temperatures between 1000 and 1300°C in low concentrations of water vapour, calcium oxide and tricalcium phosphate form crystalline hydroxyapatite. A

truly monoclinic calcium hydroxyapatite is formed by the thermal hydrolysis of stoichiometric calcium chlorapatite (Eliot, 1971). The OH^- ion displaces the chloride ion in an ordered fashion after two weeks of steam treatment without disrupting the crystals.

1.1.2 Octacalcium Phosphate (OCP) $Ca_8H_2(PO_4)_6.5H_2O$

Octacalcium phosphate is one of the major crystalline components of dental calculi. It usually co-exists with whitlockite and or apatite. The similarity in structure between OCP and hydroxyapatite gave rise to the theory that OCP is a precursor for biological apatites (Brown et al., 1962; Brown et al., 1979; Chickerur et al., 1980).

In synthetic systems, the formation of OCP is sensitive to pH and temperature changes and to the presence of trace elements. It co-exists with apatite when the starting pH is high and with β-tricalcium phosphate in the presence of magnesium.

OCP usually forms needle-like crystals which grow from a common centre (Legeros, 1977). The OCP crystals are similar to apatite needles morphologically.

1.1.3 Whitlockite, β-Tricalcium Phosphate(TCP), $Ca_9(PO_4)_6$ or β-Tricalcium Magnesium Phosphate(TCMP), $(CaMg)_9(PO_4)_6$

Pure whitlockite is β-TCP, $Ca_9(PO_4)_6$. It is not found in biological systems and cannot be prepared from aqueous

systems. β-TCP can only be prepared at high temperatures (900°C) by solid state reaction (Legeros, 1977). Biological whitlockite usually contain varying amounts of magnesium. Whitlockite is found mostly in salivary stones and dental calculi but rarely in urinary stones.

The presence of Mg^{2+} in biological and synthetic whitlockites stabilizes them from being hydrolyzed to apatite. Other ions such as Mn^{2+}, Fe^{2+}, Co^{2+} and Ni^{2+} also promote the formation of β-TCP at the expense of apatite from aqueous systems (Legeros and Legeros, 1980).

However, the Mg/Ca ratio in biological systems is the main determining factor in the formation of whitlockite phase at the expense of apatite. Similarly, in gel systems, increase in Mg/Ca ratio causes the formation of TCP and OCP instead of apatite and OCP.

1.1.4 Struvite, $MgNH_4PO_4.6H_2O$

Struvite is mostly found in association with apatite as a component of urinary stones which usually forms as a result of bacterial infection (Elliot, 1973). The formation of struvite may also be induced by alkalinization using ammonia solution.

Struvite crystals in gel systems grow very readily in the presence of mg^{2+}, HPO_4^{2-}, PO_4^{3-}, NH_4^{+} while the simultaneous presence of $P_2O_7^{2-}$ results in reduction in crystallite size habit modification and twinning of the struvite crystals. The simultaneous presence of Ca^{2+} with Mg^{2+} also affect the formation of struvite.

1.2 Research Objectives

The purpose of this work is to investigate the individual effects of some cations on the formation and some properties of apatites in synthetic systems. It is undertaken as part of an on-going attempt to clarify factors influencing the nature of the interaction of cations with apatitic systems.

The choice of the metal-metal hydroxyapatite systems for this study was guided by consideration of the individual effects of such metal ions on the human system (biological apatite being the principal inorganic phase of human bones and teeth), with a view to gaining better understanding of among other things the effect of:

i) pH of mediating solutions;

ii) cationic size; and

iii) method of preparation on the nature of the products and extent of isomorphous substitution in apatite systems.

The study has been carried out by the method of co-precipitation from basic and acidic media at specified temperatures (Legeros et al., 1980; Patel, 1979; Bigi et al., 1982) and in some cases by solid state reactions (Bigi et al., 1984 and 1989). Products of these reactions were characterized by atomic absorption spectrometry, infra-red and UV spectrophoto-metry and by X-ray powder diffraction analysis. The cases studied include:

i) the replacement of Ca^{2+} by Mg^{2+} and Zn^{2+} in calcium

hydroxyapatite in aqueous medium at specified pH (pH 12 for Mg^{2+}; pH 10.5 and pH 5-6 for Zn^{2+});

ii) the substitution of $Ca^{2+}$by Pb^{2+} in calcium hydroxyapatite by solid state reaction;

iii) the replacement of Sr^{2+} in strontium hydroxyapatite by each of Zn^{2+}, Cd^{2+} and Pb^{2+} in basic medium (pH = 10.5) and acidic medium (pH 5-6);

iv) isomorphous substitution of lead by cadmium and barium in lead hydroxyapatite in basic medium (pH = 10.5) and acidic medium (pH 5-6);

v) isomorphous substitution of lead by barium in lead hydroxyapatite by solid state reaction; and

vi) a modified method for a high yield preparation of lead hydroxyapatite.

CHAPTER TWO

REVIEW OF RELATED LITERATURE

2.1 Substitution in Apatite Systems

The structure of the hydroxyapatite easily accommodates a great variety of substituents, both anionic and cationic. Some of these ions (e.g., Sr^{2+}, Ba^{2+}, Cd^{2+}, etc) are able to substitute for Ca^{2+} in synthetic hydroxy-, fluor- and chlor- apatites (Legeros et al., 1980, Collin, 1959; Chiranjeevirao et al., 1982, Thomas et al., 1989; Bigi et al., 1984, 1989, 1991; Narasaraju et al., 1972; Patel, 1979; Koutsoukos and Nancollas, 1981; Baravelli et al., 1984; Casonovas et al., 1980; Pearce, 1981; Verbeeck et al., 1981). While ions such as Cl^- and F^- substitute for the OH^- ions, CO_3^{2-}, ASO_4^{3-}, and to a limited extent, MnO_4^{3-}, SiO_4^{3-} substitute for the phosphate ion, PO_4^{3-}. Exchange of cation in the hydroxyapatite structure is the basis for incorporation of lead in human skeletal system which leads to lead poisoning (Narasaraju et al., 1972).

Substitution of other ions into the apatite lattice affect the crystallinity (reflecting crystallite size and/or strain), morphology and lattice parameters of the apatite (Baud, 1975; Baud et al 1977) and as a result cause stability or instability to the human tissues involved in the case of biological apatites. Some of these "impurities" are associated with the susceptibility or resistance of human tooth enamel to acid dissolution (caries) and of bone to resorption process (Baud et al.,

1977). The effects of some of these ionic substitutions on the formation and stability of apatite are briefly examined in the following sections.

2.1.1 Effects of Anion Substitutions on the Formation and Stability of Apatite

i). Carbonate, CO_3^{2-}

The incorporation of carbonate in synthetic and biological apatite is coupled with the incorporation of sodium ions. Carbonated apatites are of two types: type A is that in which the carbonate ion, CO_3^{2-} replaces the hydroxyl ion, OH^-. This is mostly found in synthetic non-aqueous (1000°C) systems; type B occurs in aqueous systems (25 - 100°C) in which the CO_3^{2-} exchanges for the phosphate ion, PO_4^{3-}. In biological apatites the carbonate ion, CO_3^{2-}, predominantly exchanges for PO_4^{3-} (Pearce, 1981; Doi et al., 1982; Nelson, 1981).

The extent of carbonate incorporation is determined by the presence of other ions which include Na^+, K^+ and Sr^{2+}. Sodium and to a lesser extent potassium enhance high incorporation of carbonate into the apatite structure while Sr^{2+} limits it. Generally, the incorporation of carbonate into the apatite structure causes (Nelson, 1981).

(a) Changes in morphology from needle-like rods to equi-axial crystals;

(b) Reduction in crystallite size;

(c) Contraction in the a-axis and expansion in the c-axis dimension compared to the unsubstituted calcium hydroxyapatite;

(d) Internal strain and

(e) Chemical instability - such as increase in solubility and decrease in thermal stability (Legeros 1977).

On the whole, the apatite with least carbonate content (e.g. enamel) has greater crystallinity (i.e. greater crystallite size and/or less strain) than the apatite with more carbonate (e.g., bone or dentine). For similar reasons, enamel is less soluble than dentine or bone mineral in acid buffers.

ii) Fluoride, F^-

The fluorapatites, idealized as $Ca_{10}(PO_4)_6F_2$, are the most abundant mineral apatites containing carbonate in most cases. The hard impervious enamel that covers the soft porous interior dentine of mammalian teeth usually contains a modest amount of fluoride ions isomorphically substituted for the hydroxyl ion, OH in the hydroxyapatite crystal lattice. This results from reactions of ingested or topically applied fluoride with enamel or bone apatites (Eanes, 1979; Baud et al., 1977).

The incorporation of fluoride in biological and synthetic apatites causes:

(a) increase in crystallite size;

(b) decrease in strain due to increased stability of the apatite structure;

(c) contraction of the a-axis and no significant change in the c-axis when compared to unsubstituted calcium hydroxy-apatite;

(d) increase in chemical stability (decrease in solubility) and

(e) increase in thermal stability (Barone et al., 1976; Baud et al., 1977).

iii) Chloride, Cl^-

In non-aqueous systems, two chloride ions substitute for two hydroxyl ions in the apatite crystal lattice, but in apatites from aqueous medium, the maximum substitution is 40 mole percent. The formation of apatite in biological systems strongly discriminates against chloride incorporation, for example, the average chloride content of human enamel apatite is about 0.25 weight % while that for bone or dentine is less than 0.01 ~~weight~~ %.

The exchange of Cl for OH in apatite to form $Ca_{10}(PO_4)_6Cl_2$ or $Ca_{10}(PO_4)_6(OH)(Cl)$ from non-aqueous and aqueous systems respectively causes the expansion of the a-xis and contraction of the c-axis dimensions. Chloride ions contribute to the instability of the apatite structure and its properties. Chloride containing apatites are less stable thermally than either OH - or F-apatites (Legeros and Legeros, 1980).

iv). Acid Phosphate (HPO_4^{2-}

The acid phosphate, HPO_4^{2-}, is able to substitute for PO_4^{3-} in the apatite crystal lattice. Its exchange for PO_4^{3-} results in the expansion of the a-axis and slight contraction in the c-axis dimensions. It also causes instability in the apatite, thus, making the apatite to be more susceptible to acid dissolution. The non-stoichiometry of biological apatites especially that of human enamel is partly due to the presence of the HPO_4^{2-} ions. The HPO_4^{2-} may be either surface bound, lattice bound (substituting partially for PO_4^{3-}) or as constituent of octacalcium phosphate interlayered with apatite (Brown et al., 1979).

v) Pyrophosphate, $P_2O_7^{4-}$

Pyrophosphate suppresses crystal growth if present in a solution from which apatite forms. Its presence in biological fluids, urine and saliva is associated with the inhibition of dental and urinary calculi formation.

vi) AsO_4^{3-}, VO_3^{3-}, CrO_4^{3-}, and MnO_4^{3-}

Arsenate can completely or partially replace phosphate in either hydroxyapatite or fluorapatite in a continuous range of solid solutions. With less than 70% AsO_4^{3-} substitution in fluorapatite, the crystals retain the hexagonal symmetry of fluorapatite, but above this point, the symmetry is reduced.

As, V and Cr each can replace phosphorus in both

fluor- and chlor-apatites of calcium, strontium and barium (Grisafe and Hummel, 1970). Maganese (v) completely replaces phosphorus only in barium apatites. With this exception, the substitution of arsenic, vanadium, chromium or maganese for phosphorus with a given halide and metal ion takes place over a continuous range of solid solutions. Substitution of vanadium, arsenic or chromium for phosphorus in calcium fluorapatite distorts the hexagonal symmetry of the crystal.

2.1.2 Effects of Cation Substitutions on the Formation and Stability of Apatite

Substitution of various cations for Ca^{2+} in the hydroxyapatite is usually accompanied by changes in the lattice parameters, crystallinity and morphology of the apatite (Legeros et al., 1980; Fowler, 1974; Patel, 1979; Bigi et al., 1984, 1989 and 1991). Substitution of cations having smaller ionic radii than Ca^{2+} show unit cell contraction (e.g., Fe^{2+}, Co^{2+}, Ni^{2+}, Mg^{2+}, Zn^{2+}, etc) while the replacement of Ca^{2+} in hydroxyapatite by cations possessing larger ionic radii than Ca^{2+} (e.g., Sr^{2+}, Ba^{2+}, Pb^{2+}, etc) causes expansion of the unit cell parameters. (Patel, 1979; Collin, 1959, Legeros et al., 1980).

The exclusion of calcium from the hydroxyapatite lattice results in changes in the crystal field acting upon the phosphate ion (Fowler, 1974; Klee and Engel, 1970). Such changes are manifested in the form of a shift or

broadening of the infra-red absorption bands for the phosphate ions and the hydroxyl ions in the hydroxyapatite lattice. For example, the infra-red absorption spectra of apatites obtained from solution containing concentrations of Al^{3+}, Cr^{3+}, Zn^{2+}, Cu^{2+}, Fe^{2+}, of Fe^{3+} show shifts while lesser effects are observed in the spectra of apatites obtained in the presence of similar concentrations of Ba^{2+}, Pb^{2+}, Sr^{2+}, Mn^{2+}, and Cd^{2+}, yet no significant shift occurs in the presence of Na^{+}, Li^{+} and K^{+} when their infra-red absorption spectra were compared with that of unsubstituted calcium hydroxyapatite.

Unsatisfactory explanation abound in the literature as to why some cations substitute for calcium in the hydroxyapatite structure in the whole compositional range giving a complete series of solid solutions of the type $Ca_{10-x}M_x(PO_4)_6(OH)_2$ (x = 0 to 10; M = substituting cation) while others do not. A seemingly popular view is that the replacement of Ca^{2+} in the apatite structure by other metal ions is related to the ionic radii of the cations (Legeros et al., 1980; Patel, 1979). Cations larger than Ca^{2+}, e.g., Sr^{2+} and Pb^{2+} have been reported to exchange for calcium, giving a complete range of solid solutions in the entire compositional range (Legeros, 1980; Bigi et al., 1989; Narasaraju et al., 1972). Cations with smaller ionic radii than Ca^{2+}, such as Cd^{2+} and Mg^{2+} have also been reported to replace Ca^{2+} in the apatite structure to give solid solutions in the whole range (Patel, 1979; Inikori,

Thomas and Ayoko, 1989; Chiranjeevirao et al., 1982).

2.1.2.1 Magnesium Substitution (Mg^{2+})

Substitution of magnesium is still a matter of controversy as earlier reports (Legeros et al., 1980; Klee and Engel, 1972) show that magnesium if incorporated, is incorporated to a very limited extent, suppresses the crystal growth of apatites and promotes the formation of β-tricalcium phosphate (TCP) at the expense of apatite (Legeros et al., 1980). The formation of β-TCP by heat treatment of the inorganic deposits of different biological and pathological calcifications has been correlated with the magnesium contents of the mineral phases (Bigi et al., 1980). The limited amount of magnesium (less than 1 weight %) in mineral, synthetic and biological apatites and the preferential release of Mg^{2+} during the initial dissolution of enamel skeletal and synthetic apatites are taken to indicate that Mg^{2+} in biological apatite is surface limited and not lattice bound (Williams and Sallis, 1982; Nacollas, 1984; Boskey and Posner, 1974).

The clear evidence of the role of magnesium in affecting the biological apatite deposits has prompted numerous studies on the interaction of magnesium ion with hydroxyapatite in aqueous and non-aqueous systems (Legeros et al., 1980; Baravelli et al., 1984; Patel, 1979; Inikori, Thomas and Ayoko, 1989). Two studies, (Patel, 1979 and Chiranjeevirao et al., 1982) have suggested that at pH

values above 9, magnesium replaces calcium in calcium hydroxyapatite to give solid solutions in the whole compositional range. Both studies attributed the ability of Mg^{2+} to substitute for Ca^{2+} to the similarity in their ionic radii (Ca^{2+} = 1.00Å; Mg^{2+} = 0.72Å). This assertion is still debatable because other cations whose ionic radii are either similar, e.g. Hg^{2+}, Na^{+}, Yb^{2+} etc or smaller than Ca^{2+} (e.g. Co^{2+}, Zn^{2+}, AI^{3+} etc) have not been reported to substitute Ca^{2+} in the hydroxyapatite in the whole range (Legeros et al., 1980). It follows therefore that the ionic radii of cations alone cannot be used as a basis for predicting the extent to which a certain cation can substitute for Ca^{2+} in the hydroxyapatite lattice. Recourse may have to be made to factors which influence the values of such radii before a meaningful rationalization can be made. Coordination number of the cations involved and occupancy of cationic sites in the apatite lattice may also affect the degree of substitution (Bigi et al., 1989; Thomas, 1988).

2.1.2.2 Strontium Substitution (Sr^{2+})

The calcium form of hydroxyapatite will exchange Ca^{2+} for Sr^{2+} in aqueous medium to form solid solutions in the entire compositional range (Koutsoukos and Nancollas, 1981; Fowler, 1974; Collin, 1959).

The ultimate site and mechanism of strontium incorporation into the bone structure of the human body

have been of great concern since the release of radioactive strontium into the atmosphere from nuclear tests. In contrast to the variable levels of this element in bones, the strontium deposited in teeth varies little in concentration (Jenkins, 1978).

Experiments in rats showed that lack of strontium in the diet causes a high incidence of dental caries and poor growth condition. Addition of strontium to the diet were found to reverse these changes although it resulted in rickets.

It is believed that incorporation of strontium into the lattice of calcium hydroxyapatite is due to the similarity of its ionic radius with that of calcium (Ca^{2+} = 0.99A°; Sr^{2+} = 1.12A°) (Elliot, 1973). This assertion as already pointed out is still debatable. A complete series of solid solutions of strontium with hydroxyapatite was prepared by Collin (1959) with unit cell parameters linearly dependent on the extent of strontium incorporation into the apatite lattice. The Sr: Ca ratios in the solid, however, were smaller than those in the solution phase. These results were confirmed by the synthesis of a continuous series of solid solutions of strontium and hydroxyapatite by solid state reaction (Heijligers et al., 1979). It was suggested that there is a slight preference of strontium for the 6-fold axis and that the solution behaved ideally. At higher strontium contents however, there was evidence for another phase co-existing with the

solid solutions of Ca-Sr apatite. Koutsoukos and Nancollas (1981) reported that changes in the unit cell lattice parameters and infra-red absorption spectra of Sr-Ca hydroxyapatite solid solutions are also linearly related to the strontium content of the precipitated solid phases. The presence of strontium in crystallizing strontium - calcium hydroxyapatite solid solution reduces the size of the developing Sr-Ca hydroxyapatite crystallite. With strontium having a larger ionic radii than Ca^{2+}, the substitution of Sr^{2+} for Ca^{2+} in the hydroxyapatite produces expansion effects on the lattice parameters of the apatite formed (Legeros et al., 1980; Collin, 1959 and 1960). Legeros et al (1980) reported that the incorporation of strontium in the apatite directly depends on Sr^{2+}: Ca^{2+} ratio in the media and is facilitated at higher pH (9 > 7 > 5) and temperatures 100 > 60 > 37°C).

In bone and tooth minerals, strontium is found as one of the minor constituents or impurities (Baud et al., 1977). The incorporation of strontium in bone mineral has been correlated with changes in the a-axis dimension of the bone apatite, but in enamel apatite, the effect of strontium substitution for calcium was obscured by simultaneous fluoride substitution for hydroxy which causes opposite effect on the axis (Bartels et al., 1982; Tanaka et al., 1981). Nevertheless, the interaction of strontium with bone is reported to be similar to that with synthetic calcium hydroxyapatite. Report by Koutsoukos and Nancollas

(1981) showed that in the presence of strontium, the crystallization of hydroxyapatite from metastable calcium phosphate solutions at low supersaturation results in the creation of cationic vacancies in the lattice and insignificant incorporation of the strontium ions.

2.1.2.3 Lead Substitution (Pb^{2+})

The replacement of lead in the hydroxyapatite structure in aqueous medium to form solid solutions in the entire range has been carried out based on the following equation (Narasaraju et al., 1972):

$10M(No_3)_2 + 6(NH_4)_2 HPO_4 + 2H_2O = M_{10}(PO_4)_6(OH)_2 + 12NH_4NO_3 + 8HNO_3$, where M = Ca^{2+} or Pb^{2+} for the respective end members and (Ca^{2+} + Pb^{2+}) for the solid solutions, the proportion of Ca to Pb being varied as desired at a pH of 12. Lead-calcium hydroxyapatite solid solutions have also been obtained by solid state reaction of appropriate mixtures of lead hydroxyapatite and calcium hydroxyapatite at a temperature of 900°C overnight (Bigi et al., 1989). Legeros et al (1980) also reported the substitution of Pb^{2+} for Ca^{2+} in the hydroxyapatite structure to form solid solutions in the entire compositional range by the drop-wise addition of calcium and lead acetate solution to a stirring phosphate solution maintained at 95 - 100°C for 5 hours.

The replacement of calcium by lead in the hydroxyapatite causes an expansion of the unit cell.

However, while the c- and a-axes dimensions of strontium - calcium apatites vary linearly with composition, contradictory data are reported for lead-calcium hydroxyapatite. Earlier reports (Narasaraju et al., 1972) indicated that the lattice parameters of lead-calcium hydroxyapatite vary linearly with composition but more recently, deviation of the c-parameters from Vegard's law has been reported (Bigi et al., 1989 and 1991). Report by Bigi et al., (1989) indicated that incorporation of lead into the hydroxyapatite causes a destabilizing effect on the hydroxyapatite structure and provokes its thermal conversion into β-tricalcium phosphate (β-TCP). The extent of this conversion was found to reduce with increasing lead concentration up to about 50 lead atom %. At lead concentrations higher than 50%, the stability of the solid solutions to heat treatment decreases. The researchers noted that the inhomogeneous distribution of lead in two non-equivalent cation sites of the hydroxyapatite structure or a preference of Pb^{2+} ion for site (2) of the hydroxyapatite structure causes a structural difference which can be considered responsible for the deviation of the c-axis from Vegard's law and thermal stability with composition of lead-calcium hydroxyapatite. Lead incorporation in the hydroxyapatite structure was also found to cause small displacement of the phosphorus atoms from the origin of the unit cell and affects significantly, the position of the hydroxyl group.

2.1.2.4 Barium Substitution (Ba^{2+})

The substitution of barium for calcium in the hydroxyapatite structure has been studied in aqueous system and by solid state reaction (Legeros et al., 1980; Bigi et al., 1984). According to Bigi et al., (1984), the precipitates obtained at 100°C by drop-wise addition of calcium and barium acetate solutions into a stirring phosphate solution are constituted by solid solutions only in the range of barium concentration in solution from 0 to 25 atom %. Amorphous precipitates were obtained from solutions containing a barium concentration of 25 to 60 atom %. At higher barium concentrations, tribarium phosphate was obtained. After heat treatments at 1200°C, apatitic precipitates from aqueous solution were converted into a crystalline phase corresponding to α-tricalcium phosphate. The study also showed that products obtained by solid state reactions at 1200°C are solid solutions over the range of barium concentration 60-100 atom %. The lattice dimensions and the frequency in the infra-red absorption spectra of the solid solutions were found to vary linearly with the atom % of barium. Concentration of barium in the solid solution was found to be less than that in the aqueous solution from which it was precipitated. This is in agreement with the results obtained by Legeros et al., (1980).

Incorporation of more than 25 atom % barium in the

calcium hydroxyapatite in aqueous medium was found to produce broadening in the X-ray powder diffraction peaks. The cell dimensions increased with barium atom % as expected due to the larger size of the barium ion compared with calcium ion. Inspite of the presence of a zone of immiscibility, the a-axis and c-axis dimension were found to expand according to Vegard's Law which is in agreement with that reported by Legeros et al., (1980) for Ba-Ca hydroxyapatite obtained from aqueous solution containing 5 and 10 atom % of barium.

2.1.2.5 Tin Substitution (Sn^{2+})

The extent to which tin can substitute for Ca^{2+} in the hydroxyapatite structure is still a matter of controversy. Studies by Legeros et al., (1980) showed that tin does not substitute for calcium in the hydroxyapatite to any significant extent. They reported that in an attempt to incorporate Sn^{2+} in the hydroxyapatite lattice in aqueous medium at 100°C, amorphous precipitates were obtained from solutions containing Sn^{2+} : Ca^{2+} mole ratio of 3:97 respectively.

A recent study by Thomas et al., (1989), however showed that Sn^{2+} can substitute calcium in the hydroxyapatite structure to form solid solutions over the range of Sn^{2+} concentration of 0 to 20 atom % by solid state reaction at 500°C; the amount of tin (II) incorporated in the calcium hydroxyapatite by precipitation

from aqueous medium was insignificant. Products obtained by solid state reactions in the study showed an expansion of the a-axis and c-axis lattice parameters in the range of 0 to 10 atom % tin which are similar to those reported by Legeros et al., (1980) for other cations.

2.1.2.6 Substitution by Other Cations

Not much work has been done on the substitution for Ca^{2+} in calcium hydroxyapatite by other cations, such as, Fe^{2+}, Co^{2+}, Ni^{2+}, Zn^{2+}, Mn^{2+}, Cu^{2+}, AI^{3+}, Fe^{3+}, Cr^{3+}, Li^{+}, Na^{+}, K^{+}, etc. In a survey of the individual effects of some cations on the formation, stability and some of the properties of apatites Legeros et al., (1980) reported that incorporation of Fe^{2+}, Co^{2+} and Ni^{2+} even in small amounts of not less than 10% relative to Ca^{2+}, destabilises the hydroxyapatite structure and promotes the formation of tricalcium phosphate (TCP); the presence of 5-10% of Zn^{2+}, Mn^{2+}, Cu^{2+}, Fe^{2+}, AI^{3+}, Fe^{3+} or Cr^{3+} relative to Ca^{2+} in the mediating solution was found to suppress the growth of the hydroxyapatite crystals. Similarly, the presence of not more than 10% Cr^{3+} or Cr^{6+} relative to calcium in the mediating solution caused the formation of apatite with differing crystallinity. While the presence of Cr^{3+} gave apatite with smaller crystallite size, no remarkable change was observed with Cr^{6+} relative to calcium hydroxyapatite.

2.1.3 Factors Affecting Cation Substitution in Hydroxyapatite

Proper understanding of the interaction of cations with calcium hydroxyapatite requires an examination of those factors which can influence these interactions. Attempts at explaining the extent of cationic replacement of Ca^{2+} in the hydroxyapatite on the basis of ionic radii (Legeros et al., 1980; Patel, 1979; Collin, 1959; Bigi et al., 1991) have not been too successful as it failed to account for some observed substitutions. For example, cations larger than Ca^{2+} such as Sr^{2+} and Pb^{2+} have been reported to substitute for Ca^{2+} in the hydroxyapatite structure giving a series of solid solutions in the complete composition range. Cadmium and Magnesium ions with smaller ionic radii than Ca^{2+} have also been shown to substitute for Ca^{2+} in the hydroxyapatite to form solid solutions in the entire range. Some other cations whose ionic radii are either similar or smaller than that of Ca^{2+} have not been reported to form complete series of solid solutions with hydroxyapatite.

Factors other than cationic size which influence the nature and extent of incorporation of metal ion in the hydroxyapatite structure may be inferred from the experimental observations in the above survey. The pH of the medium from which the solid solutions are precipitated may affect the nature and extent of incorporation of cation in the hydroxyapatite structure.

Table 2.1 Radii of Some Ions

Cation	Radii (A)	Anion	Radii (A)
Ca^{2+}	0.99	OH^-	1.53
Sr^{2+}	1.13	Cl^-	1.81
Ba^{2+}	1.35	F^-	1.36
Pb^{2+}	1.21	PO_4^{3-}	1.55
Fe^{2+}	0.76	CO_3^{2-}	1.29
Fe^{3+}	0.64		
Co^{2+}	0.74		
Ni^{2+}	0.69		
Zn^{2+}	0.74		
Mn^{2+}	0.80		
Cu^{2+}	0.72		
AI^{3+}	0.50		
Cr^{3+}	0.53		
Na^+	0.95		
Li^+	0.60		
K^+	1.33		
Mg^{2+}	0.65		
Cd^{2+}	0.97		

Source: Cotton and Wilkinson (1972)

For example, the higher the pH (9>7>5), the greater the amount of Sr^{2+} that can be incorporated in the hydroxyapatite structure (Legeros et al., 1980). The formation of lead-calcium hydroxyapatite in aqueous system

is facilitated at a pH of 12 (Narasaraju et al., 1972). Similarly, the incorporation of Mg^{2+} in the hydroxyapatite structure is favoured at higher pH values. At pH less than 9, the tricalcium phosphate is formed at the expense of magnesium-calcium hydroxyapatite (Patel, 1979; Inikori, Thomas, and Ayoko, 1991). Manganese (II) forms only apatite at a pH of 7, but at a pH of 5, apatite mixed with tricalcium phosphate are obtained (Legeros et al., 1980) from solutions containing 10 Mn^{2+}/90 Ca^{2+}.

The valency of a cation has also been found to influence the extent of formation of tricalcium phosphate at the expense of apatite and the nature of the crystallite size (Legeros, et al., 1980). Fe^{3+} in similar concentrations as Fe^{2+} partially replaces calcium in the hydroxyapatite in the ratio of 10/90 Ca to form tricalcium phosphate mixed with apatite, while apatite alone is obtained with Fe^{2+}. Also, Cr^{3+} and Cr^{6+} when present in similar amounts, 10/90 Ca^{2+}, in the mediating solution, causes the formation of apatite with differing crystallite size; and smaller crystallite size in the case of Cr^{3+} relative to that of hydroxyapatite.

The method of preparation may also influence the extent of cationic exchange in the hydroxyapatite structure. Ba^{2+} replaces Ca^{2+} in the apatite structure over a range of barium concentration of 60-100 atom % by solid state reaction at 1200°C. However, only small amounts of Ba^{2+} can be incorporated in the hydroxyapatite by

precipitation from aqueous medium (Bigi et al., 1984). Similarly, Sn^{2+} substitutes for Ca^{2+} in the hydroxy-apatite structure over a range of Sn^{2+}, 0 to 20 atom % by solid state reaction whereas only insignificant amounts of Sn^{2+} can be incorporated in the hydroxyapatite by precipitation from aqueous system (Thomas et al.,1989; Legeros et al.,1980; Legeros, 1977).

2.1.4 Methods for Investigating Cation Substitutions in Apatite System

Various physical methods are in use for studying substitution processes in apatite systems. These methods include:

i) Atomic absorption spectrophotometry;

ii) Infra-red absorption spectrophotometry;

iii) UV-Visible spectrophotometry; and

vi) X-ray powder diffraction analysis.

v) Transmission and Scanning Electron Microscopy.

These methods are often complimentary to each other and in practice a combination of a few of them is able to give enough information about the nature of the precipitates formed. Each of these methods and their application to the investigation of substitution reactions in apatite systems have been surveyed.

2.1.4.1 Infra-red Absorption Spectroscopy

The infra-red region is that portion of the electromagnetic spectrum between visible light and radio waves. Radiation absorbed in the infra-red region produces changes in the vibrational energy levels of the bonds in the molecule. Either wave number or wavelength is used to plot the positions of the absorption bands in the infra-red spectrum which in modern instrument covers 4000-200cm^{-1}. The infra-red region possesses a great array of characteristic bands which provide a wealth of structural information about the molecule.

Infra-red radiation will be absorbed by a molecule provided three conditions (Gadsden, 1975); are met:

i) a natural frequency of vibration of the molecule must be equal to the frequency of incident radiation;

ii) the change in bond length or bond angle due to vibrational or rotational motion must cause a net change in the dipole moment of the molecule and

iii) the energy must correspond to the energy difference of the ground and excited states of the molecules.

It is important that moisture be avoided during infra-red measurements. Strong absorption bands due to moisture which usually appear at 3710cm^{-1} and 1625cm^{-1} may interfere in the analysis (Fowler, 1974).

Infra-red spectra of organic compounds generally exhibit sharp well defined bands, assignable to the vibrations of the individual functional groups of which the

molecule is comprised. However, the infra-red spectra derived from inorganic compounds usually have absorption bands that are broad and overlapping, thus making assignments and specific identification of a cation-anion pair more difficult (Gadsden, 1975).

Four main areas in which infra-red spectroscopy can be useful in mineral analysis have been identified (Gadsden, 1975). These include:

i) identification of minerals of different but constant chemical compositions;

ii) identification of minerals of constant compositions but with different crystal structures;

iii) distinguishing between minerals that exhibit a range of composition within a group; and

iv) distinguishing between minerals that vary in both structural modification and chemical composition.

Early application of infra-red spectroscopy to the study of inorganic compounds proved the usefulness of the technique for the identification of polyatomic anions of the type, XO_4^{2-}, XO_3^- and others. A major set back suffered was the range of the spectrophotometers at the early days which was limited ($4000-650cm^{-1}$) and this made a large number of inorganic vibrations which occur in the far infra-red region (e.g. inter-atomic vibrations in binary compounds, such as borides, oxides, sulphides, etc) remain undetected. Today, most infra-red spectrophotometers cover the range $4000-200cm^{-1}$ and even

beyond. The availability of this modern instrumentation coupled with advances in coordination chemistry has awakened new interest in the application of infra-red spectroscopy to inorganic compounds.

Generally, the frequencies at which a material absorbs infra-red energy depends upon the internal vibrations of the molecule and hence upon composition. Polyatomic anions of the type, PO_4^{3-}, SO_4^{2-}, CO_3^{2-} and others absorb infra-red energy of different wavelengths and can be distinguished from the other. As the position of the maximum absorption in the infra-red spectrum is sensitive to changes in mass and charge of the constituent ions (Klee and Engel, 1970), the infra-red spectrum provides useful information regarding shift in absorption bands when one ion is replaced by another in a given compound (Fowler, 1974; Klee and Engel, 1970). Such information when correlated with the amount of the ions incorporated serves a suitable guide for following the extent and effects of incorporation of another ion in the lattice of a given compound (Bigi et al., 1984). This approach has been of immense assistance in the investigation of the extent and effects of cationic replacement in apatite systems.

Several workers have investigated the properties of apatites using infra-red spectroscopy (Klee and Engel, 1970; Fowler, 1974; Bigi et al., 1984; Patel, 1979; Koutsoukos and Nancollas, 1981; Bigi et al., 1991; Thomas et al., 1991; Baravelli et al., 1984). According to Fowler

(1974) infra-red spectroscopy is an effectual physical method for studying both compositional and structural details of apatites. This requires the complete assignment and characterization of the vibrational spectra of the pure apatite end members of controlled chemical and physical properties.

Klee and Engel (1970) have correlated the internal PO_4^{3-} frequencies of various apatites ($M_{10}(PO_4)_6X_2$, M = Ca, Sr, Ba, Cd, Pb, X = OH, F, Cl, Br) with various properties of the M and X ions including cation mass and lattice position, size and mass of the X ions.

Table 2.2: Vibrations of the Phosphate Ions in Substances Having the Apatite Structure (cm^{-1})

Apatite	V_1	V_{3a}	V_{3b}	V_{4a}
$Ca_5(PO_4)_3$ F	964	1092	1042	601
$Ca_5(PO_3)_3$ OH	962	1088	1042	601
$Ca_5(PO_4)_3$ Cl	960	1079	1040	605
$Ca_5(PO_4)_3$ Br	961	1080	1044	607
$Sr_5(PO_4)_3$ F	949	1075	1026	590
$Sr_5(PO_4)_3$ OH	947	1072	1032	592
$Sr_5(PO_4)_3$ Cl	949	1069	1028	591
$Sr_5(PO_4)_3$ Br	945	1061	1024	593
$Cd_5(PO_4)_3$ F	946	1058	1012	591
$Cd_5(PO_4)_3(OH)$	950	1064	1012	593
$Cd_5(PO_4)_3$ Cl	942	1058	998	598
$Cd_5(PO_4)_3$ Br	940	1054	996	600
$Ba_5(PO_4)_3$ F	933	1051	1010	579
$Ba_5(PO_4)_3$ Cl	934	1045	1008	579
$Ba_5(PO_4)_3$ Br	931	1041	1002	580
$Pb_5(PO_4)_3$ F	-	1032	982	569
$Pb_5(PO_4)_3$ OH	-	1030	976	572
$Pb_5(PO_4)_3$ Cl	925	1024	966	570
$Pb_5(PO_4)_3$ Br	920	1026	954	571

Source: Klee and Engel, (1970).

Klee and Engel (1970) concluded that:

i) For a given anion X, the mean wavenumbers are dependent essentially on the mass of the cation. The variation of the mean wavenumbers with the mass of M is practically linear for M = Ca, Sr and Ba. In most cases, lead compounds show a smaller and the cadmium compounds a larger deviation from this linear relationship;

ii) the degree of splitting of the bands, for a given anion X, does not seem to be related to the mass of the cation. In particular, the splitting of V_3 is of the same order of magnitude for the three alkaline earth metal compounds and is larger for certain lead and cadmium apatites;

iii) neither the masses of X nor their positions in the apatite structure have an influence on the mean wavenumbers comparable in magnitude to that of the cations; and

iv) for a given cation M, the influence of the X anion on the degree of splitting of the bands is rather complex. In the case of calcium and strontium apatites the splitting of V_3 decreases while that of V_4 increases when going from the fluoride to the bromide compounds.

On the whole, the mass of the cation seems to have significant influence on the mean frequencies of the internal PO_4^{3-} vibrational modes. Patel, (1979) also

reported that the V_3 and V_4 frequencies corresponding to OH-ions are shifted to lower frequencies in Ca-Mg hydroxyapatite solid solutions precipitated from aqueous solution at pH = 9 as the magnesium atom concentration increases. Similarly, Bigi et al., (1984) showed that except for the frequency of the OH- stretching mode which increases with increase of barium atom concentration, all the other infra-red frequencies decrease nearly linearly with increasing barium content in the Ca-Ba hydroxyapatite solid solutions. According to Legeros et al., (1980), if the PO_4^{3-} groups of the apatite is considered as a skeletal frame work of the structure, then it is reasonable to expect that substitutions within the structures will cause changes in the neighbourhood of these PO_4^{3-} groups. These will affect their vibrations and will be reflected in their infra-red absorption spectra. Such changes were also observed in the infra-red absorption spectra of apatites obtained from solutions containing similar concentrations of AI^{3+}, Cr^{3+}, Zn^{2+}, Cu^{2+}, Cu^{+}, Fe^{3+} and Fe^{2+}. Less band shifts were observed in the spectra of apatites obtained in the presence of similar concentrations of Ba^{2+}, Pb^{2+}, Sr^{2+}, Mn^{2+}, Cd^{2+} and no significant shift occurred in the presence of K^{+}, Li^{+}, or Na^{+} when these infra-red spectra were compared with those of unsubstituted calcium hydroxyapatite (Legeros et al., 1980). According to Fowler (1974), as the cation - anion bond becomes stronger, the frequencies of the internal modes of the anion should

become more cation dependent and in turn sensitive to cation mass.

The internal PO_4^{3-} frequencies of cadmium and lead are reported to deviate from the nearly linear cation mass-frequency trends characteristic of apatites of calcium, strontium and barium (Klee and Engel 1970; Fowler, 1974). Klee and Engel (1970) attributed this observation to the more covalent cation-anion bond character in the cadmium and lead apatites as compared to the calcium, strontium and barium apatite.

Most of the infra-red absorption bands of mixed Ca-Sr hydroxyapatite are broadened especially the hydroxyl bands as compared to the bands of the end members, calcium hydroxyapatite and strontium hydroxyapatite. This band broadening according to Fowler (1974) reflects the heterogeneity introduced by the different cations in the crystal fields about the vibrating anions.

While studying the infra-red spectra of apatites, the OH vibrational modes are of primary interest especially the OH libration mode which is very sensitive to its environment. For example, in Ba-Sr- and calcium hydroxyapatite, the OH stretching modes occur at 3606, 3592 and 3572cm^{-1} respectively and the OH librational modes at 430, 535 and 630cm^{-1} respectively. Marked increase in the OH stretching frequency and decrease in librational frequency are observed in barium-calcium and strontium-calcium hydroxyapatites which according to Fowler (1974)

are suggestive of hydrogen bond arising from decreasing OH--O separations.

The Barnes (1944) equation:

$$V = \frac{(k\mu)^{1/2}}{2\pi C}$$

where

V = frequency

k = restoring force

μ = reduced mass

C = velocity of light

may be used to explain why the infra-red frequencies of the PO_4 group in calcium hydroxyapatite are shifted when compounds of the type, $Ca_{10-x}M_x(PO_4)_6(OH)_2$ are formed. (X = 0 -10; M = cation).

When the equilibrium distance between the positive and negative atoms of the molecules is decreased, k, generally increases in the Barnes equation. This equilibrium distance depends on the ionic radius of the participating atoms in the molecule. Substitution of Ca^{2+} (ions radius = 0.99A) with a nucleus like Mg^{2+} (ionic C radius = 0.65A) gives rise to a stronger coordination of the PO_4 group to the Mg^{2+} ion through oxygen. This in turn weakens to P-O bond lowering K (increasing P - O bond length) and the frequency lowered.

The introduction of infra-red spectroscopy into the field of mineral and related inorganic compounds analysis has been limited due to excellence of the X-ray diffraction

techniques. However, the infra-red absorption technique is quick, simple, relatively inexpensive and serves as a useful supplementary technique in the identification of mineral species (Gadsden, 1975; Hertzberg, 1945).

2.1.4.2 X-ray Analysis

X-ray as an analytical tool consists of three main types (Pease, 1980).

i) X-ray absorption;

ii) X-ray diffraction; and

iii) X-ray fluorescence.

Each of these techniques depends on a different property of the radiation and each has specific application in analytical chemistry.

X-ray absorption is used to detect imperfection in the internal structure of a physical body through which it passes; x-ray diffraction is used mainly to determine crystalline structure and can be done on a single crystal or on a powder sample; x-ray fluorescence on the other hand is used qualitatively and quantitatively for elemental analysis. All three techniques are non-destructive.

X-ray spectra lines result when incident electrons knock orbital electrons out of an atom. If an ejected electron is from one of the inner orbitals of the atom, an electron from an outer shell will fall into the inner orbit to fill the vacancy. The decrease in potential energy of this electron in approaching the nucleus (ΔE), results in

the emission of an x-ray photon having energy exactly equal to that lost by the electron. The wavelength λ, for such photons is related to ΔE by;

$$\lambda = \frac{hc}{\Delta E}$$

where c is the velocity of electromagnetic energy and h is Planck's constant. The X-ray photons have definite wavelengths which are characteristic of the atom. X-rays resulting from an electron vacancy in the innermost shell of an atom are known as K- X-rays or K- lines; those from L-shells are known as L-lines. The K-lines are mostly used for powder diffraction method.

X-ray powder diffraction technique serves as one of the most reliable methods for following substitution process in apatite systems. The principle of diffraction is based on the combined effects of interference and reinforcement that occur between two wave fronts that are either in pure or out of phase.

X-rays penetrating below the surface of crystalline materials are scattered (diffracted) by the individual parallel layers of atoms; each atomic layer acts as a new although weak source of x-rays. To be reinforced in a given direction at an angle θ, the spacing, d, between crystal planes must be rigorously related to the wavelength of the x-ray radiation. At a given angle, X-rays of one definite wavelength will be constructively reinforced. The variables are related by the Bragg's law (Pease, 1980).

$\lambda n = 2d \sin\theta$

where n is the order of diffraction.

As already stated, the diffraction method can be carried out on either a single crystal or on a powder sample. The diffracted X-rays may be recorded either photographically or by means of counting devices such as scintillation counters. For a single crystal using a film method, the diffraction pattern is comprised of a series of spots produced by the various planes in the crystal as it is rotated in the plane of the x-rays. The final result usually gives a three-dimensional picture of the molecule, showing all atoms present and the relative molecular configuration.

Powdered samples usually contain many small crystals (crystallites) arranged at random angles and the combined effects of all their various crystal planes is to produce a series of cones of scattered x-rays. Powder diffraction patterns may be obtained with a rotating detector. The read out from the system is a series of peaks, the heights and areas of which are proportional to the intensity of the lines and the positions are in terms of 2θ degree. The angle may be readily translated into d-values where the wavelength of the incident radiation is known.

The x-ray powder diffraction technique is often used as a "finger printing" method. It involves comparing the x-ray powder diffraction patterns of the sample under test with standard powder patterns provided by the Joint

Committee on Powder Diffraction Standards (JCPDS) as cards. Matching is normally judged in terms of the tabulated d-spacing and relative intensities of the corresponding peaks. The powdered patterns are usually sufficient to characterise the compound under test and also provide information on the number of phases present in the compound. Where the compound is sufficiently crystalline, unit cell parameters of the compound can be obtained through rigorous calculations from the powder diffraction patterns which often involves the use of computer. Refinement of the structure of the compound may also be carried out from the X-ray powder diffraction patterns as reported by Bigi et al., (1989).

X-ray powder diffraction method has been widely applied in the study of apatite systems. Several research workers including Thomas et al., 1989, Inikori, et. al., 1991; Collin, 1959; Narasaraju et al., 1972; Trautz, 1955; Koutsoukes and Nancollas, 1981; Patel, 1979; Mayer and Fowler, 1982; Brown et al., 1979, Bigi et al., 1984; Baravelli et al., 1984; Bigi et al., 1991; Legeros et al., 1980, have used the x-ray powder diffraction method to investigate the individual effects of some elements on the formation and some properties of apatites in synthetic and biological systems. Reports from these studies show that lattice parameters indicate unit cell expansion when cations larger than Ca^{2+} are incorporated in the hydroxyapatite structure; those cations with smaller ionic

radii than Ca^{2+} lead to unit cell contraction (Legeros et al., 1980; Koutsoukos and Nancollas, 1981; Narasaraju et al., 1972; Collin, 1959; Patel 1979). Thomas et al., 1989, have reported the expansion of the a-and c-lattice parameters in the range of 0-10% Sn in solid solutions of tin-calcium hydroxyapatite similar to those reported by Legeros et al., (1980) for other cations. Narasaraju et al., (1972) also reported that the substitution of Ca^{2+} by Pb^{2+} dilates the unit cell of the hydroxyapatite, which confirms the formation of solid solutions. They observed that such a dilation with increase in lead content of the Pb-Ca apatite could be inferred from the excellent regularity with which the unit cell volumes of the sample precipitates, calculated on the basis of experimentally determined lattice constants increased with the proportion of lead in the solid solutions.

X-ray powder diffraction studies have also shown that both a - and c-axis dimensions increase with increasing strontium incorporation in the solid solution of the calcium-strontium hydroxyapatite (Collin, 1959). Such an effect could not be accounted for by surface absorption and it has been suggested that strontium shows a preference for the six fold position in the hydroxyapatite (Heijligers et al., 1979). Koutsoukos and Nancollas (1981) have also reported that the proportionality between unit cell lattice parameters and the strontium concentration of precipitates obtained from the interaction between

strontium ions and hydroxyapatite suggests that solid solutions are formed during crystallization reactions rather than discrete Ca-Sr apatites. Baud and Very (1973) measured the unit cell parameters of the inorganic components of the bones of mice that had been fed a strontium rich diet and showed that higher doses of strontium resulted in increase in a-axis.

According to Patel, (1979), when lattice constants of suspected solid solutions are plotted against atom % of the substituting metal in the solution, and a straight line joining the two end members is obtained, it is a conclusive real evidence that the preparations are not mixtures of two components or one component with adsorbed materials but solid solutions in that series. This observation has been corroborated by other researchers (Legeros et al., 1980; Koutsoukos and Nancollas, 1981; Collin, 1959).

Among the cations which can be incorporated in the hydroxyapatite structure, only cadmium, strontium, lead and recently magnesium are known to replace calcium over the whole range. The a- and c-axis dimensions of both strontium-calcium apatites and cadmium-calcium apatites have been reported to vary linearly with composition according to Vegard's Law (Verbeeck et al., 1981). Bigi et al., (1984) have also reported that the products obtained by solid state reaction between barium and calcium hydroxyapatite at 1200°C are solid solutions over the range of barium concentrations, 60-100 atom %, and these exhibit

lattice parameters which vary linearly with the barium atom concentration.

Crystallographic studies of the mineral phase associated with human subcutaneous deposits revealed two distinct type of calcium phosphate deposits in the x-ray diffraction patterns. The main crystalline inorganic phase was hydroxyapatite while β-tricalcium phosphate, a partial replacement of calcium with magnesium was present just in small amounts (Bigi et al., 1980).

2.1.4.3 Atomic Absorption Spectrometry (AAS)

Atomic absorption spectroscopy is one of the widely used analytical techniques for the detection and determination of metal concentrations especially those that occur at trace levels. This is due to its high sensitivity, accuracy, reproducibility, ease of sample preparation and handling. These qualities of the Atomic Absorption Spectrophotometer have made it a very important tool in the determination of metal-atom concentrations present as cations in biological, geological and synthetic apatites.

The principle of atomic Absorption Spectroscopy is based on the ability of atoms in their ground state to absorb radiant energy of their own specific wavelength which is passed through a flame containing their vapour (Pease, 1980). The radiant source (hollow cathode lamp) used is specific to each element. This helps in overcoming overlap of spectra bands and inter-elemental interference.

Following the absorption of some of the incident light by the vaporised atoms, the decrease in intensity is measured by a monochromator (which enables the selection of the particular wavelength for measurement) and then to a detector.

In early years, the flames used in absorption spectroscopy were pre-mixed air-coal gas, air-propane or air-acetylene and a slot burner type nebulizer (Walsh, 1955). Such flames could only vaporize atoms of alkalis and alkaline earth metals, chromium, molybdenum and tin, but too low for the detection of oxides which do not dissociate easily in such flames. The nitrous oxide acetylene flame is however characterised by its high temperature and reductive atmosphere which permits the determination of very low concentrations of non-dissociable compounds that are not detected with air-acetylene flame (Willis, 1965). Some of such elements include Ba, Be, Al, Sr, Si, Ti, V, W, Eu, Gd, Hf, Fr, La, Nb. Se, Zr, and others. These elements can form oxides which require high energy for dissociation, for which, the temperature of the air-acetylene is too low, but the nitrous oxide-acetylene flame is adequate.

Both the air acetylene and nitrous oxide acetylene flames have been widely used in determining the concentration of a given metal ion in biological, geological and synthetic apatite samples (Legeros et al., 1980; Berry, 1967; Bigi et al., 1980; Koutsoukos and

Nancollas, 1981; Mayer and Fowler, 1982; Baravelli et al., 1984).

Results of metal concentrations in apatite samples determined by atomic absorption spectrometry are utilized for computing weight percent of the metal per mole of the apatite, molecular formula and also used along with phosphorus levels for computing the mole-atom ratio for each sample. The mole-atom ratio is the ratio of the metal atom concentration to phosphorus per mole of an apatite sample. For pure apatites, the mole-atom ratio is theoretically 1.67. This figure serves as a guide as to when a solid solution results from a cationic substitution in the hydroxyapatite structure (Partington, 1957). Patel, (1979) reported a mole-atom ratio of 1.656 for Ca-Mg solid solutions. For the same system, Chiranjeevirao et al., (1982) reported values ranging from 1.67 to 1.68. Narasaraju et al., (1972) reported 1.62, 1.66 and 1.67 for calcium-lead solid solutions. A comparison of results from atomic absorption determinations such as metal weight percent and molecular formula with calculated values for each sample also provide a guide as to whether cationic substitution produced solid solutions.

Various types of interferences are often encountered in Atomic Absorption Spectrophotometric determinations. Chemical and ionization interferences are the most common type of interferences (Pease, 1980).

When a compound or complex ions of the element being

determined dissociates incompletely into the atoms, low absorbance results are obtained. This incomplete dissociation is a chemical interference and may be removed by the use of high flame temperature or by chemical means. For example, magnesium and aluminium give thermally stable metal oxides. Due to this thermal stability, low results for magnesium are obtained in the presence of aluminium. However, such interference may be removed by the addition of lanthanum to the system. Since the mixed oxide of lanthanum and aluminium is more stable than that of magnesium and aluminum, lanthanum-aluminium oxide is formed and magnesium oxide is released. Magnesium is then determined after this latter compound is reduced and vaporized in the flame.

Similarly, the presence of phosphate ions, PO_4^{3-}, suppresses the absorbance of calcium atoms, (Vogel, 1961). This may be due to the formation of refractory calcium phosphate which is not dissociated into its constituent atoms in the flame. The addition of salts such as lanthanum chloride, strontium nitrate and others, can reduce this interference probably by preferential combination of the lanthanum or strontium ions with the phosphate ions, thus freeing the calcium ions for maximum absorbance.

Ionization interference is another draw-back in atomic absorption spectroscopy. This arises if the flame temperature is too high. When this occurs, some of the vaporized atoms become ionized. The resulting ions absorb

at a different wavelength from the vaporized atoms; this new wavelength will not be selected by the monochromator and low absorbance values are consequently obtained. Attempts at lowering the flame temperature so as to alleviate the ionization interference may result in complete dissociation and greater chemical interference.

Ionization interference may be corrected for by the addition of large quantities of sodium or potassium salts to the solution. Since each of these elements has a lower ionization potential than calcium, their electrons are relatively easier to remove, thereby allowing it to be freely determined.

2.1.4.4. UV-Visible Spectroscopy

Ultraviolet spectrum is recorded over the wave number range 50,050 to 25,000cm^{-1} (185-400nm). The 25,000 - 12,000cm^{-1} region (400 - 800nm) records absorption in the visible region. Absorption of electromagnetic radiation in these regions involves the promotion of electrons from the ground state to the higher energy states. An ultraviolet-visible spectrophotometer provides a reliable means of determining minute quantities of an absorbing species.

Two limitations however govern the use of UV-visible spectrophotometer. These are instrument limitation and reagent limitation. Most of the reagent limitations are brought about by a change in the nature and concentration of the absorbing species. Any change in the system brought

about by other factors such as pH, oxidation-reduction, reaction with solvent or even dilution which causes a shift in equilibria might lead to increase or decrease in concentration and a change in measured absorbance. For example, assume a chelation equilibria system used in the determination of copper, the copper being determined as a chelate. If the chelating agent exists in three equilibria species as follows:

$$\underset{\text{Green}}{H_2KE^+} \longrightarrow \underset{\text{Yellow}}{HKE} + H^+ \quad - - - - \text{(i)}$$

$$\underset{\text{Yellow}}{HKE} \longrightarrow H^+ + \underset{\text{Red}}{KE^-} \quad - - - - \text{(ii)}$$

where H_2KE, is the acidic form, HKE, is the neutral form and KE^- is the basic form of the chelating agent, HKE. If it is desired to determine copper as the red $CU(KE)^+$, which forms according to the following reaction:

$$\underset{\text{Yellow}}{HKE} + Cu^{2+} \longrightarrow \underset{\text{Red}}{[Cu\ (KE)]^+} + H^+ \quad - - - \text{(iii)}$$

then, it is obvious that an excess of acid (low pH) would shift the equilibrium to the left in equation (iii) and as a consequence, the measured concentration of $[CU\ (KE)]^+$ would not accurately reflect the total Cu^{2+} in the solution. Care must also be taken to avoid the use of excess base as this would lead to the formation of excess KE^-. Since KE^- and $[Cu\ (KE)]^+$ are both red and absorb at the same wavelength, any measurement at this wavelength would reflect the concentration of both species, KE^- and $[Cu\ (KE)]^+$ and high absorbance values would be obtained.

Instrumental deviation from Beer-Lambert's Law may also occur. The law requires monochromatic radiation because absorptivity is a constant at a single wavelength and varies with a change in wavelength. The possibility of error due to the practical impossibility of obtaining monochromatic radiation can be minimized by selection of a spectral region where a change in absorptivity with a change in wavelength is very small.

Generally, in order to avoid the numerous possibilities of an error arising from deviation, in practice, a calibrated curve for the absorbance-concentration relationship is prepared at the chosen wavelength for each analysis.

The UV-Visible spectrophotometer is widely used in the determination of the concentration of phosphorus in apatite samples. By comparing the combined metal concentration with the phosphorus concentration in the sample, an indication as to whether the desired solid solution has been prepared may be obtained.

A metal atom concentration to phosphorus concentration ratio of 1.67 is usually an evidence of the formation of an apatite sample. According to Patel (1979), the fact that the observed value of mole-atom ratios of Ca/P, Mg/P for end members and (Ca+Mg)/P for intermediate members for a Ca-Mg apatite system = 1.656, is consistent with the formation of solid solutions (Partington, 1957) in the entire range. This procedure has been widely applied by

various researchers to the study of substitution processes in apatite systems (Berry, 1967; Bigi et al., 1980; Legeros et al., 1980; Baravelli et al., 1984). Some non-stoichiometric apatites have been reported with composition of Ca/P = 1.33 to 1.67 (Berry, 1967).

The concentration of phosphorus in apatite systems is more often determined spectrophotometrically as molybdovanado-phosphoric acid (Quinlan and Dessesa, 1955). In common with arsenic, germanium and silicon, phosphorus forms a yellow heteropoly acid with excess molybdate. These heteropoly acids may be utilized directly in spectrophotometric procedures or they may be reduced to molybdenum blue with an increase in intensity (Vogel, 1961). Either of these methods can be used for phosphorus determinations. However, both methods are subject to serious interference if arsenic, germanium or silicon is also present. Both methods are therefore suitable for the determination of phosphorus in synthetic apatites which are free of the interference elements.

Another popular spectrophotometric method for phosphorus determination is that based on the formation of the yellow molybdovanadophosphoric acid as originally proposed by Misson (1908) and later developed by Quinlan and Dissesa (1955). This method has been used by various research workers (Bigi et al., 1980; Baravelli et al., 1984) for the determination of phosphorus in apatite systems.

CHAPTER THREE

ISOMORPHOUS SUBSTITUTION IN CALCIUM HYDROXYAPATITE (CaHA) BY MAGNESIUM, ZINC AND LEAD

3.1 Introduction

$Ca^{2+} \longrightarrow Mg^{2+}$ replacement reactions in Calcium Hydroxyapatite is of extreme biological significance as it explains the mechanism of incorporation of Mg^{2+} in human skeletal systems, (Patel, 1979). The exchange process, is known to occur according to the following equation:

$Ca_{10}(PO_4)_6(OH)_2 + xMg^{2+} \longrightarrow Ca_{10-x}Mg_x(PO_4)_6(OH)_2 + x\ Ca^{2+}$

(where x = 0 to 10).

There are conflicting reports regarding the interaction of Mg^{2+} with Calcium hydroxyapatite. Some studies have suggested that the interaction of Mg^{2+} with Calcium hydroxyapatite is limited to the apatite crystal surface with no significant substitution of Mg^{2+} for Ca^{2+} (Williams and Sallis, 1982; Nancollas, 1984; Neuman and Neuman, 1969, Bosler and Posner, 1974). Other studies have shown that the presence of a significant amount of Mg^{2+} in the mediating solution tends to favour the formation of amorphous calcium phosphate or β-tricalcium phosphate (Legeros et al., 1980).

Patel (1979) and Chiranjeevirao et al., (1982), have shown that at pH values greater than 9, Mg^{2+} undergoes isomorphous substitution with Ca^{2+} in Calcium hydroxyapatite to form solid solutions in the entire range. Solid solutions of calcium and magnesium hydroxyapatite

were prepared earlier (Vanwazer, 1966) by fixing mixtures containing various portions of calcium and magnesium hydroxyapatite at about 1300°C. These samples prepared by solid state reaction were however found to be non-homogeneous and discontinuous.

In the present study, homogeneous solid solutions of Ca-Mg hydroxyapatite over the entire compositional range have been prepared by the method of co-precipitation (Patel, 1979; Legeros, et al., 1980; Chiranjeevirao et al., 1982). The products obtained have been studied by colorimetry, infra-red absorption method (Herzberg, 1945), atomic absorption spectroscopy and x-ray analysis (Klug and Alexander, 1974). The study was undertaken as part of on-going attempt to clarify factors influencing the nature of the interaction of Mg^{2+} with Calcium hydroxyapatite.

As stated earlier, the apatites of human teeth and bones are "impure calcium hydroxyapatite" because they contain "impurities". Based on studies on synthetic calcium hydroxyapatite systems (Thomas et al., 1989; Thomas, 1989; Bigi et al., 1989; Bigi et al., 1984; Chiranjeevirao et al., 1982; Baravelli et al., 1984; Mayer et al., 1982; Koutsoukos and Nancollas, 1981; Legeros et al., 1980; Brown et al., 1979; Elliot, 1979; Narasaraju et al., 1972; Berry, 1967; Fowler, 1974; Klee and Engel, 1970), Sn^{2+}, Sr^{2+}, Na^{+}, Li^{+}, Mg^{2+}, Pb^{2+}, Ba^{2+}, Zn^{2+}, Fe^{2+}, Cd^{2+} and other cationic trace elements are presumed associated with biological apatite.

The nature, role and extent of incorporation of Zn^{2+} among others in the Calcium hydroxyapatite lattice is still not clear. The incorporation of Zn^{2+} in the apatite system has not been extensively studied. This may be attributed to the fact that the element, zinc, has not been known to produce very adverse effects on the human system.

Though zinc has an ionic radius smaller than that of calcium, (Zn^{2+} = 0.74A; Ca^{2+} = 0.99A), it has not been shown to form complete series of solid solutions with Ca^{2+}. It has been reported that Zn^{2+} can be incorporated in the Calcium hydroxyapatite lattice to a limited extent and significant incorporation of it suppresses crystal growth (Legeros et al., 1980).

In this study, an attempt has been made to replace Ca^{2+} with Zn^{2+} in the calcium hydroxyapatite in aqueous medium to form solid solutions in the entire compositional range. Samples obtained have been analysed by the colorimetric method, atomic absorption spectrometry and infra-red absorption spectroscopy.

Also of significance among the cationic exchange reactions of calcium hydroxyapatite is the replacement of Ca^{2+} by Pb^{2+} to form a continuous series of solid solutions of Ca-Pb hydroxyapatite (Narasaraju et al., 1972; Legeros et al., 1980; Bigi et al., 1989; Bigi et al., 1991). Such an exchange is considered to be the basis for the incorporation of lead in human skeletal system which brings about lead poisoning.

The incorporation of lead and other foreign ions in the hydroxyapatite crystal lattice have been reported to affect the crystallinity, morphology, lattice parameters and consequently the stability of the apatite structure (Collin, 1959; Baravelli et al., 1984; Thomas et al., 1989; Patel, 1979; Bigi et al., 1984, 1989 and 1991; Heijligers, et al., 1979; Muller, 1947; Narasaraj et al, 1972; Engel et al., 1975; Verbeeck et al., 1981; Andres-Verges et al., 1983).

The substitution of lead for calcium in the calcium hydroxyapatite structure causes enlargement of the unit cell which reflects the larger size of the Pb^{2+} ion (ionic radius = 1.20Å) compared to that of Ca^{2+} (ionic radius = 0.99Å). While the a- and c-axis dimensions of both strontium-calcium and cadmium-calcium hydroxyapatites have been reported to vary linearly with composition according to Vegard's law (Bigi et al., 1986; Heijligers et al., 1979), there are conflicting reports regarding the variation of the lattice constants with composition of Ca-Pb hydroxyapatite solid solutions. Muller (1947), Narasaraju et al., (1972) and Rao (1979) have reported that the lattice parameters of the Pb-Ca hydroxyapatite solid solutions vary linearly with composition. More recent reports (Engel et al., 1975; Heijligers et al., 1979; Verbeeck et al., 1981; Andres-Verges et al., 1983; Bigi et al., 1989), however show a deviation of the c-parameter from Vegard's law. A linear variation of both a- and c-

axis dimensions with the composition of the Pb-Ca hydroxyapatite is usually an indication that the substitution of Pb^{2+} for Ca^{2+} in the Calcium hydroxyapatite is homogeneous in all axes as also manifested by the regularity of the dilation of the unit cell with the proportion of lead in the apatite as reported by Narasaraju et al., (1972). On the other hand, the non-linearity of the c-parameter with the proportion of lead in lead-calcium hydroxyapatite solid solutions in the whole range may imply that the substitution of Pb^{2+} for Ca^{2+} in the Calcium hydroxyapatite is not homogeneous in the two equivalent cation sites of the hydroxyapatite structure.

In this chapter an attempt has also been made to investigate the role of lead in the lead-calcium hydroxyapatite solid solutions. Lead hydroxyapatite and calcium hydroxyapatite were prepared from aqueous medium and the exchange reactions carried out by solid state process at 900°C. The lead substituted calcium hydroxyapatite solid solutions were then analysed by crystallographic and spectroscopic methods. The X-ray powder diffraction analysis were carried out for this study in Italy.

3.2 Experimental

3.2.1 Preparation of Calcium Hydroxyapatite.

Reagents

Unless where stated, all reagents were of analytical grade. All aqueous solutions were prepared in doubly distilled water.

Calcium Nitrate Solution

A 8.0 x 10^{-3} M solution of calcium nitrate was prepared by dissolving a calculated amount of the salt in water.

Ammonium Dihydrogen Phosphate Solution

A 1.9 x 10^{-2} M solution of ammonium dihydrogen phosphate was prepared by dissolving stoichiometric amount of the salt in water.

Procedure

The calcium nitrate and ammonium dihydrogen phosphate solutions were separately brought to pH = 12 with ammonia solution. The calcium nitrate solution was then heated to boil and the phosphate solution carefully added drop-wise with constant stirring and the temperature maintained at about 100°C (Legeros et al., 1975; Bigi et al., 1980).

After precipitation, the contents of the flask were refluxed for about 1 hour to enhance homogeneity and crystallinity of the apatite (Chiranjeevirao et al., 1982). The precipitate was filtered, washed with warm water till washings were neutral and dried at 105°C for about 6 hours.

pH Measurement

pH values were determined with W.G. Pye Model 290 pH meter.

3.2.2 Preparation of Magnesium Hydroxyapatite

Reagents

Magnesium Nitrate Solution

An 8.0 x 10^{-3} M solution of magnesium nitrate was prepared by dissolving a stoichiometric amount of the salt in water.

Ammonium Dihydrogen Phosphate Solution

This was prepared as stated in section 3.2.1.

Procedure

Magnesium hydroxyapatite was prepared as described for calcium hydroxyapatite, but using magnesium nitrate solution (8.0 x 10^{-3} M) instead of calcium nitrate.

3.2.3 Preparation of Calcium-Magnesium Hydroxyapatites

Calcium-magnesium hydroxyapatite solid solutions were prepared from aqueous medium by the method of co-precipitation (Chiranjeevirao et al., 1982; Legeros et al., 1980; Patel, 1979; Bigi et al., 1980).

A mixed solution of calcium and magnesium nitrate Ca/Mg in mole ratios ranging from 100/0 to 0/100 respectively was added drop-wise to a stirring ammonium dihydrogen phosphate solution maintained at about 100°C. The pH of the mediating solution was maintained at 12 with

ammonia solution. The mixed metal nitrate solutions were prepared in such a way that the total cation concentration was exactly 8.0 x 10^{-3} mol dm^{-3} while the phosphate concentration was fixed at 1.9 x 10^{-2} mol dm^{-3}. The precipitate obtained in each case was treated as described for calcium hydroxyapatite in section 3.2.1.

3.2.4 Preparation of Zinc Hydroxyapatite

Zinc hydroxyapatite was prepared as described for calcium hydroxyapatite in section 3.2.1 but using zinc acetate dihydrate solution (8.0 x 10^{-3} M) and pH of 10.5 enhanced with ammonia solution.

3.2.5 Preparation of Calcium-Zinc Hydroxyapatite

Solid solutions of calcium-zinc hydroxyapatite were prepared as described for calcium-magnesium hydroxyapatite but using mixed solutions of calcium acetate monohydrate and zinc acetate dihydrate and maintaining the pH of the solution at 10.5 with ammonia solution in the first instance and secondly without enhancing the pH of the mediating solution (pH 5-6).

3.2.6 Preparation of Lead Hydroxyapatite

Lead hydroxyapatite was prepared as described for calcium hydroxyapatite in section 3.2.1 but using lead acetate trihydrate solution ((8.0 x 10^{-3} M) and pH of 10.5.

3.2.7 Preparation of Lead-Calcium Hydroxyapatite by Solid State Process

Lead-calcium hydroxyapatite in the composition range of $Pb_{20}Ca_{80}$, $Pb_{45}Ca_{55}$, $Pb_{65}Ca_{35}$, and $Pb_{80}Ca_{20}$ were prepared by solid state reaction process. This was carried out by mixing appropriate quantities of lead hydroxyapatite and calcium hydroxyapatite and allowing the mixture to react at 900°C for 15 hours (Bigi et al., 1989).

3.2.8 Chemical Analyses of Samples

3.2.8.1 Colorimetric Determination of Phosphorus Content of Apatite Samples

The concentrations of phosphorus in the prepared apatite samples were determined colorimetrically using the molybdenum blue method (Basset et al., 1978; Quinlan and Dessesa, 1955).

This method is based on the fact that acidified solutions of orthophosphate and molybdate ions condense to form the heteropoly acid, molybdophosphoric acid which on reduction with hydrazine sulphate forms molybdenum blue. The intensity of the blue colour of the molybdenum is a function of the quantity of phosphate initially incorporated in the molybdophosphoric acid and therefore serves as a highly reliable method for estimating the phosphorus concentrations in hydroxyapatite spectrophotometrically.

The method is however subject to serious interference if arsenic, silicon or germinarium is also present (Quinlan and Desesa, 1955).

Reagents

Molybdenum Solution

Molybdenum solution was prepared by dissolving 12.5g of sodium molybdate ($Na_2MoO_4.2H_2O$) in 5.0 M sulphuric acid and diluting to 500cm ^{3} with 5.0 M H_2SO_4.

Hydrazinium Sulphate Solution

A stock solution of hydrazinium sulphate solution was prepared by dissolving 1.5g of hydrazinium sulphate in water and diluting to 1.0 dm^3.

Standard Phosphate Solution

A stock solution of phosphate was prepared by dissolving 0.2197g of dried potassium dihydrogen phosphate (KH_2PO_4) in water and diluting to 1.0 dm^3, yielding a solution of 5.0 x 10^{2-}mg phosphorus per cm^3.

Working standard phosphate solutions in the range of 1-10ppm were prepared by serial dilution of the stock solution.

Sample Solution

1.0 x 10^{-2}g of each sample was dissolved with 3-drops of concentrated nitric acid, transferred to a 50cm^3 graduated flask and made to the mark with doubly distilled water.

Instrument Used

A Unicam SP 1750B (Pye Unicam Ltd., England) spectrophotometer was used for absorbance measurements.

Procedure

5.0cm^3 of the molybdate solution was added to each standard solution in a 50cm^3 pyrex graduated flask followed by 2.0cm^3 of the hydrazinium sulphate solution and diluting to the mark with doubly distilled water. After thorough mixing, the flask was immersed in a boiling water bath for about 10 minutes, removed, allowed to cool and the volume adjusted. The absorbance of each standard solution was read at 830 nm. A calibration curve was constructed from the results obtained.

For the sample solutions, 2.0cm^3 of each was transferred to a 10cm^3 graduated flask to which was added 5.0cm^3 of the molybdate solution followed by 2.0cm^3 of the hydrazinium sulphate solution, and then treated as in the case of standard solutions. Absorbance for each sample solution was read at 830nm as in the case of standard solutions. The calibration curve obtained from the standard solutions was used in estimating the phosphorus concentrations of the sample solutions.

3.2.8.2 Determination of Ca, Mg, Zn and Pb Content of Apatite Samples by Atomic Absorption Spectrometry

Reagents

Lanthanum Solution, 10% m/v

Lanthanum solution was prepared by dissolving 31.20g Lanthanum nitrate hexahydrate, $La(NO_3)_3.6H_2O$ in a $100cm^3$ graduated flask and making it to mark with 50% hydrochloric acid.

Calcium Standard Solution

Standard calcium solution in ampoule was diluted with water to obtain 1000 ppm. Working standard solutions were subsequently prepared by serial dilution of the standard stock solution.

Magnesium Standard Solution

Standard magnesium solution in ampoule was diluted with water to give a 1000 ppm Mg^{2+} solution. Working standard solutions of Mg^{2+} were then obtained by serial dilution of the standard stock solution.

Standard Zinc Solution

Standard zinc solution (1000 ppm) was prepared by dissolving 1.2450g reagent grade zinc oxide, ZnO(BDH) in $5.0cm^3$ of water to which $25cm^3$ of 5.0 M hydrochloric acid solution was subsequently added in a 1 dm^3 graduated flask. The solution was made to mark with water and standardized by titrimetry (Vogel, 1961). Working standard solutions were prepared by serial dilution.

Lead Standard Solution

Standard solutions of lead were prepared from lead nitrate. The lead nitrate was first standardized by titration with standard solution of sodium hydroxide and disodium ethylenediamine tetracetate, EDTA (1.0×10^{-1} M) solution using methyl red indicator (Schwarzenbach, 1960).

Standardization Procedure

The Lead nitrate solution was treated with lead ammonium chloride (1.0M and $10cm^3$ for each $100cm^3$ of solution), and after adding the indicator, it was brought to pH = 5.0 with sodium hydroxide solution. Few drops of the EDTA were added and neutralization effected with standard sodium hydroxide solution. A further small amount of EDTA was added and neutralization carried out again. These operations were repeated until finally the addition of EDTA no longer caused the pH to sink below pH=5.

The amount of lead present was calculated from the volume of standard alkali required. $1.0cm^3$ of 1.0×10^{-1}M NaOH thus corresponding to 10.36 mg of lead. From the titration results, stock solution of lead was prepared. 1.599 of lead nitrate was dissolved in $25cm^3$ of nitric acid (1% v/v) and this was made up to 1.0 dm^3 with water. Working standard solutions in the range of 0-10 ppm lead were prepared by serial dilution of the stock solution.

Sample Solution

1.0 x 10^{-2}g of each sample was dissolved with 3-drops of concentrated nitric acid, transferred to a 50cm^3 graduated flask and made to the mark with water. 2.0cm^3 of the solution was transferred to a 10cm^3 graduated flask to which 5.0cm^3 of Lanthanum solution was added to suppress interference by phosphate ions.

Instrument Used

A Pye Unicam SP 1900 atomic absorption spectrometer equipped with a pre-mixed chamber and burner head suitable for air-acetylene flame was used. Radiation sources were hollow cathode lamps of the element being determined.

Instrumental Conditions

(i) Calcium

Wavelength	-	422.67 nm
Flame	-	Air/acetylene
Slit setting	-	0.15 mm
Air-flow rate	-	5.0 dm^3 min^{-1}
Acetylene flow rate	-	1dm^3 min^{-1}
Lamp current	-	7.0 mA
Sensitivity	-	526

(ii) Magnesium

Same as for calcium except for energy source and;

Wavelength	-	285.2 nm
Lamp current	-	3.0 mA
Sensitivity	-	450

(iii) Zinc

Wavelength	-	213.86 nm
Flame	-	Air/acetylene
Slit setting	-	0.15 mm
Air-flow rate	-	5.0 dm^3 min^{-1}
Acetylene flow rate	-	1dm^3 min^{-1}
Lamp current	-	7.0 mA

(iv) Lead

Wavelength	-	217.67 onm
Flame	-	Air/acetylene
Slit setting	-	0.15 mm
Air-flow rate	-	5.0 dm^3 min^{-1}
Lamp current	-	8.0 mA
Acetylene flow rate	-	1.0dm^3 min^{-1}

Procedure

All instrumental conditions were adjusted and the hollow cathode lamp (calcium hollow cathode lamp for calcium determination, Mg lamp for magnesium, and Pb lamp for lead determination) was set and allowed to stabilize.

The standard and sample solutions were each treated

with 5cm^3 of the 10% lanthanum solution. (Bigi et al., 1980). The standard solutions were then aspirated into the flame. The absorption intensities were measured and used to prepare a calibrated curve.

Sample solutions were subsequently aspirated into the flame and their absorption intensities obtained. The corresponding concentration of each cation was read off from the appropriate calibration curve.

3.2.8.3 Infra-red Absorption Analysis

For infra-red absorption analyses, about 1.0mg of each powdered sample was mixed intimately with 300 mg of potassium bromide (infra-red grade) and pelleted under vacuum. The pellets were analysed using a Pye Unicam Model SP 1100 infra-red spectrophotometer.

Instrumental Conditions

Baseline	-	0
Expansion	-	1.0
Range	-	4000 - 400cm^{-1}
Slit	-	Normal

3.1.9 X-ray Powder Diffraction Analysis

X-ray powder diffraction patterns of calcium-magnesium hydroxyapatite were taken using a Philips Powder Diffractometer with Nickel-filtered Copper-α radiation at the Centre for Energy Research, Ahmadu Bello University, Zaria.

3.2.9.1 Instrumental Conditions

Radiation..... Cu, Kx, Ni-filtered (45KV, 30mA).

Divergent slit ..... 0.5°

Receiving slit..... 0.1 mm

Scattering slit ..... 0.5°

Step width..... 0.03 (2θ)

Count time ..... 30 seconds each step

2θ range ..... 8 - 80°

Temperature ..... Room temperature.

3.3 Results

The results of the atomic absorption spectrometry, colorimetric and infra-red spectrophotometer for calcium-magnesium hydroxyapatites are shown in table 3.1. In table 3.2, the expected and observed contents of calcium, magnesium and phosphorus are compared. The main products of the interaction between Mg^{2+} and calcium hydroxyapatite are compared with those reported by other workers at various pH values in table 3.3. The X-ray Powder

diffraction patterns of calcium hydroxyapatite and some solid solutions of calcium-magnesium hydroxyapatite are shown in figure 3.2. The spectrum for magnesium hydroxyapatite $Mg_{10}(PO_4)_6(OH)_2$ obtained under similar conditions is shown in figure 3.2. The infra-red frequencies are reported in table 3.1. They range from 1040 to 1100cm^{-1} attributable to the PO_4 group and 3400 to 3440cm^{-1} corresponding to the OH group. The variation of the infra-red frequencies for the calcium-magnesium solid solutions with atom % magnesium is linear within experimental error (Figure 3.1). The equations of the lines are shown in the legend to the figure.

The amount (weight percent) of calcium, zinc and phosphorus determined in the calcium-zinc hydroxyapatites are shown in table 3.4 for reactions done in aqueous ammonia solution (pH = 10.5) and in table 3.4 for reactions carried without the addition of ammonia solutions (pH 5-6). The expected and observed cationic concentrations and phosphorus contents of the apatite samples are compared in tables 3.6 and 3.7 for reactions in basic and acidic media respectively. The mole-atom ratios for the samples are contained in tables 3.4 and 3.6. The infra-red absorption bands for samples prepared in basic medium (Zn_{100}; $Zn_{80}Ca_{20}$; $Zn_{40}Ca_{60}$ and Ca_{100}) are shown in figure 3.6. These range from 630 to 640 cm^{-1}, corresponding to the OH librational mode; 1040 to 1100 cm^{-1} corresponding to the PO_4 group and 3420 to 3440 cm^{-1} attributable to the OH

stretching mode.

The results of the Chemical analyses for the calcium-lead hydroxyapatite solid solution obtained by solid state reaction are shown in table 3.8. The solid state reaction of mixtures of lead and calcium hydroxyapatite at 900°C gave solid solution in the entire compositional range. The infra-red frequencies are also contained in table 3.8. These range from 3560 to 3572 cm^{-1} corresponding to OH stretching mode, V_4, and the other two, 940 to 962 cm^{-1} and 1050 to 1090 cm^{-1} attributable to the V_1 (PO_4) and V_3 (PO_4) respectively.

The variation of the infra-red frequencies for the calcium-zinc hydroxyapatite solid solutions with the zinc concentrations expressed as zinc atom percent is shown in figures 3.4 and 3.5 for basic and acidic media respectively. The variation of infra-red frequencies of calcium-lead hydroxyapatite solid solutions with the lead concentration expressed as atom percent is shown in figure 3.8. The plots are linear within experimental error as shown by the equation of the lines in figure 3.8. The infra-red absorption bands for lead-calcium hydroxyapatites are shown in figure 3.9. Table 3.10 contains the lattice parameters of lead-calcium hydroxyapatite solid solutions. The variation of the lattice constants with atom % lead is shown in figure 3.10

Table 3.1 Calcium, Magnesium and Phosphorus Contents (Weight Percent) of Calcium-magnesium Solid Solutions Precipitated from Aqueous Ammonia Solution (pH = 12) and Their Infra-red (I.R) Frequencies

Mg Content (atom %)	Weight (%) Ca	Mg	P	Molecular Formula	Mole-Atom Ratio Ca+Mg/P	I.R Frequencies (cm^{-1}) $V_3(PO_4)$	V_4 (OH)
0	40.13	-	18.50	$Ca_{10}(PO_4)_6(OH)_2$	1.67	1100	3440
20	32.95	4.82	18.97	$Ca_{8.01}Mg_{1.95}(PO_4)_6(OH)_2$	1.65	1080	3425
40	25.70	9.87	19.66	$Ca_{8.05}Mg_{3.82}(PO_4)_6(OH)_2$	1.65	1080	3420
50	21.35	12.40	19.89	$Ca_{4.94}Mg_{4.72}$	1.61	1050	3400
60	17.34	16.13	20.26	$Ca_{3.946}Mg_{6.04}(PO_4)_6(OH)_2$	1.66	1060	3400
100	-	27.84	21.77	$Mg_{9.70}(PO_4)_6(OH)_6$	1.62	1040	3400

Table 3.2 Expected[e] and Observed Calcium, Magnesium and Phosphorus Contents (Weight Percent) of Calcium-magnesium Hydroxyapatite Precipitated from Aqueous Ammonia Solution (pH=12) Based on the Molecular Formula, $Ca_{10-x}Mg_x(PO_4)_6(OH)_2$

Ca[o]	Ca[e]	Mg[o]	Mg[e]	P[o]	P[e]
40.13	39.88	-	-	18.50	18.51
32.95	32.93	4.82	4.94	18.97	19.11
25.70	25.50	9.87	10.33	19.66	19.75
21.35	21.60	12.40	13.14	19.89	20.08
17.34	17.59	16.13	16.03	20.26	20.43
-	-	27.45	28.70	21.77	21.94

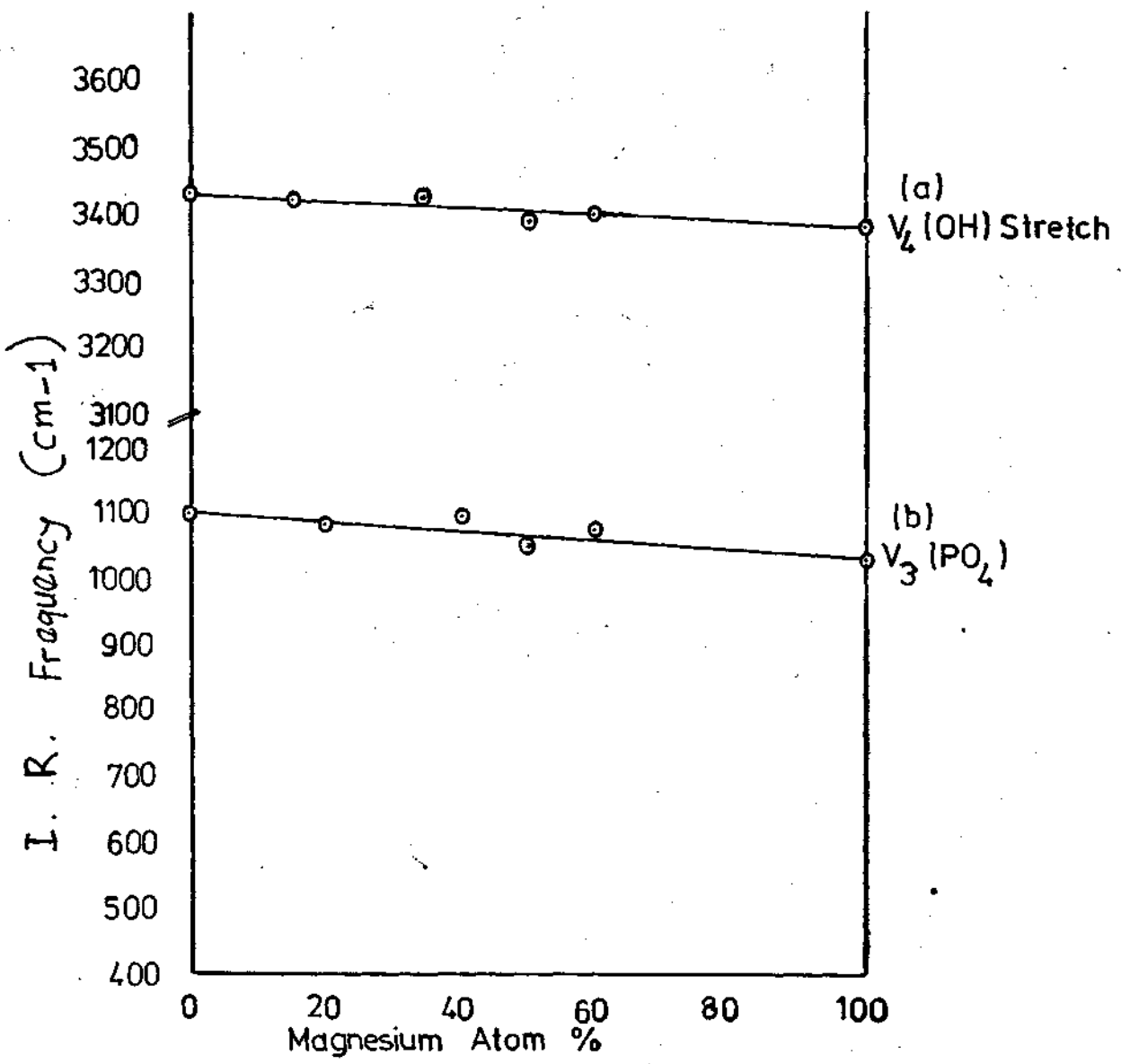


Fig 3.1

Infra-red frequencies for calcium-magnesium hydroxyapatite solid solution against magnesium atom %

Equations for the lines:

(a) $y = 3433.3 - 0.42x$ ($n=6$, $\sigma = 0.13$)

(b) $y = 1095.2 - 0.6x$ ($n=6$, $\sigma = 0.6$)

(y = infra-red frequency; x = atom % magnesium; σ = standard deviation)

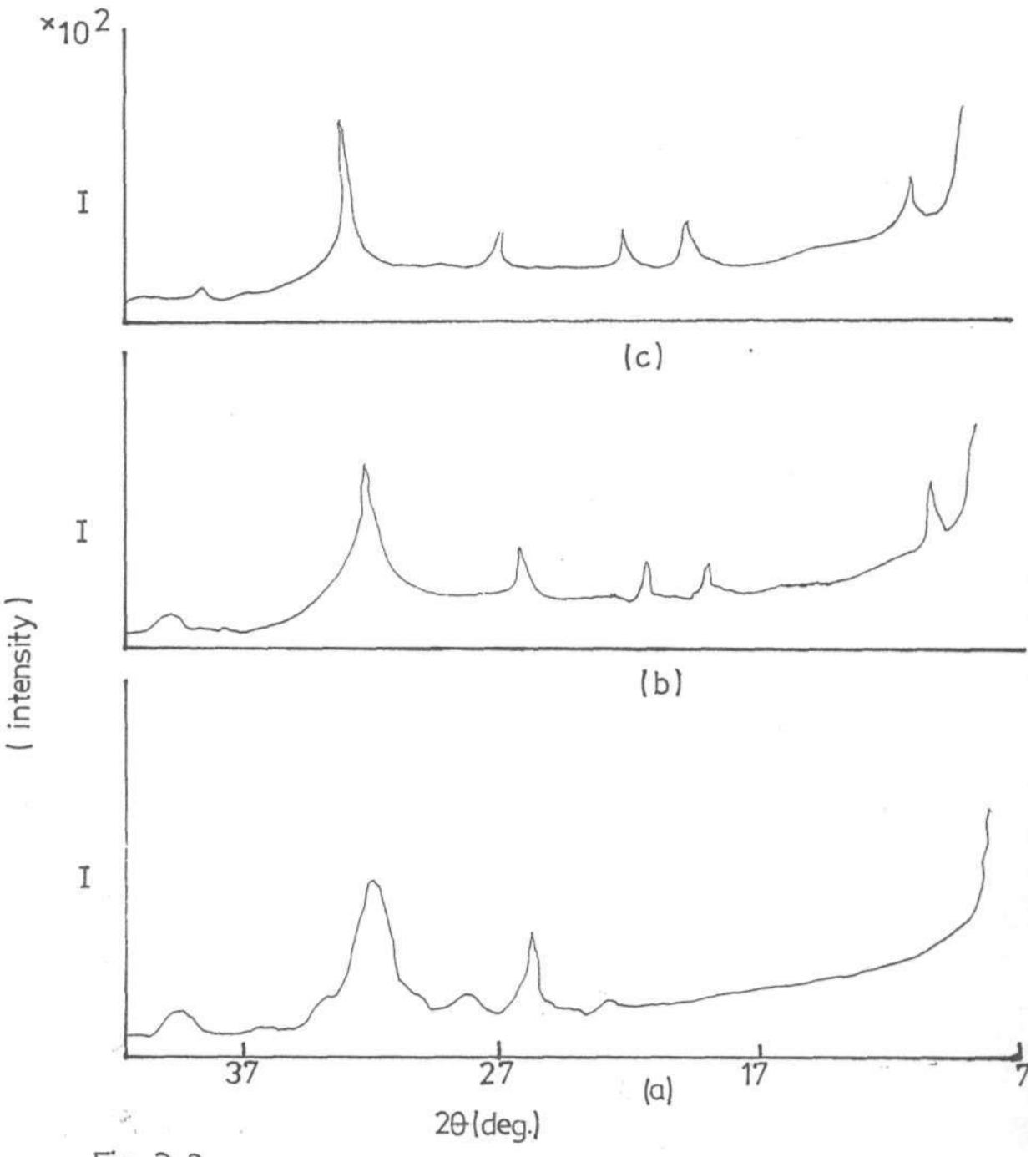


Fig. 3.2

X-ray powder diffraction pattern of (a) Calcium hydroxyapatite $Ca_5(PO4)_3OH$ (b) $Ca_{2.5}Mg_{2.5}(PO4)_3OH$ and (c) $Ca_2Mg_3(PO4)_3OH$

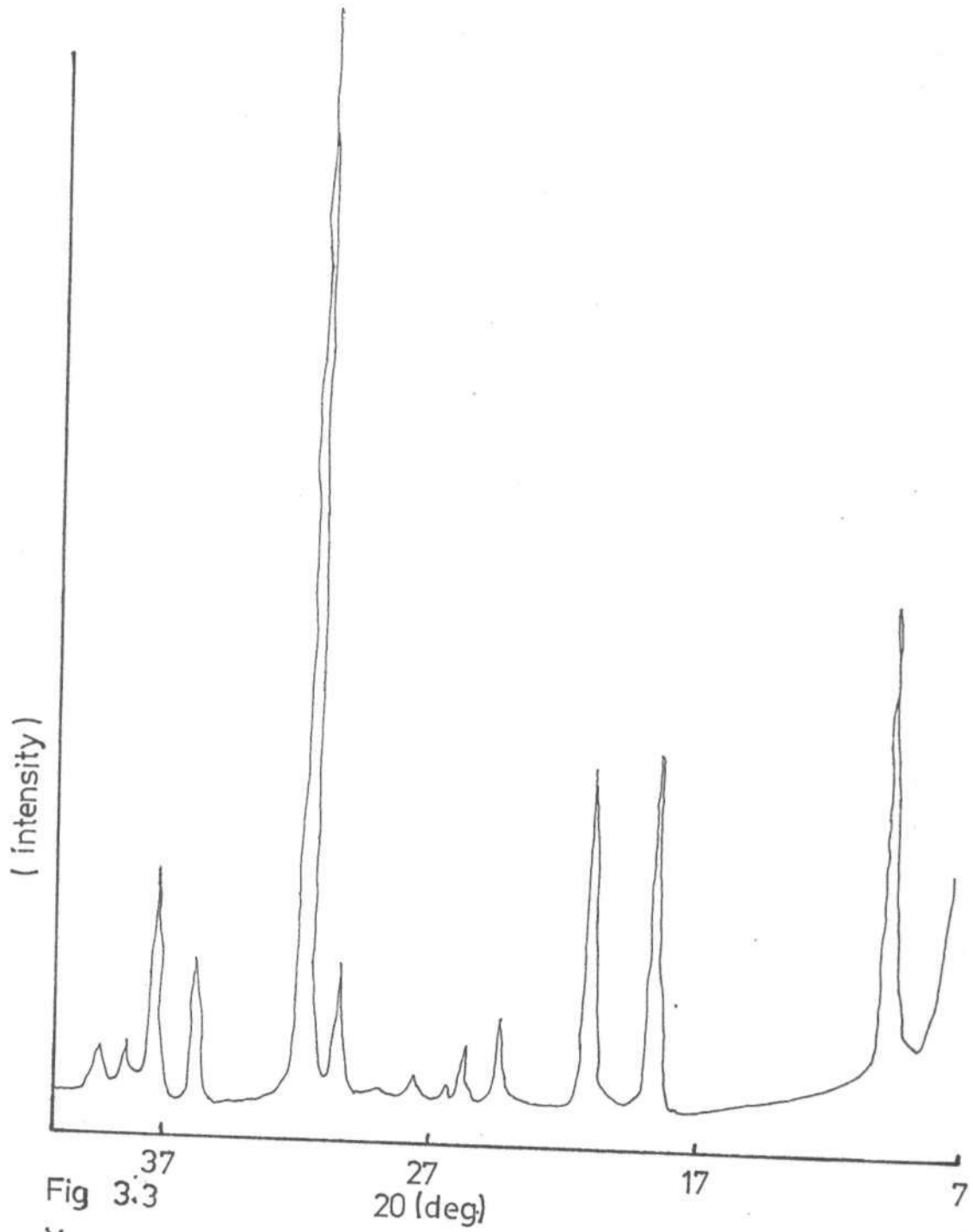


Fig 3.3 X-ray powder diffraction pattern of $Mg_5 (PO4)_3 OH$.

Table 3.3 Some Literature Reports on the Interaction of Magnesium with Calcium Hydroxyapatite in Aqueous Medium

pH of Mediating Solution	$\frac{[Mg^{2+}]}{[Ca^{2+}]}$%	Main Product	Reference
< 7	10/90	tcp	Legeros et al., 1980
< 7	15/85	tcp	Legeros et al., 1980
7 - 9	30/70	Acp	Legeros et al., 1964
7 - 9	50/50	Acp	Legeros et al., 1964
7 - 9	>25/<75	tcp to Acp	Gazzano, M. 1988
12	complete range	hydroxyapatite	this work
> 9	complete range	hydroxyapatite	Patel, 1979
> 9	complete range	hydroxyapatite	Chiranjeevirao et al 1982

tcp = tricalcium phosphate or derivatives containing some magnesium
Acp = Amorphous calcium phosphate Hydroxyapatite includes solid solutions of calcium-magnesium apatite.

Table 3.4 Calcium, Zinc and Phosphorus Contents (Weight Percent) of Calcium-Zinc Hydroxyapatite Solid Solutions Precipitated from Aqueous Ammonia Solution (pH = 10.5) and their Infra-red (I.R) Frequencies.

Zn Content (atom %)	Weight (%) Zn	Ca	P	Molecular Formula	Mole-Atom Ratio Zn+Ca/P	I.R Frequencies (cm^{-1}) $V_3(PO_4)$	$V_1(OH)$	$V_4(OH)$
100	51.86	-	14.10	$Zn_{9.61}(PO_4)_6(OH)_2$	1.66	1070	630	3540
						*1070	*625	*3540
80	43.25	6.28	14.95	$Zn_{7.99}Ca_{1.99}(PO_4)_6(OH)_2$	1.65	1070	630	3545
60	33.88	13.69	15.85	$Zn_{5.99}Ca_{3.95}(PO_4)_6(OH)_2$	1.66	1075	630	3550
50	28.86	17.57	15.90	$Zn_{4.99}Ca_{4.95}(PO_4)_6(OH)_2$	1.66	1080	638	3560
40	23.40	21.80	16.37	$Zn_{3.96}Ca_{6.01}(PO_4)_6(OH)_2$	1.66	1080	638	3565
0	-	39.79	18.41	$Ca_{9.93}(PO_4)_6(OH)_2$	1.67	1095	640	3570
						*1100	*640	*3575

* Infra-red frequency for sample at 500°C

Table 3.5

Expected [e] and Observed [o] Calcium, Zinc and Phosphorus Contents (Weight Percent) of Calcium-Zinc Hydroxyapatite Solid Solutions Precipitated from Aqueous Ammonia (pH = 10.5) Based on the Molecular Formula, $Ca_{10-x}Zn_x(PO_4)_6(OH)_2$

Zn[o]	Zn[e]	Ca[o]	Ca[e]	P[o]	P[e]
51.86	51.98	-	-	14.10	14.78
43.25	43.33	6.28	6.64	14.95	15.40
33.88	33.92	13.69	13.86	15.85	16.07
28.86	28.90	17.57	17.72	15.90	16.43
23.40	23.65	21.80	21.75	16.37	16.80
-	-	39.79	39.85	18.41	18.50

Table 3.6

Calcium, Zinc and Phosphorus Contents (Weight Percent) of Calcium-Zinc Hydroxyapatite Precipitated from Acidic Medium and Their Infra-red (I.R) Frequencies

Zinc (Atom %)	Weight (%) Zn	Ca	P	Molecular Formula	Mole-Atom Ratio	I.R Frequencies (cm-1) $V_3(PO_4)$	$V_4(OH)$	$V_1(OH)$
0	0	39.64	17.80	$Zn_{9.95}(PO_4)_6(OH)_2$	1.66	1095	640	3570
40	23.75	21.72	16.38	$Zn_{4.02}Ca_{5.99}(PO_4)_6(OH)_2$	1.67	1080	635	3565
50	28.20	17.65	16.01	$Zn_{4.88}Ca_{4.98}(PO_4)_6(OH)_2$	1.65	-	-	-
60	34.00	13.18	12.21	$Zn_{6.01}Ca_{3.8}(PO_4)_6(OH)_2$	1.64	1068	635	3560
80	42.50	6.60	14.69	$Zn_{7.85}Ca_{1.99}(PO_4)_6(OH)_2$	1.64	1060	630	3560
100	49.85	0	14.52	$Zn_{9.59}(PO_4)_6(OH)_2$	1.60	1050	630	3558

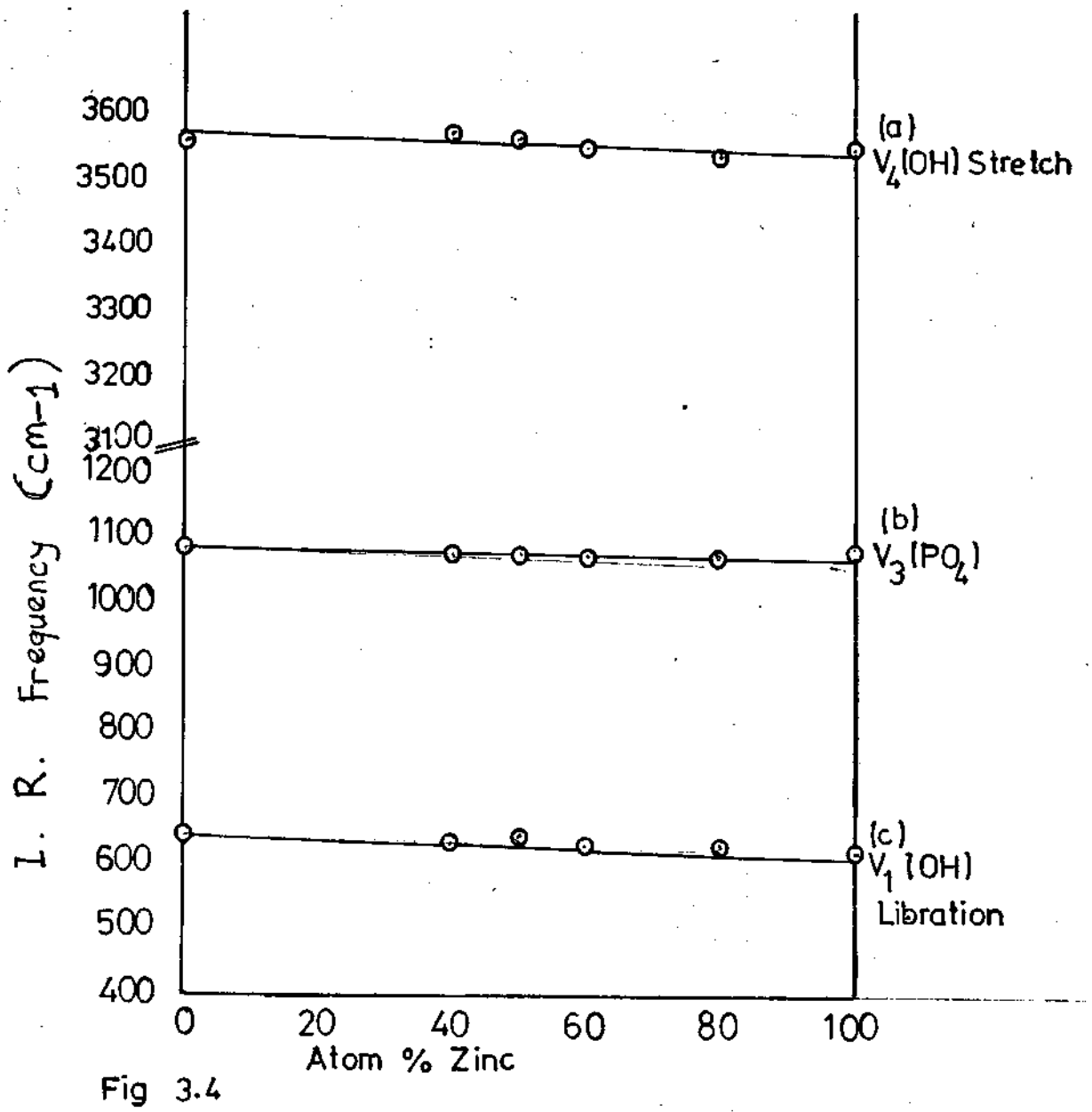


Fig 3.4

Infra-red frequencies for calcium-zinc hydroxyapatite solid solutions against Atom % zinc

(Basic medium, PH = 10.5)

Equations for the lines:

(a) $y = 3573 - 0.33x$ ($n = 6, \sigma = 1.31$)

(b) $y = 1092.70 - 0.26x$ ($n = 6, \sigma = 4.69$

(c) $y = 640.90 - 0.12x$ ($n = 6, \sigma = 2.22$

(y = infra-red frequency; x = atom% zinc; σ = standard deviation)

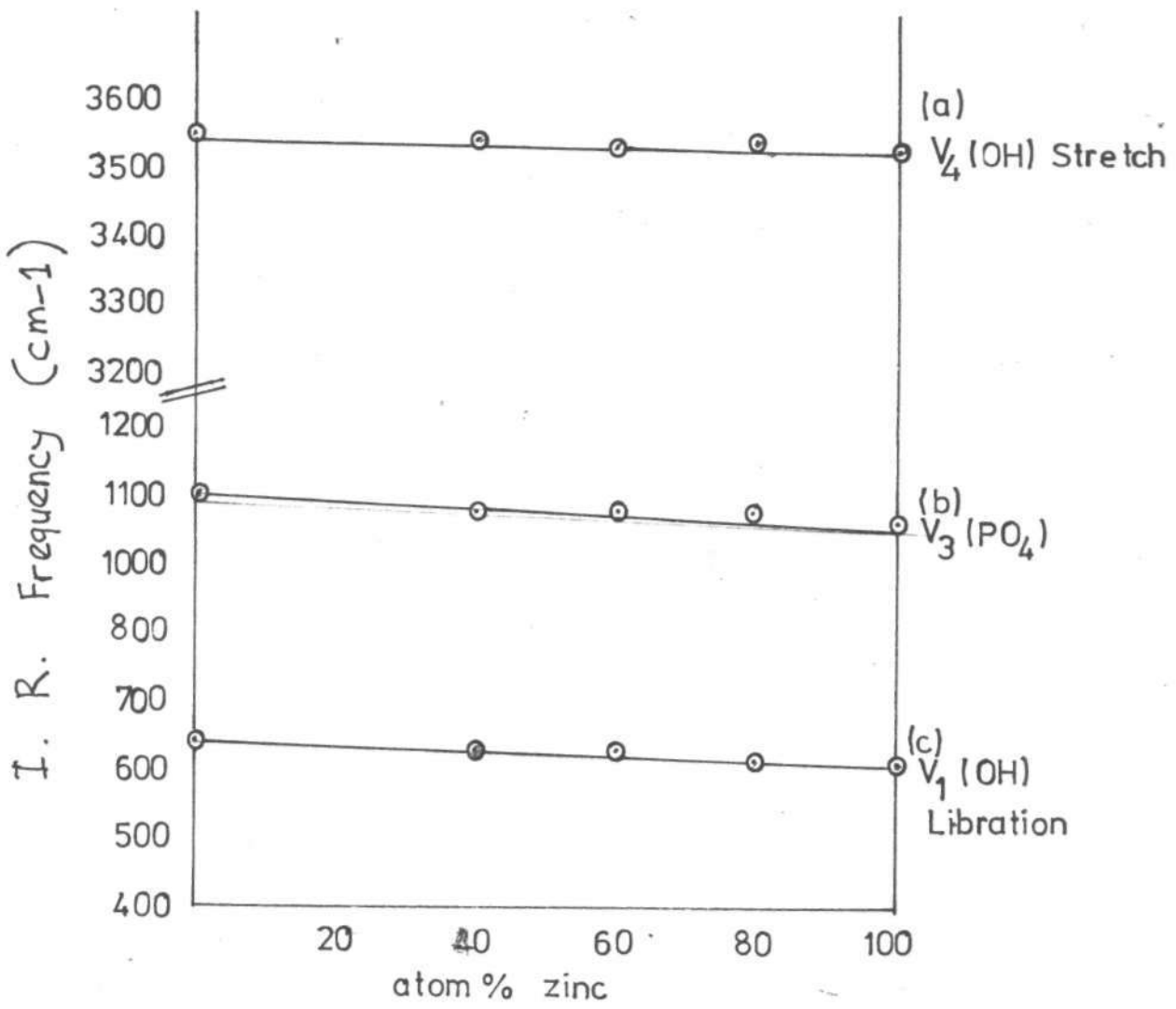


Fig 3.5

Infra-red frequencies for calcium—zinc hydroxyapatite solid solutions against atom % zinc

(Acidic medium, PH 5-6)

Equations for the lines:

(a) $y = 3569.50 - 0.12x$ ($n = 5$, $\sigma = 1.31$)

(b) $y = 1095.80 - 0.4x$ ($n = 5$, $\sigma = 2.63$)

(c) $y = 639.86 - 0.10x$ ($n = 5$, $\sigma = 1.31$)

(y = infra-red frequency; x = atom % zinc; σ = standard deviation)

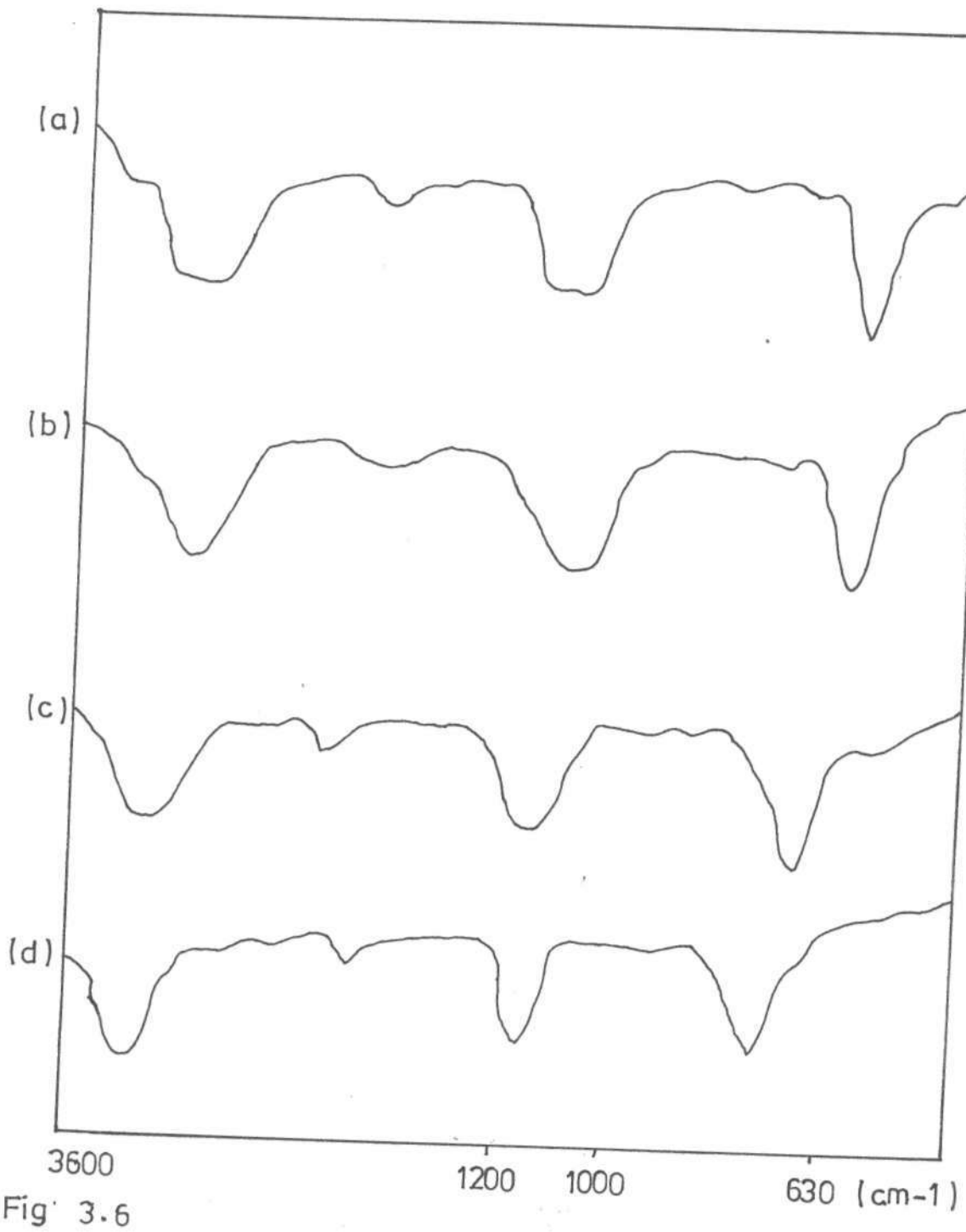


Fig 3.6

Infra-red absorption spectra for calcium-zinc hydroxyapatite solid solutions. (a) Zn_{100}; (b) Zn_{80} Ca_{20} (c) Zn_{40} Ca_{60} and (d) Ca_{100}.

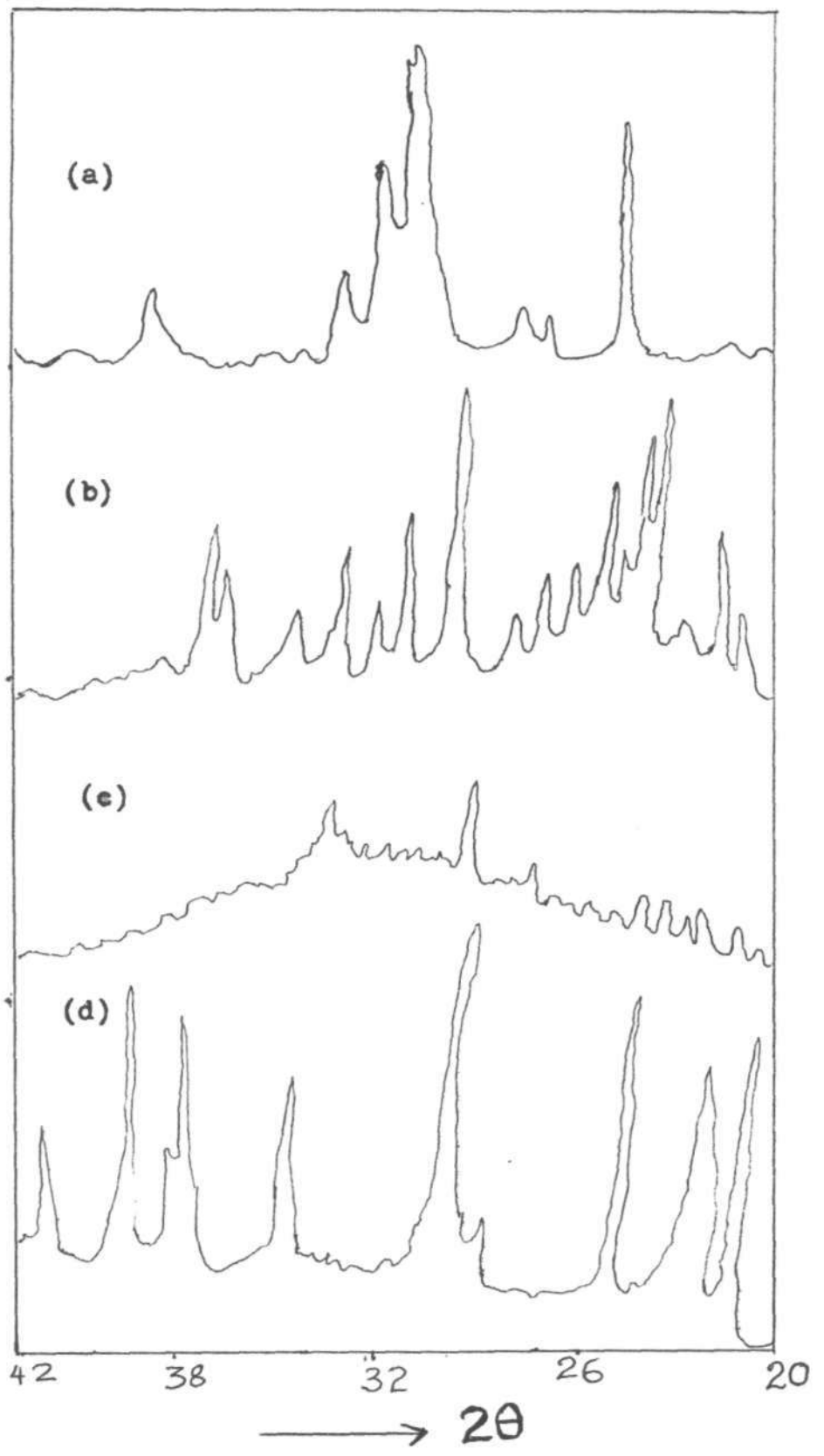


Fig. 3.7

X-ray Powder diffraction Pattern of
(a) Calcium hydroxyapatite (Ca100)
(b) Zn80Ca20 Predominantly $Ca_2Zn_2(PO_4)_2$ and $Zn_2P_2O_7$
(c) Zn50Ca50 Completely amorpheus.
(d) Zn100 Predominantly $Zn_2P_2O_7$

Table 3.7

Expected [e] and Observed [o] Calcium, Zinc and Phosphorus Contents (Weight Percent) of Calcium-Zinc Hydroxyapatite Precipitated from Acidic Medium Based on the Molecular Formula, $Ca_{10-x}Zn_x(PO_4)_6(OH)_2$

Zn[o]	Zn[e]	Ca[o]	Ca[e]	P[o]	P[e]
49.85	51.98	-	-	14.52	14.78
42.50	43.33	6.60	6.64	14.69	15.40
34.00	33.92	13.18	13.86	15.21	16.07
28.20	28.90	17.65	17.72	16.01	16.43
23.75	23.65	21.72	21.75	16.38	16.80
-	-	39.64	39.85	17.80	18.50

Table 3.8 Calcium, Lead and Phosphorus Contents (Weight Percent) of Calcium-lead Hydroxyapatite Prepared by Solid State Reaction at 900°C and Their Infra-red (I.R.) Frequencies

Zinc (Atom %)	Weight (%) Pb	Ca	P	Molecular Formula	Mole-Atom Ratio	I.R Frequencies (cm^{-1}) $V_4(PO_4)$	$V_3(PO_4)$	$V_1(PO_4)$
0	-	39.84	17.80	$Ca_{9.99}(PO_4)_6(OH)_2$	1.67	3572	1090	962
20	31.00	24.10	13.84	$Ca_{7.96}Pb_{2.02}(PO_4)_6(OH)_2$	1.66	3570	1082	955
45	52.90	12.50	10.45	$Ca_{5.48}Pb_{4.49}(PO_4)_6(OH)_2$	1.66	3565	1070	948
65	64.42	6.66	8.80	$Ca_{3.48}Pb_{6.5}(PO_4)_6(OH)_2$	1.66	3560	1060	945
80	70.70	3.38	7.75	$Ca_{1.98}Pb_{7.99}(PO_4)_6(OH)_2$	1.66	3560	1050	940

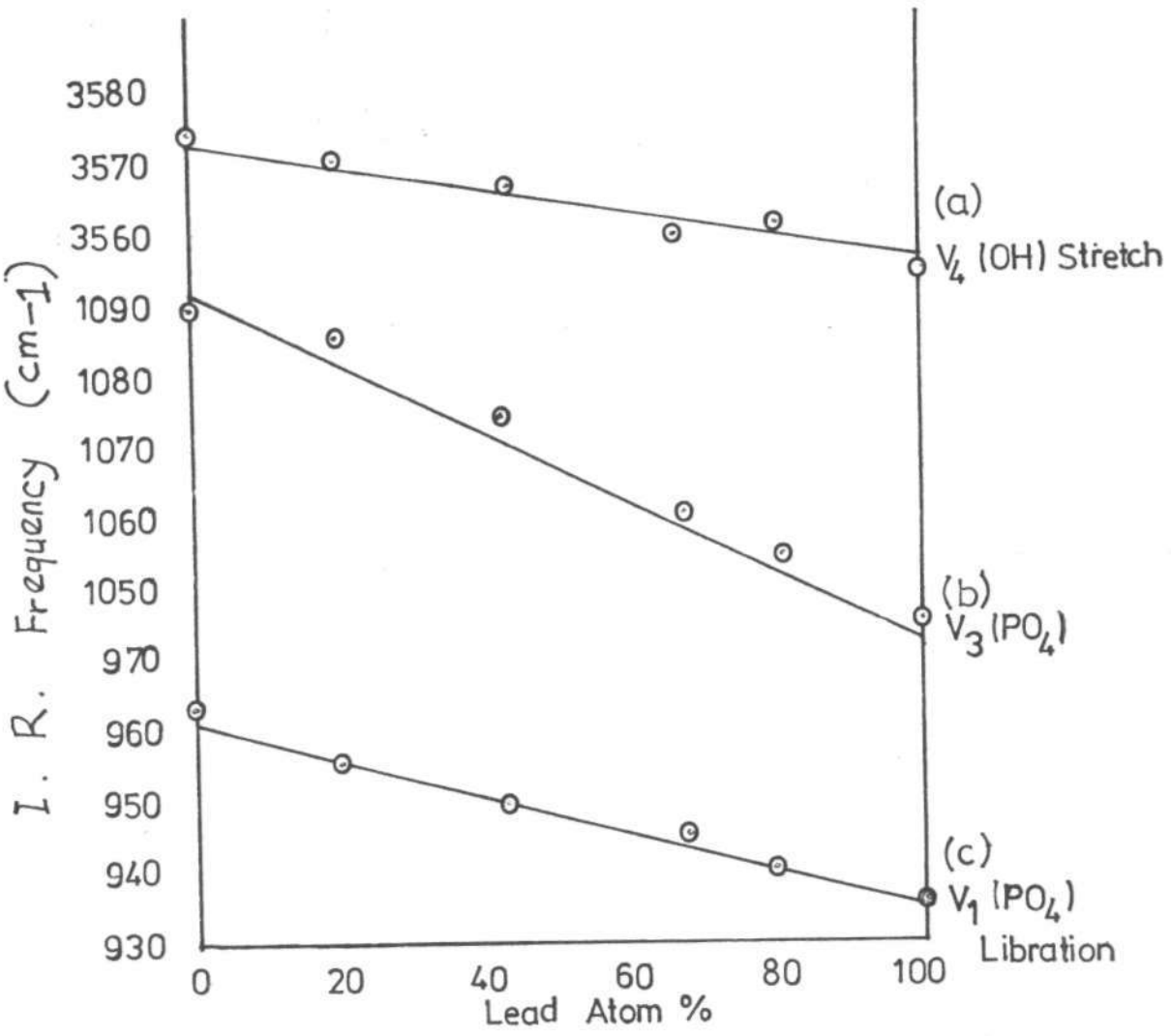


Fig 3.8

Infra-red frequencies for calcium–lead hydroxyapatite solid solutions against atom % of lead.
(solid state synthesis)

Equations for the lines:

(a) $y = 3572.04 - 0.16x$ ($n=6$, $\sigma = 1.87$)

(b) $y = 1091.20 - 0.5x$ ($n=6$, $\sigma = 1.33$)

(c) $y = 961.07 - 0.26x$ ($n=6$, $\sigma = 1.44$)

(y = infra-red frequency; x = atom % lead; σ = standard deviation)

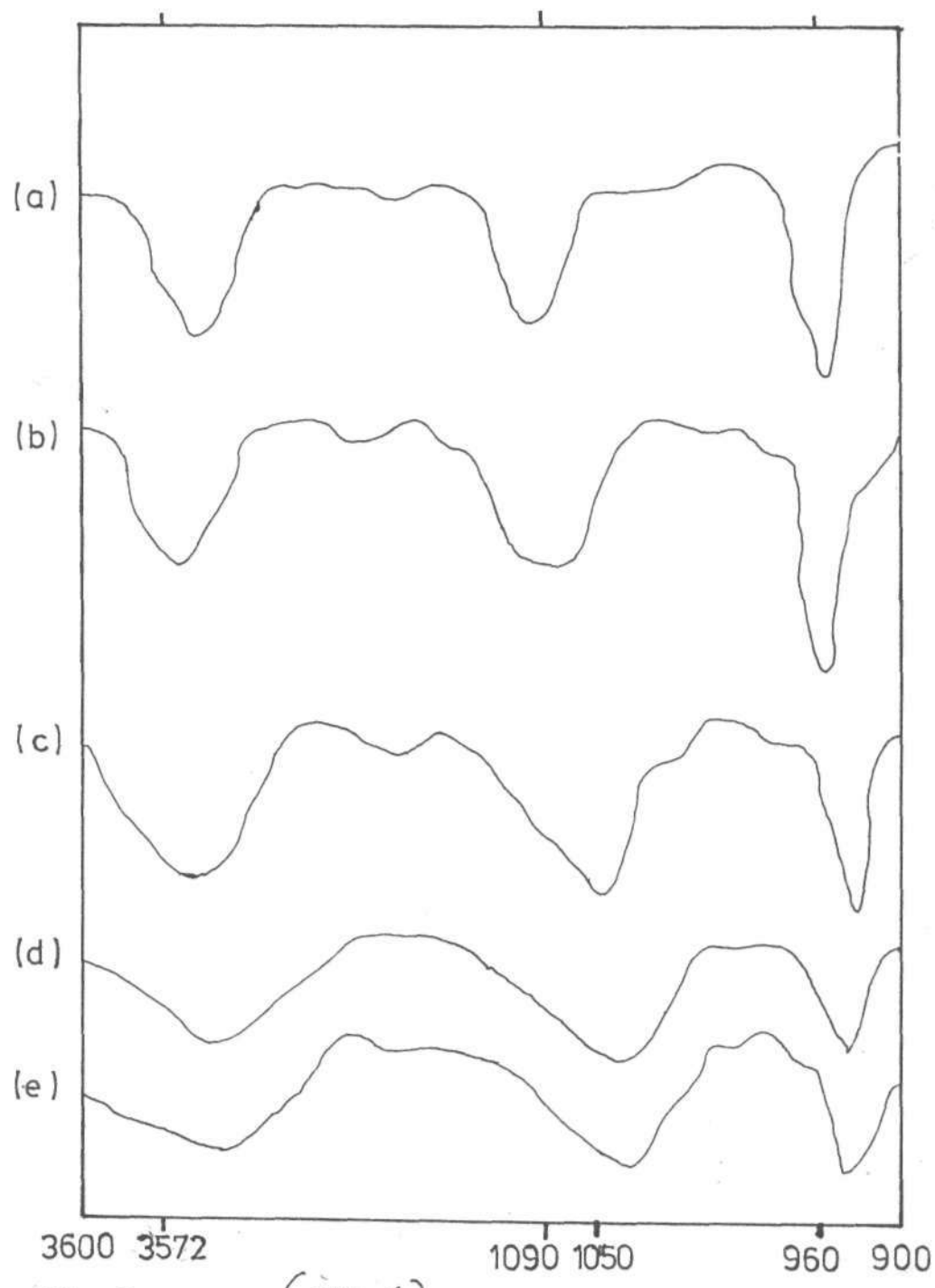


Fig. 3.9

Infra-red absorption spectra for calcium-lead hydroxyapatite solid solutions.

(a) $Pb_0\ Ca_{100}$ (b) $Pb_{20}\ Ca_{80}$; (c) $Pb_{45}\ Ca_{55}$; (d) $Pb_{60}\ Ca_{35}$. and (e) $Pb_{80}\ Ca_{20}$.

Table 3.9

Expected[e] and Observed[o] Contents (Weight Percent) of Lead,Calcium and Phosphorus in Calcium-lead Hydroxyapatite Prepared by Solid State Reaction at 900°C based on the Molecular Formula, $Ca_{10-x}Pb_x(PO_4)_6(OH)_2$

Pb Atom %	Pb[o]	Pb[e]	Ca[o]	Ca[e]	P[o]	P[e]
0	-	-	39.64	39.85	17.80	18.50
20	31.00	31.15	24.10	23.85	13.84	13.86
45	52.90	53.06	12.50	12.53	10.45	10.60
65	64.42	64.39	6.66	6.70	8.80	8.90
80	70.70	70.77	3.38	3.42	7.75	7.95

Table 3.10 Lattice Constants of Lead-calcium Hydroxyapatite Solid Solutions Synthesized by Solid State Reaction

Lead Content (Atom %)	Lattice Constants a(Å)	c(Å)
0	9.42	6.88
20	9.49	6.95
45	9.61	7.08
65	9.70	7.17
80	9.77	7.32
100	9.82	7.40

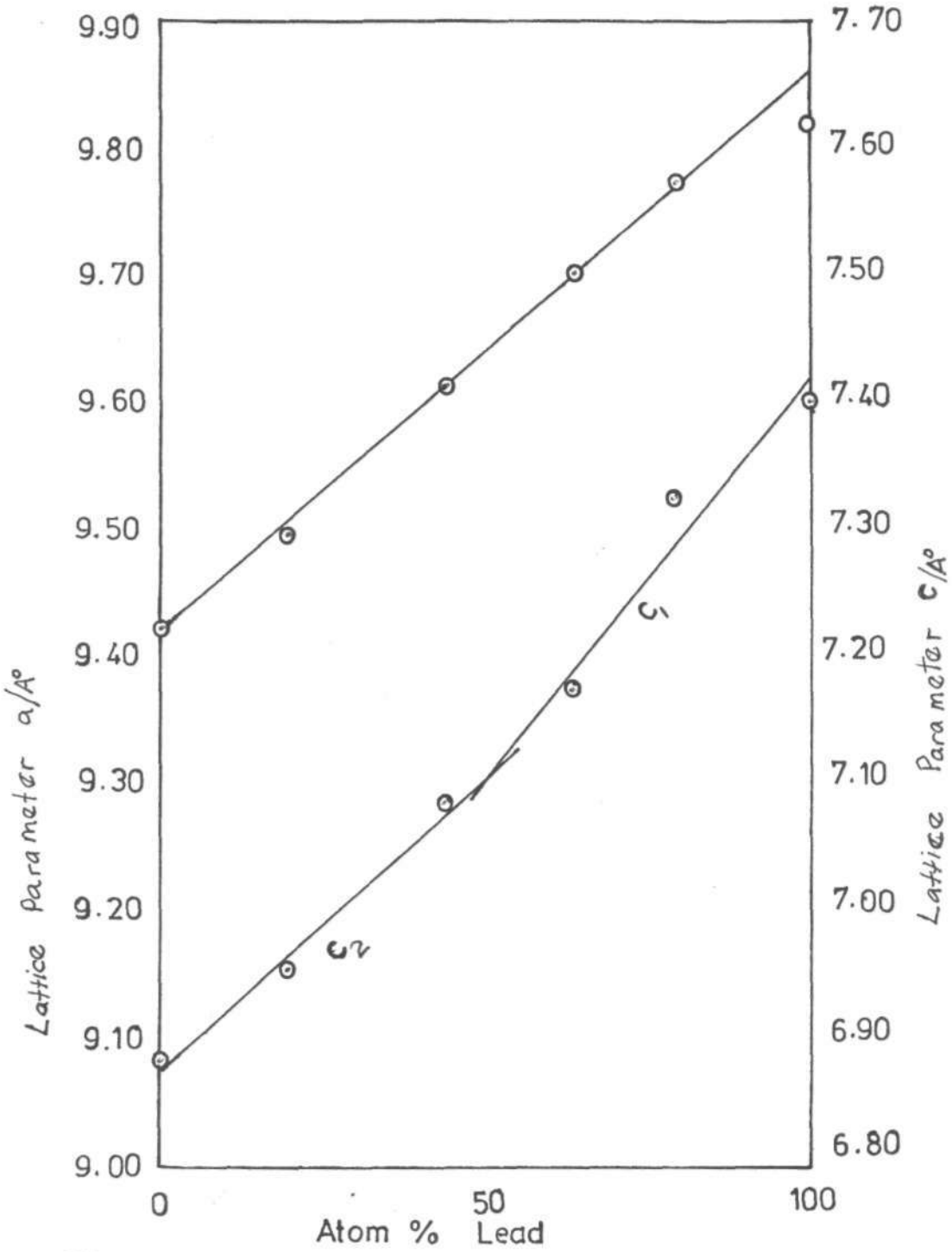


Fig 3.10

Lattice constants for Lead-calcium hydroxyapatite solid solutions against atom % Lead

Equations for the lines:

(a) $y = 9.41 + 0.005x$ $(n = 6, \sigma = 0.004)$

(c_1) $y = 6.87 + 0.005x$ $(n = 6, \sigma = 0.002)$

(c_2) $y = 6\ 71 + 0.008x$ $(n = 6, \sigma = 0.004)$

(Y = Lattice constant ; X = atom % lead; σ = standard deviation)

3.4 Discussion

The analytical data (tables 3.1 and 3.2) show that the concentration of magnesium in the solid solution is generally slightly less than the concentration in the mediating solution. The same applies to the concentrations of zinc in the calcium-zinc hydroxyapatites (tables 3.4 and 3.6). A similar observation has also been reported for the interaction of barium with calcium hydroxyapatite in aqueous medium (Bigi et al., 1984). However, the amount of magnesium rejected at this pH in each case is less than that rejected in the case of barium. Such differences may be ascribed to the loss of magnesium as the acid phosphate, the formation of which is probably encouraged in an acidic medium (Rathje, 1941 as quoted by Narasaraju et al., 1972). However, the amount of zinc rejected by the calcium-zinc solid solution (0.12 to 0.63%) is smaller than the amount of magnesium rejected by the calcium-magnesium hydroxyapatite. This also indicates a smaller rejection of added cation compared to that reported by Bigi et al., (1984) for barium. This may be due to the nature of the mediating solution which is basic for the calcium-magnesium and calcium-zinc but acidic for the calcium-barium system. Another possible reason for the observed cation rejection trend is the closer ionic sizes

of Zn^{2+} and Ca^{2+} which are respectively, 0.74Å and 0.99Å (Mg^{2+} = 0.65Å; Ba^{2+} = 1.35Å).

In the case of calcium-lead hydroxyapatite solid solutions prepared by solid state reactions, the concentration of lead in the solid solution did not show any significant deviation from that contained in the calcium-lead hydroxyapatite (table 3.8). It shows that greater amount of lead is incorporated in the apatite lattice than magnesium. Bigi et al., (1984) also reported smaller acceptance of barium for calcium-barium hydroxyapatite in aqueous medium. This observation is in agreement with the findings by Fowler (1974). He reported that the stoichiometry and purity of solid state apatite preparations are limited, primarily, only by the purity of the starting materials. In addition, if sufficient time is allowed for thermal diffusion for reaction completion, there is no volatilization of essential components during ignition. The observation may also be attributed to the high atomic mass of lead and the proximity of the apatitic channels which favours ionic exchange (Bigi et al., 1991).

The infra-red absorption spectra of the samples show that the V_3 frequencies attributable to the PO_4 group and the V_1 frequencies corresponding to the OH stretch are shifted to lower frequencies as the concentration of the substituting cation increases (Figure 3.1, 3.4, 3.5 and 3.8). This observation is in agreement with that reported by Patel, (1979). The shift of the V_3 of PO_4 group to

lower frequencies may be attributed to the effects of binding energy and atomic mass (Klee and Engel, 1970; Patel, 1979). This may be explained on the basis of the Barnes equation (1944). According to the equation, the vibrational frequencies depend on the mass of the participating atoms and restoring forces between the atoms. If the equilibrium distance between the positive and the negative atoms of the molecule is increased, the restoring force, **k**, generally increases. Since the equilibrium distance depends on the ionic radii of the participating atoms in the molecule, it may be inferred that when Ca^{2+} is replaced with an ion like Mg^{2+}, Zn^{2+} or Pb^{2+}, a stronger coordination of the PO_4 group to the substituting cation through oxygen should occur. Consequently, the phosphorus-oxygen bond (P-O), is weakened and thus causing the lowering of the frequency which is observed. The shift of the infra-red frequencies of the PO_4 internal modes to lower values may also be attributed to the smaller cationic size of Mg^{2+} and Zn^{2+} (ionic radii for Mg^{2+} = 0.65; Zn^{2+} = 0.74A°) and the tendency of Pb^{2+} towards covalent bonding. According to Fowler (1974), the shift of the OH band to lower frequencies is due to OH bonding.

The solid solutions of calcium-zinc and calcium magnesium hydroxyapatite gave more intense and sharper infra-red absorption bands at 500°C (table 3.2) which is in agreement with the report of Baravelli et al., (1984) for calcium hydroxyapatite.

The frequencies of the vibrational modes for the calcium-magnesium, and calcium lead hydroxyapatite samples gave values which varied almost linearly with the atom % of each substituting cation (figures 3.1, 3.4, 3.5, 3.6 and 3.8) in the whole composition range. This suggests that solid solutions have been formed in the whole series and that the preparations are not mixtures of two components or one component with adsorbed materials (Patel, 1979; Bigi et al., 1984; Bigi et al., 1991; Collin, 1959; Partington, 1957). The variation of infra-red frequencies of Ca-Zn solid solutions tend to show that zinc replaced calcium in the whole composition range. However, the x-ray powder diffraction results (figure 3.7) show that solid solution of Ca-Zn hydroxyapatites are not obtained in the whole series. Though there is peak enhancement in the x-ray pattern as zinc replaced calcium in the hydroxyapatite, the pyrophosphate group, $P_2O_7^{4-}$ is predominant.

The results summarised in table 3.1 are in agreement with a recent suggestion (Thomas, 1988), that the interaction of magnesium with calcium hydroxyapatite could depend on the pH of the mediating solution. Thus, table 3.3 clearly shows that the formation of either amorphous calcium phosphate (ACP) or tricalcium phosphate (TCP) in the presence of magnesium is favoured at pH values less than 9. It seems that at acidic/physiological pH, the interaction of Mg^{2+} with the apatite is a surface phenomenon. However, at alkaline pH, there is possibility

of the incorporation of Mg^{2+} into the apatite lattice. This leads to only growth sites at the apatite lattice which are blocked, and thus leading to the formation of other phases such as tricalcium phosphate and its derivatives. In the case of zinc, solid solutions of calcium-zinc hydroxyapatite were not formed in basic (pH = 10.5) and mild acidic (pH 5-6) media. In this case, the mode of interaction of Zn^{2+} with calcium hydroxyapatite is such that does not allow its incorporation into the apatite lattice in both basic and acidic media. It therefore follows that a total rationalization of isomorphous substitution of magnesium for calcium in the hydroxyapatite on the basis of cationic size only does not totally account for obtained results (Patel, 1979; Chiranjeevirao et al., 1982). A thorough understanding of the cationic morphology at various pH seems necessary in order to properly comprehend and answer the question of why isomorphous substitution of Mg^{2+} for Ca^{2+} in the hydroxyapatite takes place in the whole compositional range only in highly alkaline aqueous medium.

The x-ray powder diffraction patterns for the calcium-magnesium hydroxyapatite sample (figures 3.2 and 3.3) show that the incorporation of magnesium in the hydroxyapatite lattice produces a sharpening of the x-ray diffraction peaks and enhancement of peak intensity. This is in contrast to barium which causes peak broadening. Peak sharpening and intensity enhancement suggest that there is

an increase in crystallite size and a concomitant increase in crystallinity. This is in agreement with an earlier scanning electron microscope study (Chiranjeevirao et al., 1982) which showed large hexagonal shaped crystals for magnesium hydroxyapatite, $Mg_{10}(PO_4)_6(OH)_2$ compared to tiny crystals obtained for calcium hydroxyapatite.

The results of the x-ray powder diffraction table show that the replacement of calcium by lead in the hydroxy-apatite structure causes an expansion of the lattice parameters which is consistent with the larger ionic radius of lead (1.21A) with respect to that of calcium (0.99A). Such a dilation with the proportion of lead atom % is in agreement with those reported by Narasaraju et al., (1972), Bigi et al., (1984); Bigi et al., (1989 and 1991) and Collin (1959). The plot of cell parameters, a and c against atom % lead (figure 3.10) shows that the a-axis varies linearly with increasing lead concentration which follows the Vegard's Law (Andres-Verges et al., 1983). However, the lattice parameter shows a discontinuity at about 50 atom % lead. While these results agree with those of the researchers (Engel et al., 1975; Verbeeck et al., 1981; Andres-Verges et al., 1983), they are in disagreement with those of earlier researchers (Narasaraju et al., 1972; Rao, 1976).

The discontinuity observed for c-parameter is attributable to a preference of the Pb^{2+} ion for site (2) of the apatite structure (Bigi et al., 1989). When lead

replaces calcium in the apatite structure, it fills almost exclusively site (2), until at lead atom concentration higher than 45%, when it begins to fill site (1). The substitution of lead for calcium in site (1) provokes a greater dilation of the c-axis dimension than that induced by lead substitution in site (2).

The occupancy factors of Pb^{2+} ions on site (2) have been found to be 20.1, 42.6 and 58.4% for Pb_{20}, Pb_{45} and Pb_{80} (Bigi et al., 1989). This probably explains the discontinuity observed for the variation of the cell parameter, c, at about 50 atom percent lead.

It may therefore be concluded that the observed trends in cell parameters, infra-red absorption frequencies and the amount of lead incorporated in the hydroxyapatite can be explained on the basis of:

i) cationic size;

ii) cation-oxygen interaction; and

iii) structural differences caused by inhomogeneous distribution of lead in the two non-equivalent cation sites of the hydroxyapatite structure.

CHAPTER FOUR

ISOMORPHOUS SUBSTITUTION IN LEAD HYDROXYAPATITE (PbHA) BY CADMIUM AND BARIUM

4.1 Introduction

The replacement of calcium by lead in the hydroxyapatite has been identified as the basis for the incorporation of lead in the human skeletal system (Boyd, 1962). The replacement of Lead by a less poisonous metal is therefore considered a beneficial process to the human system. Cadmium, strontium and lead are known to replace calcium in the whole range of composition in aqueous medium (Collin, 1959; Bigi et al, 1989 and 1991; Narasaraju et al, 1972). It has also been reported that barium replaces calcium in the hydroxyapatite from 0 to 25 barium atom percent in aqueous medium while solid solutions of calcium-barium hydroxyapatite are obtained only over the range of barium concentration of 60-100 atom percent by solid state reaction (Bigi et al, 1984). The replacement of calcium in the hydroxyapatite by these cations have been explained generally on the basis of cationic sizes (Legeros et al, 1980; Patel, 1979; Collin, 1959, Bigi et al 1984; Narasaraju et al, 1972).

In the present study an attempt has been made to investigate the roles and interactions of cation smaller in size (Cd^{2+}) and that larger in size (Ba^{2+}) than Pb^{2+} ion (Table 2.1) with lead hydroxyapatite.Exchange reactions were carried out between cadmium and lead hydroxyapatite

and between barium and lead hydroxyapatite in aqueous medium. Barium hydroxyapatite was prepared by solid state reaction and then made to react with lead hydroxyapatite by solid state process at 900°C. Products obtained in both processes were analysed by crystallographic and spectroscopic methods.

4.2 Experimental

4.2.1 Preparation of Lead Hydroxyapatite

Lead hydroxyapatite was prepared as described for calcium hydroxyapatite in section 3.2.1 but using lead acetate trihydrate solution (8.0×10^{-3}M) and a pH of 10.5.

4.2.2. Preparation of Cadmium Hydroxyapatite (CdHA).

Reagents.

(i) Cadmium acetate solution

A 8.0×10^{-3}M Cadmium acetate solution was prepared by dissolving stoichiometric amount of cadmium acetate dihydrate (BDH) in doubly distilled water.

(ii) Ammonium dihydrogen Phosphate solution

A 1.9×10^{-2}M ammonium dihydrogen phosphate solution was prepared as described in section 3.2.1.

Procedure

Cadmium hydroxyapatite was prepared as described for calcium hydroxyapatite in section 3.2.1 but using cadmium acetate trihydrate solution (8.0×10^{-3}M) and a pH of 10.5.

4.2.3 Preparation of Barium hydroxyapatite.

Reagents

(i) Barium acetate solution

A 8.0×10^{-3}M barium acetate solution was prepared by dissolving stoichiometric amount of barium acetate monohydrate in doubly distilled water.

Procedure

Barium hydroxyapatite was prepared as described for calcium hydroxyapatite in section 3.2.1, but using barium acetate (8.0×10^{-3}M) at pH = 10.5.

4.2.4 Preparation of Led-cadmium hydroxyapatite

Solid solutions of lead-cadmium hydroxyapatite were prepared by the method of co-precipitation as described for calcium-magnesium hydroxyapatite in section 3.2.3, but using mixed solutions of lead and cadmium acetates. Preparation was first carried out in a basic medium enhanced with ammonia (pH = 10.5) solution and secondly in an acidic medium (pH 5-6).

4.2.5 Preparation of Lead-barium hydroxyapatite

Preparations were carried out as described for calcium-magnesium hydroxyapatite in section 3.2.3, but using mixed solutions of lead and barium acetates at pH = 10.5 and pH 5-6.

4.2.6 Preparation of barium hydroxyapatite by solid state reaction.

Barium hydroxyapatite was prepared by mixing barium hydroxide and diammonium phosphate in the molar ratio of 1.67:1 respectively and heating the mixture at 700°C for 15 hours. The mixture was then allowed to cool and mixed thoroughly. It was subsequently re-heated at 900°C for 15 hours so as to eliminate carbonate which may be present (Bigi et al, 1984).

4.2.7. Preparation of Barium-Lead hydroxyapatite by solid state reaction.

Solid solutions of Lead-barium hydroxyapatite were prepared by mixing stoichiometric amounts of lead hydroxyapatite and barium hydroxyapatite with the barium concentration ranging from 0 to 100 atom percent and heat treated at 900°C for 15 hours.

4.2.8. Chemical Analyses of Cadmium and Barium substituted Lead hydroxyapatite

4.2.8.1 Colorimetric determination of phosphorus content.

The phosphorus contents of the prepared samples were determined colorimetrically using the molybdenum blue method as described for calcium-magnesium hydroxyapatite in section 3.2.8.1. using a Unicam SP 1750B spectrophotometer for absorbance measurements.

4.2.8.2 Determination of Lead, cadmium and barium contents of prepared samples by Atomic Absorption Spectrometry.

Reagents

(i) Cadmium Standard Solution.

Cadmium standard solutions were prepared from cadmium nitrate. The cadmium nitrate was first standardized by using the same procedures as that for the standardization of lead. 1.00 cm^3 of 0.1M NaOH however corresponding to 5.62mg of cadmium. From the titration results obtained, stock solution of cadmium containing 100ppm of cadmium was prepared. Cadmium standard solutions were prepared by serial dilution of the stock solution.

(ii) Barium Standard Solution

A stock solution of barium was prepared by dissolving 1.4380g of barium carbonate in 20cm^3 IM HCl and the

solution made up to 1.dm^3 with water. The solution was standardized by complexometric titration (Schgwarzenbach, 1960) as described for lead in chapter three. Working standard solutions were prepared by serial dilution of the stock solution.

Instrumental Conditions.

(i) Cadmium

Wavelength	-	228.8nm
Flame	-	Air/Acetylene
Slit Setting	-	0.15mm
Air Flow rate	-	5.0xm^{3}min-1
Acetylene flow rate	-	1.2xm^{3}min-1
Lamp Current	-	6.0mA

(ii) Barium

Wavelength	-	553.5nm
Flame	-	Nitrous oxide-Acetylene
Slit Setting	-	0.15mm
Acetylene flow rate	-	4.5dm^{3}min^{-1}
Lamp Current	-	12.0 mA
Nitrous Oxide flow rate	-	4.5dm^{3}min^{-1}

(iii) Lead

Instrumental conditions for lead are as stated in chapter three.

Procedure

Atomic absorption measurements for lead, cadmium and barium were carried out as described in section 3.2.8.2., but using a lead hollow cathode lamp for lead determination, cadmium lamp for cadmium and barium lamp for barium determinations. Preparation of a calibration curve for using standard solutions of each cation was carried out and their levels in the corresponding samples read off.

4.2.8.3 Infra-red Absorption Analysis.

Instrumental conditions and procedure were the same as stated in section 3.2.8.3.

4.2.9. X-ray Powder diffraction Analysis.

X-ray powder diffraction measurements were carried out as described for calcium-magnesium hydroxyapatite in section 3.2.9.

4.3 Results

Tables 4.1 and 4.2 contain the results of the atomic absorption spectrometric, colorimetry and infra-red absorption spectrophotometric analyses of the lead-cadmium hydroxyapatite samples for reactions carried out in basic medium (pH = 10.5) and in acidic medium (pH 5-6) respectively. Similar data for lead-barium system are contained in tables 4.5 and 4.6. Analytical data for lead-barium hydroxyapatite obtained by solid state reaction are

reported in table 4.9 while table 4.10 contains the expected and observed lead, barium and phosphorus contents of the prepared samples. The mole-atom ratio for the lead-cadmium system, Pb+Cd/p for each sample is reported in tables 4.1 and 4.2. They range from 1.65 - 1.67 and 1.64 - 1.67 for preparations in basic medium and acidic medium respectively. These are in agreement with the theoretical values for hydroxyapatite solid solutions.

The corresponding infra-red frequencies for the lead-cadmium hydroxyapatite solid solutions are shown in tables 4.1 and 4.2 respectively. These range from 620 to 640cm^{-1} and 3430 to 3450 cm^{-1} attributable to the OH vibrational modes, 935 to 960cm^{-1} and 1020 to 1070 cm^{-1} to PO_4 vibrational modes. While the OH stretching modes decrease with increase in atom percent cadmium, the PO_4 vibrational modes $\nu_1(PO_4)$ and $\nu_3(PO_4)$ show an increase. However, the shift in the internal vibrational mode for $\nu_1(PO_4)$ to higher frequencies is not continuous (Tables 4.1 and 4.2). It remains essentially constant after a concentration of about 60 atom percent cadmium. The infra-red frequencies of the PO_4 and OH internal modes of the various samples plotted against the cadmium atom concentrations are shown in figures 4.1 and 4.2 for preparations done in basic and acidic media respectively. The plots are linear within experimental error as shown by the equations in figures 4.1 and 4.2.

The infra-red frequencies for the lead-barium systems are shown in tables 4.5, 4.6 and 4.9. For preparations done in aqueous solution, the values range from 935 to 950cm^{-1} and 1010 to 1060cm^{-1} attributable to the PO_4 group; 600 to 630cm^{-1} and 3560 to 3580cm^{-1} attributable to the OH group. The OH vibrational modes are observed only for preparations containing about 0 to 40 atom percent barium. For the solid state reaction products, the infra-red frequencies range from 1030 to 1050 cm^{-1} corresponding to the PO_4 internal vibrational mode; 440 to 620 cm^{-1} and 3570 to 3600cm^{-1} attributable to the OH librational and stretching modes respectively. While the frequencies due to OH libration decrease with increase in barium atom concentration, that for the PO_4 group and OH stretch show an opposite trend. Most of the absorption bands of the mixed lead-barium products are broadened with increase in barium content. The plot of infra-red frequencies of lead-barium hydroxyapatite solid solutions prepared by the solid state reaction against atom percent barium is shown in figure 4.3. It reveals that the frequencies vary linearly with increasing barium content within experimental error as shown by the equations in figure 4.3.

The products obtained from the solid state reaction between lead hydroxyapatite and barium hydroxyapatite at 900°C are solid solutions in the whole range. This is evidenced by the infra-red absorption frequencies of the

products which are characteristic of apatitic samples. However, precipitates obtained at about 100°C through co-precipitation by drop-wise addition of lead and barium acetate solutions into stirring ammonium dihydrogen phosphate solutions gave solid solutions only in the range of barium concentration in solution from 0 to 40%. The absence of characteristics OH bands from the infra-red frequencies of the samples precipitated from aqueous medium beyond 40 atom percent barium confirms this.

The X-ray powder diffraction data for lead-cadmium and lead-barium precipitated from basic medium (pH = 10.5) are reported in appendices II and III respectively. The 2θ, d-spacings and relative intensities for each sample is shown. Corresponding x-ray powder diffraction patterns for lead-cadmium and lead-barium hydroxyapatites are shown in figures 4.4. and 4.5 respectively. Powder patterns for lead-cadmium system gave peaks which become sharper with increasing cadmium content. However, lead-barium system gave peaks which broadened with increase in barium content.

TABLE 4.1
Lead, Cadmium and Phosphorus contents (weight percent) of Lead-Cadmium hydroxyapatite solid solutions precipitated from basic medium (pH = 10.5) and their infra-red frequencies.

Cd Content (Atom %)	Weight (%) Pb	Cd	P	Molecular formula	Mole-Atom Ratio Pb+Cd/p	I.R Frequencies (cm-1) $V_3(PO_4)$	$V_4(OH)$	$V_1(PO_4)$
0	77.35	-	6.60	$Pb_{9.9}(PO_4)_6(OH)_2$	1.66	1035	3570	935
20	66.55	9.02	7.43	$Pb_{7.98}Cd_{2.02}(PO_4)_6(OH)_2$	1.67	1038	3540	940
40	52.20	19.46	7.73	$Pb_{5.79}Cd_{4.21}(PO_4)_6(OH)_2$	1.67	1045	3520	-
50	45.45	25.70	8.06	$Pb_{4.83}Cd_{5.04}(PO_4)_6(OH)_2$	1.65	1055	3480	945
60	38.70	33.10	8.47	$Pb_{3.73}Cd_{6.21}(PO_4)_6(OH)_2$	1.66	1065	3550	960
100		64.83	10.25	$Cd_{9.96}(PO_4)_6(OH)_2$	1.66	1070	3440	960

TABLE 4.2
Lead, Cadmium and Phosphorus Contents (weight percent) of Lead-Cadmium hydroxyapatite solid solutions precipitated from acidic medium (pH = 5-6) and their infra-red frequencies.

Cd content (Atom %)	Weight (%) Pb	Cd	P	Molecular formula	Mole-Atom Ratio Pb+Cd/p	I.R Frequencies (cm^{-1}) $V_3(PO_4)$	$V_4(OH)$	$V_1(PO_4)$
0	77.20	-	6.45	$Pb_{9.97}(PO_4)_6(OH)_2$	1.66	1030	3565	935
20	66.35	9.00	6.62	$Pb_{7.98}Cd_{1.99}(PO_4)_6(OH)_2$	1.66	1030	3550	940
40	53.94	18.97	6.81	$Pb_{5.98}Cd_{3.88}(PO_4)_6(OH)_2$	1.64	1045	3500	940
50	45.80	25.55	8.52	$Pb_{4.87}Cd_{4.97}(PO_4)_6(OH)_2$	1.64	1050	3480	945
60	39.05	32.04	8.86	$Pb_{3.97}Cd_{6.01}(PO_4)_6(OH)_2$	1.67	1060	3460	960
100	-	64.30	10.76	$Cd_{9.88}(PO_4)_6(OH)_2$	1.65	1070	3440	960

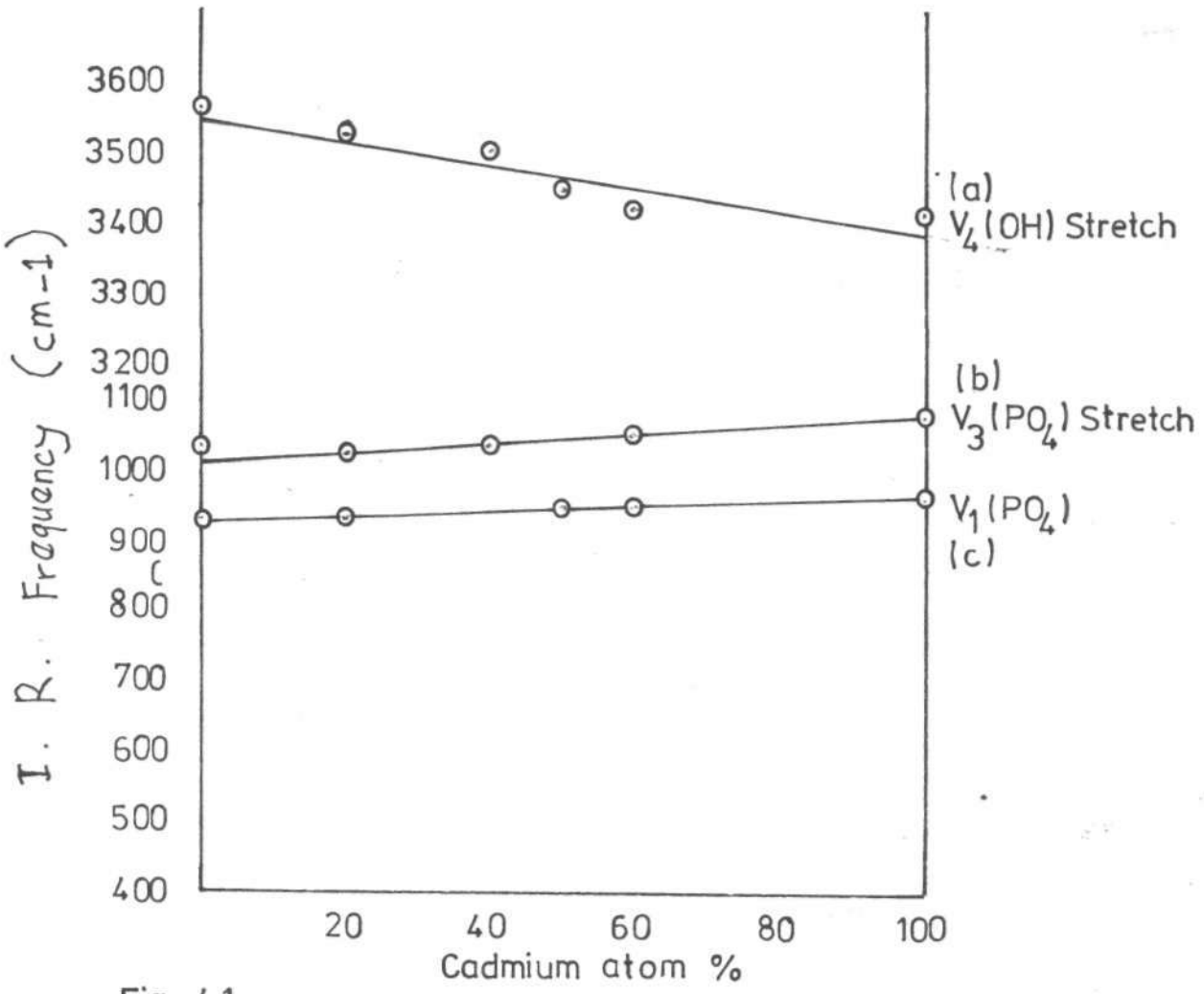


Fig 4.1

Infra-red frequencies for lead–cadmium hydroxyapatite solid solutions against cadmium atom % (PH = 10.5)

Equations for the lines

(a) $y = 3563.54 - 1.41x$ ($n = 6, \sigma = 1.40$)

(b) $y = 1032.55 + 0.41x$ ($n = 6, \sigma = 2.3$)

(c) $y = 935.5 + 0.27x$ ($n = 6, \sigma = 4.14$)

(y = infra-red fequency; x = atom % cadmium; σ = standard deviation)

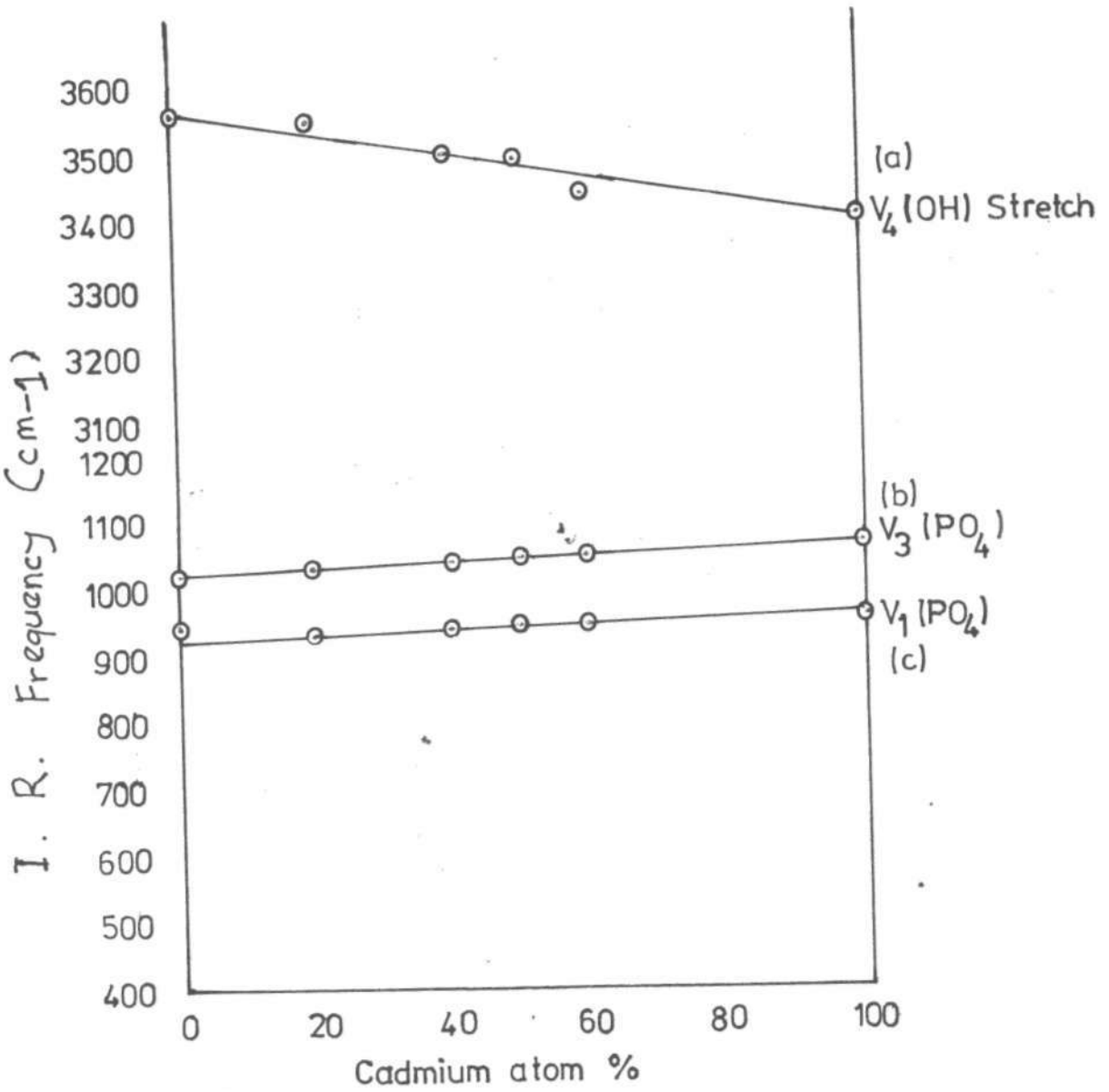


Fig 4.2
Infra-red frequencies for Lead-cadmium hydroxyapatite solid solutions against atom % Cadmium

(Acidic medium, PH 5-6)

Equations for the lines:

(a) $y = 3560.80 - 1.37x$ ($n = 6, \sigma = 12.1$)

(b) $y = 1027.25 + 0.45x$ ($n = 6, \sigma = 33$)

(c) $y = 934.10 + 0.28x$ ($n = 6, \sigma = 3.84$)

(y = infra-red frequency; x = atom % cadmium;
σ = standard deviation)

TABLE 4.3
Expected [e] and Observed [o] concentrations of Lead, cadmium and Phosphorus in lead-cadmium hydroxyapatite solid solutions precipitated from Aqueous Ammonia Solution. (pH = 10.5) based on the molecular formula, $Pb_{10-x}Cd_x(PO_4)_6(OH)_2$.

	Pb[o]	Pb[e]	Cd[e]	Cd[e]	P[o]	P[e]
1.	77.35	77.43	-	-	6.60	6.94
2.	66.50	66.67	9.01	9.04	7.43	7.47
3.	52.20	54.13	19.46	19.58	7.73	8.10
4.	45.45	47.05	25.70	25.52	8.06	8.44
5.	38.70	39.33	33.10	32.00	8.47	8.82
6.	-	-	64.85	65.05	10.25	10.75

TABLE 4.4
Expected [e] and Observed [o] contents (weight percent) of lead, cadmium and phosphorus in lead-cadmium hydroxyapatite solid solutions precipitated from acidic medium (pH = 5-6) based on the molecular formula, $Pb_{10-x}Cd_x(PO_4)_6(OH)_2$.

	Pb[o]	Pb[e]	Cd[e]	Cd[e]	P[o]	P[e]
1.	77.04	77.43	-	-	6.45	6.94
2.	66.35	66.67	9.00	9.04	7.62	7.47
3.	53.94	54.13	18.93	19.58	6.81	8.10
4.	45.80	47.05	25.55	25.52	8.52	8.44
5.	38.70	39.33	32.04	32.00	8.86	8.82
6.	-	-	64.30	65.05	10.76	10.75

TABLE 4.5 Lead, barium and phosphorus contents (weight percent) of
Lead-Barium hydroxyapatite precipitated from Aqueous Ammonia Solution
(pH =10.5) and their infra-red frequencies.

Ba content (Atom %)	Weight (%) Pb	Ba	P	Molecular formula	Mole-Atom Ratio Pb+Ba/p	I.R Frequencies (cm^{-1}) PO_4	PO_4	PO_4	OH	OH
0	77.30	-	6.44	$Pb_{9.98}(PO_4)_6(OH)_2$	1.66	935	- 1030	-	3560	
20	63.35	10.92	6.73	$Pb_{7.75}Ba_{2.0}(PO_4)_6(OH)_2$	1.63	940	- 1010	610	3578	
40	46.75	22.36	8.06	$Pb_{5.4}Ba_{3.9}(PO_4)_6(OH)_2$	1.55	940	590 -	-	3570	
50	45.70	26.10	9.20	$Pb_{4.57}Ba_{4.42}(PO_4)_6(OH)_2$	1.50	950	- -	-	-	
60	34.50	34.69	10.00	$Pb_{3.76}Ba_{5.7}(PO_4)_6(OH)_2$	1.58	-	- 1050	-	-	
100	-	63.55	12.24	$Ba_{9.15}(PO_4)_6(OH)_2$	1.53	-	590 1010	-	3606	

TABLE 4.6

Barium, lead and phosphorus contents (weight percent) of Lead-Barium hydroxyapatite precipitated from acidic medium (pH = 5-6) and their infra-red frequencies.

Ba content (Atom %)	Weight (%) Pb	Ba	P	Molecular formula	Mole-Atom Ratio Pb+Ba/p	I.R Frequencies (cm^{-1}) PO_4	PO_4	OH	OH
0	77.04	-	6.45	$Pb_{9.97}(PO_4)_6(OH)_2$	1.66	935	1040	-	3565
20	64.36	8.81	6.69	$Pb_{7.78}Ba_{1.63}(PO_4)_6(OH)_2$	1.57	940	-	620	3580
40	48.01	20.93	8.20	$Pb_{5.55}Ba_{3.65}(PO_4)_6(OH)_2$	1.53	940	1060	625	3575
50	40.60	28.90	8.41	$Pb_{4.56}Ba_{4.9}(PO_4)_6(OH)_2$	1.58	965	-	-	-
60	34.85	35.47	9.00	$Pb_{3.80}Ba_{5.83}(PO_4)_6(OH)_2$	1.61	970	-	-	-
100	-	64.36	9.96	$Ba_{9.27}(PO_4)_6(OH)_2$	1.54	950	-	-	-

TABLE 4.7

Expected [e] and Observed [o] contents (weight percent) barium, of lead, and phosphorus in lead-barium hydroxyapatite solid solutions precipitated from Aqueous Ammonia (pH 10.5) based on the molecular formula, $Pb_{10-x}Ba_x(PO_4)_6(OH)_2$.

	Pb[o]	Pb[e]	Ba[e]	Ba[e]	P[o]	P[e]
1.	77.30	77.43	-	-	6.44	6.94
2.	63.35	65.36	10.92	10.83	6.73	7.33
3.	46.75	51.88	22.36	22.93	8.06	7.76
4.	40.70	44.53	26.10	29.52	9.20	7.99
5.	34.50	36.73	34.69	36.52	10.00	8.23
6.	-	-	63.55	69.46	12.24	9.40

TABLE 4.8

Expected [e] and Observed [o] contents (weight percent) of barium, lead and phosphorus in lead-barium hydroxyapatite solid solutions precipitated from Acidic medium based on the molecular formula, $Pb_{10-x}Ba_x(PO_4)_6(OH)_2$.

	Pb[o]	Pb[e]	Ba[e]	Ba[e]	P[o]	P[e]
1.	77.04	77.43	-	-	6.45	6.94
2.	64.36	65.36	8.81	10.83	6.69	7.33
3.	48.01	51.88	20.93	22.93	8.20	7.76
4.	40.60	44.53	28.90	29.52	8.41	7.99
5.	34.85	36.73	35.47	36.52	9.00	8.23
6.	-	-	64.36	69.46	9.96	9.40

TABLE 4.9

Lead, barium and phosphorus contents (weight percent) of lead-barium hydroxyapatite solid solutions prepared by solid state reaction at 900°C and their infra-red frequencies.

Ba content (Atom %)	Weight (%) Pb	Ba	P	Molecular formula	Mole-Atom Ratio Pb+Ba/p	I.R Frequencies (cm-1) $V_3(PO_4)$	$V_1(OH)$	$V_4(PO_4)$
0	75.30	-	6.92	$Pb_{9.97}(PO_4)_6(OH)_2$	1.66	1030	-	3570
20	64.52	10.60	7.50	$Pb_{7.90}Ba_{1.94}(PO_4)_6(OH)_2$	1.64	1038	620	3575
40	49.96	21.85	7.68	$Pb_{5.78}Ba_{3.81}(PO_4)_6(OH)_2$	1.60	1040	580	3585
50	44.06	29.33	7.72	$Pb_{4.95}Ba_{4.95}(PO_4)_6(OH)_2$	1.65	1040	550	3590
60	37.50	35.87	8.04	$Pb_{4.08}Ba_{5.89}(PO_4)_6(OH)_2$	1.66	1045	530	3590
100	-	69.40	9.33	$Ba_{9.99}(PO_4)_6(OH)_2$	1.67	1050	440	3600

TABLE 4.10

Expected [e] and Observed [o] contents (weight percent) of lead-barium hydroxyapatite solid solutions prepared by solid state reaction at 900°C values based on the molecular formula, $Pb_{10-x}Ba_x(PO_4)_6(OH)_2$.

	Pb[o]	Pb[e]	Ba[e]	Ba[e]	P[o]	P[e]
1.	75.30	77.43	-	-	6.92	6.94
2.	64.52	65.36	10.60	10.83	7.50	7.33
3.	49.96	51.88	21.85	22.93	7.68	7.76
4.	44.06	44.53	29.33	29.52	7.72	7.99
5.	37.50	36.73	35.87	36.52	8.04	8.23
6.	-	-	69.40	69.46	9.33	9.40

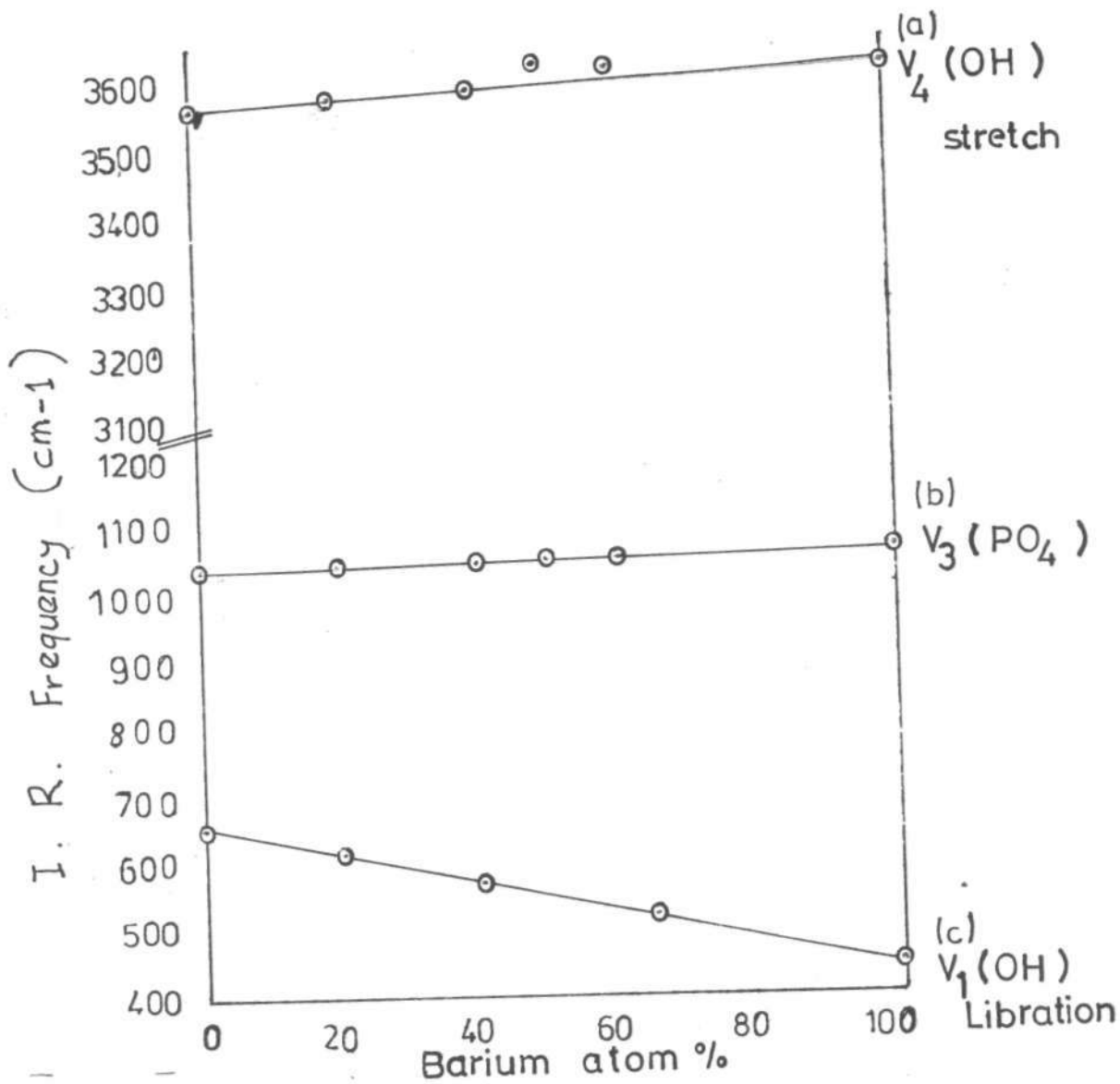


Fig 4.3

Infra-red frequencies for Pb-Ba hydroxyapatite solid solutions against atom % Barium (Solid State Process)

Equations for the lines:

(a) $y = 3571.50 + 0.3x$ ($n=6$; $\sigma = 2.75$)

(b) $y = 1031.90 + 0.19x$ ($n=6$; $\sigma = 1.20$)

(c) $y = 643 - 1.92x$ ($n=6$; $\sigma = 1.10$)

(y = infra-red frequency; x = atom % Barium; σ = standard deviation)

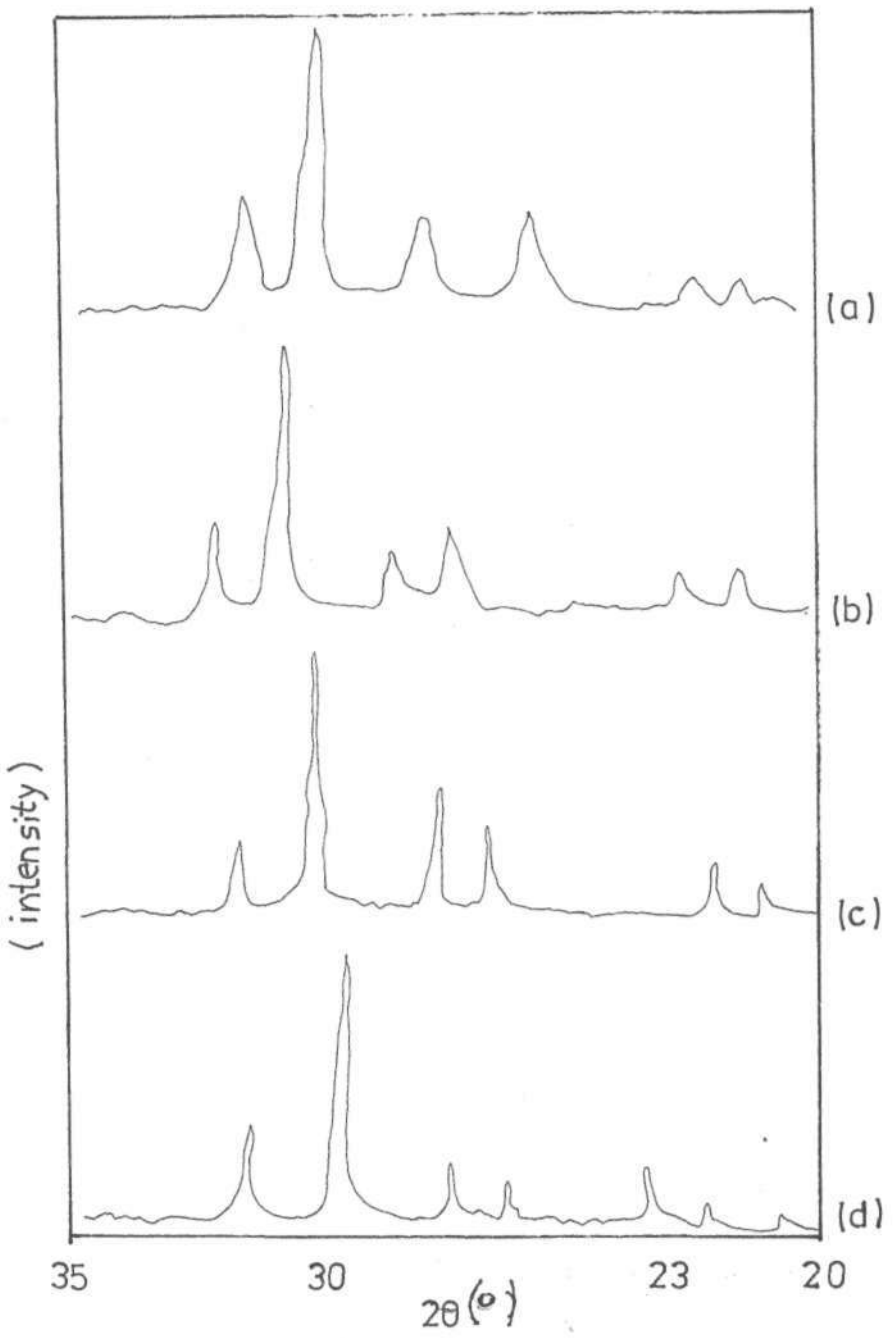


Fig 4.4

X-ray powder diffraction pattern

(a) $Pb_{9.98}(PO_4)_6(OH)_2$

(b) $Pb_{7.98}Cd_{2.02}(PO_4)_6(OH)_2$

(c) $Pb_{5.79}Cd_{4.21}(PO_4)_6(OH)_2$

(d) $Pb_{3.73}Cd_{6.2}(PO_4)_6(OH)_2$

(Basic medium, PH = 10.5)

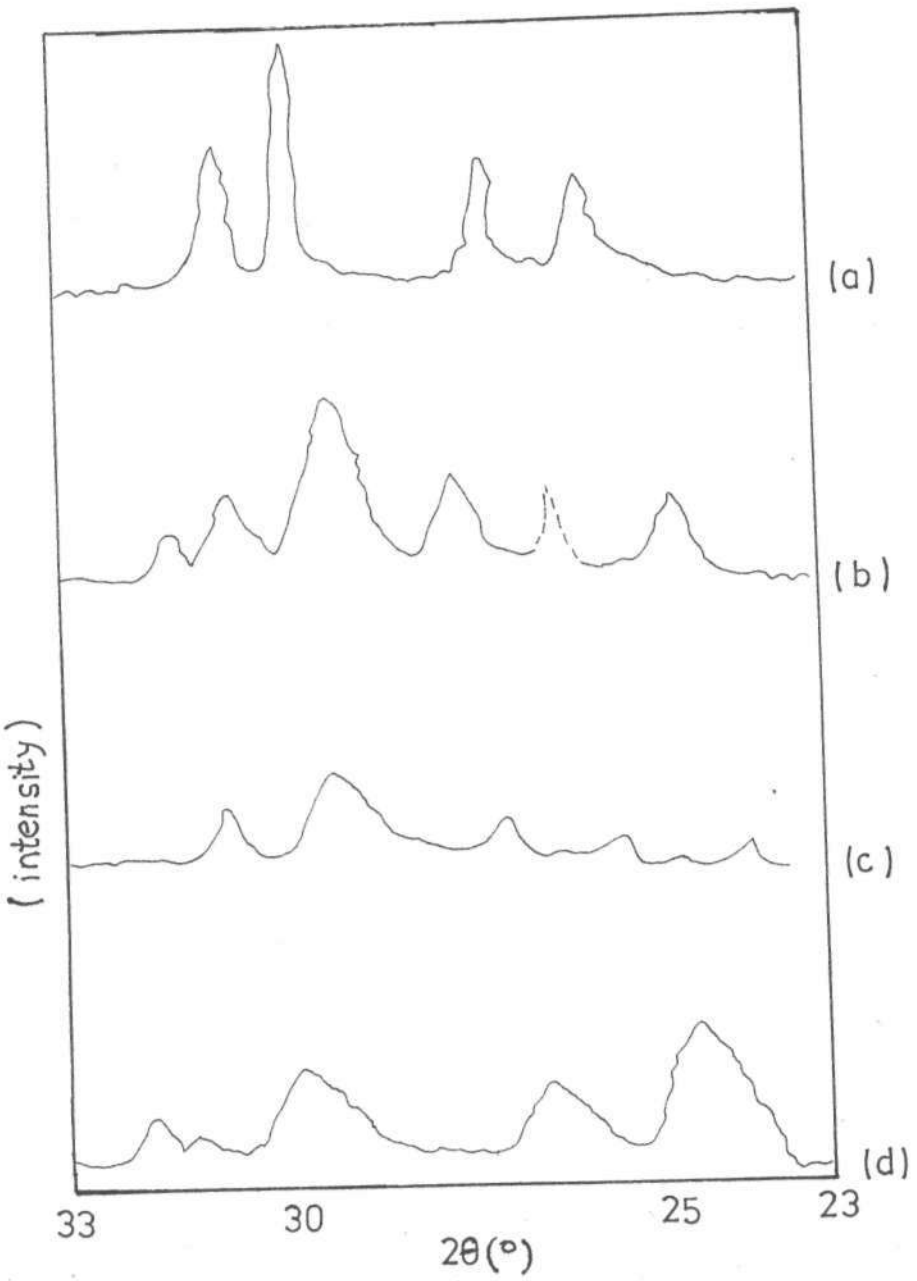


Fig 4.5

X - ray powder diffraction pattern

(a) $Pb_{7.78}Ba_{1.63}(PO_4)_6(OH)_2$

(b) $Pb_{5.55}Ba_{3.65}(PO_4)_6(OH)_2$

(c) $Pb_{4.56}Ba_{4.9}(PO_4)_6(OH)_2$

(d) $Pb_{3.80}Ba_{5.83}(PO_4)_6(OH)_2$

(Basic medium, PH=10.5)

4.4 Discussion

The replacement of lead by cadmium in the apatite structure induces a shift of the infra-red bands characteristic of the PO_4 internal modes to higher frequencies as the atom percent cadmium increases. This trend is in agreement with the *decrease* in cationic mass (Pb→Cd). The mass of the cation is indicated to have the greatest influence on the mean frequency of the internal PO_4 vibrational modes (Klee and Engel, 1970; Fowler, 1974). According to Fowler (1974), as the cation-anion bond becomes stronger the frequency of the internal modes of the anion becomes more cation dependent and in turn sensitive to cation mass. In the present case, the overall cation mass decreases as cadmium increasingly substitutes for lead in the apatite lattice thereby inducing stronger cation-anion bonding and causing the frequencies of internal vibrational modes of the phosphate ion to shift to higher values.

The shift of the OH stretching and librational modes **of** the lead-cadmium solid solutions toward lower frequencies with increase in atom percent cadmium is in agreement with the predominant role of the M-OH (M = cation) interaction with respect to OH --- O(PO_3) hydrogen bond (Fowler, 1974; Bigi et al, 1991).

The near linearity of the plot of the infra-red frequencies of lead-cadmium hydroxyapatite against cadmium

atom percent (figures 4.1 and 4.2) is suggestive that the preparations are homogeneous solid solutions in the entire compositional range. Also, the values of the mole-atom ratios, Pb/p, Cd/p and Pb+Cd/p are in agreement with that expected for apatitic samples (Partington, 1957: Patel, 1979). Higher amounts of the substituting cation (Cd^{2+}) are observed in the solid solutions prepared in basic medium (pH = 10.5) than for reactions in acidic medium. This is also in agreement with results obtained for zinc substituted calcium hydroxyapatite which indicates that the preparations are to some extent pH dependent.

The results of the infra-red analysis carried out on the products obtained from the interaction of barium with lead hydroxyapatite in aqueous solution show the formation of solid solutions for samples containing about 0-40 atom percent barium in the mediating solution. In contrast, products obtained by solid state reaction between lead hydroxyapatite and barium hydroxyapatite are solid solutions in the entire compositional range. The infra-red frequencies of the products obtained through solid state reaction assume values lying on a straight line joining the characteristic frequencies of lead and barium hydroxyapatites (figure 4.3). This indicates that the products of the solid state synthesis are not simply mixtures of two components or one component adsorbed on the other but homogenous solid solutions (Bigi et al; Collins,

1959; Fowler, 1974; Patel, 1979).

The decrease of the magnitude of the OH librational frequency with increasing barium atom concentration is similar to that observed for the lead-cadmium system and also in agreement with that reported by Fowler (1974) on strontium and barium apatites. This may be due to the displacement of the OH by the introduction of the larger cation, Ba^{2+} which causes weak hydrogen bonding of the type M-OH---OPO_3 (M = Ba^{2+}). Also, the shift of the OH stretching mode to higher frequencies with increase in barium atom concentration is in agreement with that reported by Bigi et al (1984) for calcium-barium hydroxyapatite solid solutions.

The increasing sharpness of x-ray powder peaks for lead-cadmium hydroxyapatite as the cadmium content increases, (figure 4.4) indicates that the products become more crystalline in the same order. The result is in agreement with the smaller cationic size of Cd^{2+} compared to Pb^{2+}. However, x-ray powder peaks for lead-barium system are broadened with increasing barium content. The peak broadening is more pronounced for samples containing more than about 40 barium atom percent (basic medium, pH = 10.5). The result is in agreement with observed infra-red absorption data. It also agrees with the larger cation size of Ba^{2+} compared to Pb^{2+}. The results further indicates that products obtained beyond barium concentration of about

40 barium atom percent are increasingly amorphous in character. Similar results were reported by Bigi et al (1984) for the replacement of calcium by barium in the hydroxyapatite lattice. In the latter, the substitution range was from 0 to 25 barium atom percent in aqueous medium and 60 to 100% in solid state reaction. The reluctance of barium to undergo substitution processes in hydroxyapatites in aqueous medium may be attributed to the large size of the Ba^{2+} ion. Even among the group IIA elements, Mg, Ca, Sr, Ba and Ra the tendency to form hydrates decreases with increasing size of M^{2+} (Cotton and Wilkinson, 1972). This trend may be attributed to the fact that hydration energies decrease more rapidly than the lattice energies as the size of the M^{2+} increases. This may also account for why the smaller cation, Cd^{2+}, replaces lead in the hydroxyapatite in aqueous medium in the whole series while the larger Ba^{2+} ion does not.

The value for the ratios, Pb/p and Ba/p of the end members of the lead-barium system and the Pb+Ba/p for the intermediate members range from 1.55 - 1.66 and 1.60 - 1.67 for products obtained from aqueous medium and solid state reactions respectively (theoretical value = 1.67). The values observed for the solid state reaction products are characteristic of apatitic solid solutions. The loss of cation manifested by the products obtained from the aqueous medium is attributable to possible acid phosphate formation

in that medium (Rathje, 1941 as cited by Narasaraju et al, 1972). The formation of apatitic samples of lead-cadmium in both basic and acidic media indicates that the mode of interaction may be such that allows the incorporation of Cd^{2+} into the apatite lattice.

CHAPTER FIVE

ISOMORPHOUS SUBSTITUTION IN STRONTIUM HYDROXYAPATITE BY CADMIUM, ZINC AND LEAD

5.1 Introduction

Experiments in rats have shown that lack of strontium in the diet causes dental caries and poor growth conditions. Addition of strontium to the diet has been found to reverse these changes but caused rickets. It has also been suggested that strontium has a beneficial action on the mineralization of depleted bones in persons suffering from disturbances of bone metabolism (Curzon et al, 1970; Koutsoukos and Nancollas, 1981).

It is now believed that one way through which strontium is incorporated in the human body is by its cationic replacement of Ca^{2+} in the hydroxyapatite found in bones and teeth. The complete series of solid solutions of strontium with calcium hydroxy-apatite has been prepared by various researchers (Collin, 1981; Heijligers et al, 1971; Fowler, 1974).

From the fact that strontium plays some significant role in man and its interaction with bone is similar to that with synthetic calcium hydroxyapatite, the present work is concerned with the isomorphous replacement of strontium by Cd^{2+}, Zn^{2+} and Pb^{2+} in strontium hydroxyapatite. It is aimed at ascertaining the role of these metals (cadmium, zinc and lead) in strontium

hydroxyapatite and clarifying factors influencing the nature of their interaction with strontium hydroxyapatite. Products obtained from the replacement reactions have been analysed by colorimetric, atomic absorption and infra-red absorption methods.

5.2 Experimental

5.2.1 Preparation of Strontium Hydroxyapatite.

Reagents

(i) Strontium Acetate Solution

A 8.0×10^{-3}M strontium acetate solution was prepared by dissolving stoichiometric amount of hydrated strontium acetate $Sr(CH_3COO)_2$, ½ H_2O (BDH) in doubly distilled water.

(ii) Ammonium dihydrogen phosphate solution

A 1.9×10^{-2}M solution of ammonium dihydrogen phosphate was prepared by dissolving stoichiometric amount of the salt in water.

Procedure

Strontium hydroxyapatite was prepared as described for calcium hydroxyapatite in section 3.2.1, but using strontium acetate solution first in basic medium at pH = 10.5, enhanced with ammonia solution and second in acidic medium (pH 5-6).

5.2.2 Preparation of Cadmium hydroxyapatite

Cadmium hydroxyapatite was prepared using the same reagents and procedure as in section 4.2.2.

5.2.3 Preparation of Strontium-cadmium hydroxyapatite.

Solid solutions of strontium-cadmium hydroxyapatite were prepared as described for calcium-magnesium hydroxyapatite in section 3.2.3, but using mixed solutions of strontium acetate and cadmium acetate. Two preparations were made; one in basic medium (pH = 10.5) and second in acidic medium (pH 5-6).

5.2.4 Preparation of zinc hydroxyapatite

Zinc hydroxyapatite was prepared using the same reagents and procedure as in section 3.2.4.

5.2.5. Preparation of Strontium-Zinc hydroxyapatite solid solutions.

Strontium-zinc hydroxyapatite samples were prepared by the method of co-precipitation as described for calcium-magnesium hydroxyapatite in section 3.2.3, but using mixed aqueous solutions of strontium acetate and zinc acetate in basic medium (pH 10.5) and in acidic medium (pH 5-6).

5.2.6 Preparation of Lead Hydroxyapatite

Lead hydroxyapatite was prepared using the same reagents and procedure as contained in section 3.2.6.

5.2.7 Preparation of Strontium-Lead hydroxyapatite solid solutions

Strontium-lead hydroxyapatite solid solutions were prepared by the method of co-precipitation as described for calcium-magnesium hydroxyapatite in section 3.2.3, but using mixed aqueous solutions of strontium acetate and lead acetate first in basic (pH 10.5) and second in acidic medium (pH 5-6).

5.2.8 Chemical Analyses of Cadmium, Zinc and Lead substituted Strontium Hydroxyapatite

5.2.8.1 Colorimetric determination of Phosphorus content

The concentrations of phosphorus in the prepared samples were determined colorimetrically using the molybdenum blue method and the same spectrophotometer as described for calcium-magnesium hydroxyapatite in section

5.2.8.2 Determination of Cadmium, lead, strontium and zinc contents of prepared apatite samples by Atomic Absorption Spectrometry.

Reagents

(i) Strontium Standard Solution

Stock solution of strontium was prepared by dissolving 1.6840g of strontium carbonate in 20cm^3 M-HCl and diluting to 1.0dm^3 with doubly distilled water. Working standard solutions were prepared by serial dilution of the stock solution.

(ii) Lanthanum Solution

This was prepared as described in chapter three.

(iii) Zinc Standard Solution

This was prepared as described in chapter three.

(iv) Lead Standard Solution

Lead standard solutions were prepared as described in chapter three.

(v) Cadmium Standard Solution

Cadmium standard solution were prepared from cadmium nitrate as described in chapter four.

Instrument Used

Pye Unicam SP 1900 Atomic Absorption spectrometer.

Instrumental Conditions

(i) Strontium

Wavelength	-	460.7nm
Flame	-	Nitrous oxide-Acetylene
Slit Setting	-	0.2mm
Acetylene flow rate	-	$4.4dm^3min^{-1}$
Nitrous Oxide flow rate	-	$4.5dm^3min^{-1}$
Lamp Current	-	8.0mA

(ii) Lead and Zinc

The instrumental conditions for lead and zinc are as stated in chapter three.

(iii) Cadmium

The instrumental conditions for cadmium are as stated in chapter four.

Procedure

Atomic absorption measurements for lead, cadmium and zinc in the prepared samples were carried out as described in Chapter three. Lead hollow cathode lamp was used for lead determination; cadmium hollow cathode for cadmium; strontium hollow cathode lamp for strontium determination and zinc hollow cathode lamp for zinc determination.

5.2.8.3 Infra-red Absorption Analysis.

Instrumental conditions and procedure were the same as stated in Chapter three.

5.3 Results

The results of the atomic absorption spectrometry, colorimetry and infra-red absorption spectrophotometric analyses of the cadmium, lead and zinc substituted strontium hydroxyapatite samples are shown in tables 5.1, 5.5 and 5.9 for preparations done in aqueous ammonia, solution (basic medium). Tables 5.3, 5.7 and 5.11 contain similar results for preparations carried out in acidic medium. The cationic contents and the phosphorus levels of the prepared samples are compared with calculated values in tables 5.2, 5.4, 5.6, 5.8, 5.10 and 5.12. The mole atom ratios for the samples are contained in tables 5.1, 5.3, 5.5, 5.7, 5.9 and 5.11. The values range from 1.62 to 1.67 (theoretical value = 1.67). This indicates that the preparations are homogenous solid solutions.

The infra-red frequencies are reported in tables 5.1, 5.3, 5.5, 5.7, 5.9 and 5.11. For the strontium-cadmium system, these range from 540 to 700cm^{-1} attributable to the internal $V_3(PO_4$ vibrational mode. The OH stretching mode and the $V_3(PO_4)$ are shifted to lower values as cadmium content increases. However, the OH librational mode is shifted to higher values with increasing cadmium content.

This may be due to differences in OH bonding between strontium and cadmium. (Fowler, 1974). The infra-red frequencies of the PO_4 and OH internal modes of the strontium-cadmium hydroxyapatite solid solutions are plotted against the cadmium atom concentration in figures 5.1 and 5.2 for preparations done in basic and acidic media respectively. The plots reveal a linear relationship in both cases. The equations of the lines are shown in the legend to figures 5.1 and 5.2.

The infra-red frequencies for the strontium-lead system range from 630 to 635cm^{-1} and 3440 to 3590cm^{-1} attributable to the OH vibrational modes and 930 to 950cm^{-1} corresponding to the PO_4 vibrational modes for preparations done in acidic medium; 630 to 635cm^{-1} and 3460 to 3585cm^{-1} corresponding to the OH vibrational modes and 1030 to 1090 cm^{-1}attributable to $V_3(PO_4)$ internal modes for preparations carried out in aqueous ammonia (basic medium) (Tables 5.5 and 5.7). The OH stretching modes and the $V_3(PO_4)$ internal modes are shifted to lower frequencies in a manner similar to that observed for the cadmium substituted strontium hydroxyapatite (tables 5.1 and 5.3). Plots of the infra-red absorption frequencies for the PO_4 and OH vibrational modes against atom percent lead of the strontium-lead solid solutions are shown in figures 5.3 and 5.4 for samples obtained from basic and acid media respectively. The plots are linear in both cases. The equations of the lines are

also shown in the legend to figures 5.3 and 5.4.

The infra-red frequencies for the zinc substituted strontium hydroxyapatite range from 538-640cm^{-1} and 3500-3590cm^{-1} for the OH group and 1080-1100cm^{-1} for the $V_3(PO_4)$ internal mode. The pattern of shift in the OH and PO_4 frequencies for the zinc substituted strontium hydroxyapatite is quite similar to that observed for the cadmium substituted strontium hydroxyapatite. Frequencies attributable to the PO_4 vibrational mode and the OH stretching mode are shifted to lower values with increasing zinc content while the OH librational mode is shifted to higher frequency values as the atom % zinc increases. Plots of these frequencies for the PO_4 and OH vibrational modes against atom % zinc (figures 5.5 and 5.6) show a linear relationship. The equations of the lines are shown in the legend to figure 5.5 and 5.6.

TABLE 5.1

Cadmium, strontium and Phosphorus contents of Strontium-Cadmium hydroxyapatite solid solutions precipitated from Aqueous Ammonia Solution (pH = 10.5) and their infra-red frequencies.

Cd Content (Atom %)	Weight (%) Sr	Cd	P	Molecular formula	Mole-Atom Ratio Sr+Cd/p	I.R Frequencies (cm^{-1}) $V_3(PO_4)$	$V_1(OH)$	$V_4(OH)$
0	58.75	-	17.80	$Sr_{9.92}(PO_4)_6(OH)_2$	1.65	1090	540	3590
40	32.89	28.05	16.38	$Sr_{6.93}Cd_{3.93}(PO_4)_6(OH)_2$	1.65	1080	590	3550
50	25.65	35.00	16.01	$Sr_{4.7}Cd_{4.98}(PO_4)_6(OH)_2$	1.62	1070	620	3540
60	21.20	40.85	15.21	$Sr_{3.94}Cd_{5.92}(PO_4)_6(OH)_2$	1.64	1065	640	3500
80	9.82	53.50	14.69	$Sr_{1.96}Cd_{8.96}(PO_4)_6(OH)_2$	1.65	1060	650	3460
100		64.30	14.52	$Cd_{9.89}(PO_4)_6(OH)_2$	1.65	1060	700	3440

TABLE 5.2

Expected [e] and Observed [o] contents (weight percent) of cadmium, strontium and Phosphorus in strontium-cadmium hydroxyapatite solid solutions precipitated from Basic medium (pH = 10.5) based on the molecular formula, $Sr^{10-x}Cd_x(PO_4)_6(OH)_2$.

Cd content (atom %)	*Cd[o]*	*Cd[e]*	*Sr[o]*	*Sr[e]*	*P[o]*	*P[e]*
100	*64.30*	*65.05*	-	-	*14.52*	*10.75*
80	*53.50*	*53.78*	*9.82*	*10.40*	*14.69*	*11.07*
60	*40.85*	*41.41*	*21.20*	*21.52*	*15.21*	*11.41*
50	*35.00*	*35.04*	*25.65*	*27.31*	*16.01*	*11.59*
40	*28.05*	*28.47*	*32.89*	*33.29*	*16.38*	*11.77*
0	-	-	*58.75*	*59.20*	*17.80*	*12.56*

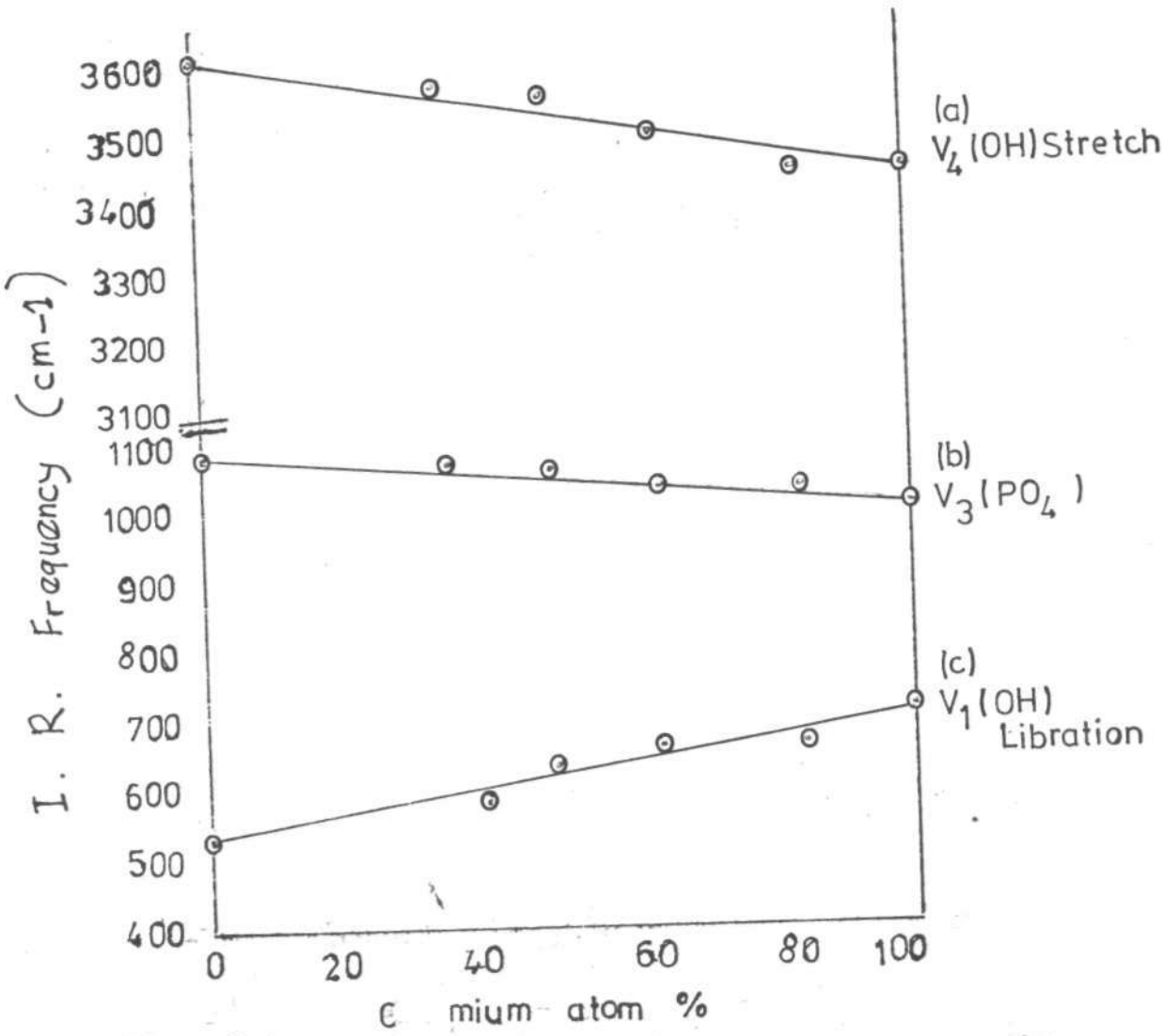


Fig 5.1

Infra-red frequencies for Sr-Cd hydroxyapatite solid solutions against atom % cadmium (PH = 10.5)

Equations for the lines:

(a) $y = 3602 - 1.61x$ ($n = 6, \sigma = 11.98$)

(b) $y = 1089.08 - 0.33x$ ($n = 6, \sigma = 3.30$)

(c) $y = 537.37 + 1.56x$ ($n = 6\ \sigma = 8.18$)

(y = infra-red frequency; x = atom % cadmium; σ = standard deviatio

TABLE 5.3

Cadmium, strontium and Phosphorus contents (weight percent) of Strontium-Cadmium hydroxyapatite solid solutions precipitated from Acidic (pH 5-6) medium and their infra-red frequencies.

Cd Content (Atom %)	Weight (%) Sr	Cd	P	Molecular formula	Mole-Atom Ratio Sr+Cd/p	I.R Frequencies (cm^{-1}) (PO_4)	(OH)	(OH)
0	57.80	-	12.06	$Sr_{9.90}(PO_4)_6(OH)_2$	1.65	1090	540	3590
40	31.73	28.40	11.52	$Sr_{5.72}Cd_{3.99}(PO_4)_6(OH)_2$	1.62	1075	610	3550
50	26.49	34.80	11.49	$Sr_{4.85}Cd_{4.97}(PO_4)_6(OH)_2$	1.64	1060	630	3550
60	19.48	42.02	11.15	$Sr_{3.62}Cd_{6.09}(PO_4)_6(OH)_2$	1.62	1055	635	3500
80	10.00	52.50	10.88	$Sr_{1.92}Cd_{7.78}(PO_4)_6(OH)_2$	1.62	1050	640	3480
100	-	63.10	10.11	$Cd_{9.7}(PO_4)_6(OH)_2$	1.62	1050	710	3460

TABLE 5.4

Expected [e] and Observed [o] contents (weight percent) of cadmium, strontium and phosphorus in strontium-cadmium hydroxyapatite solid solutions precipitated from Acidic medium (pH = 5-6) based on the molecular formula, $Sr_{10-x}Cd_x(PO_4)_6(OH)_2$.

Cd content (atom %)	Cd[o]	Cd[e]	Sr[o]	Sr[e]	P[o]	P[e]
100	63.10	65.05	-	-	10.11	10.75
80	52.50	53.78	10.00	10.40	10.88	11.07
60	42.02	41.41	19.48	21.52	11.15	11.41
50	34.80	35.04	26.49	27.31	11.49	11.59
40	28.40	28.47	31.73	33.29	11.52	11.77
0	-	-	57.80	59.20	12.06	12.56

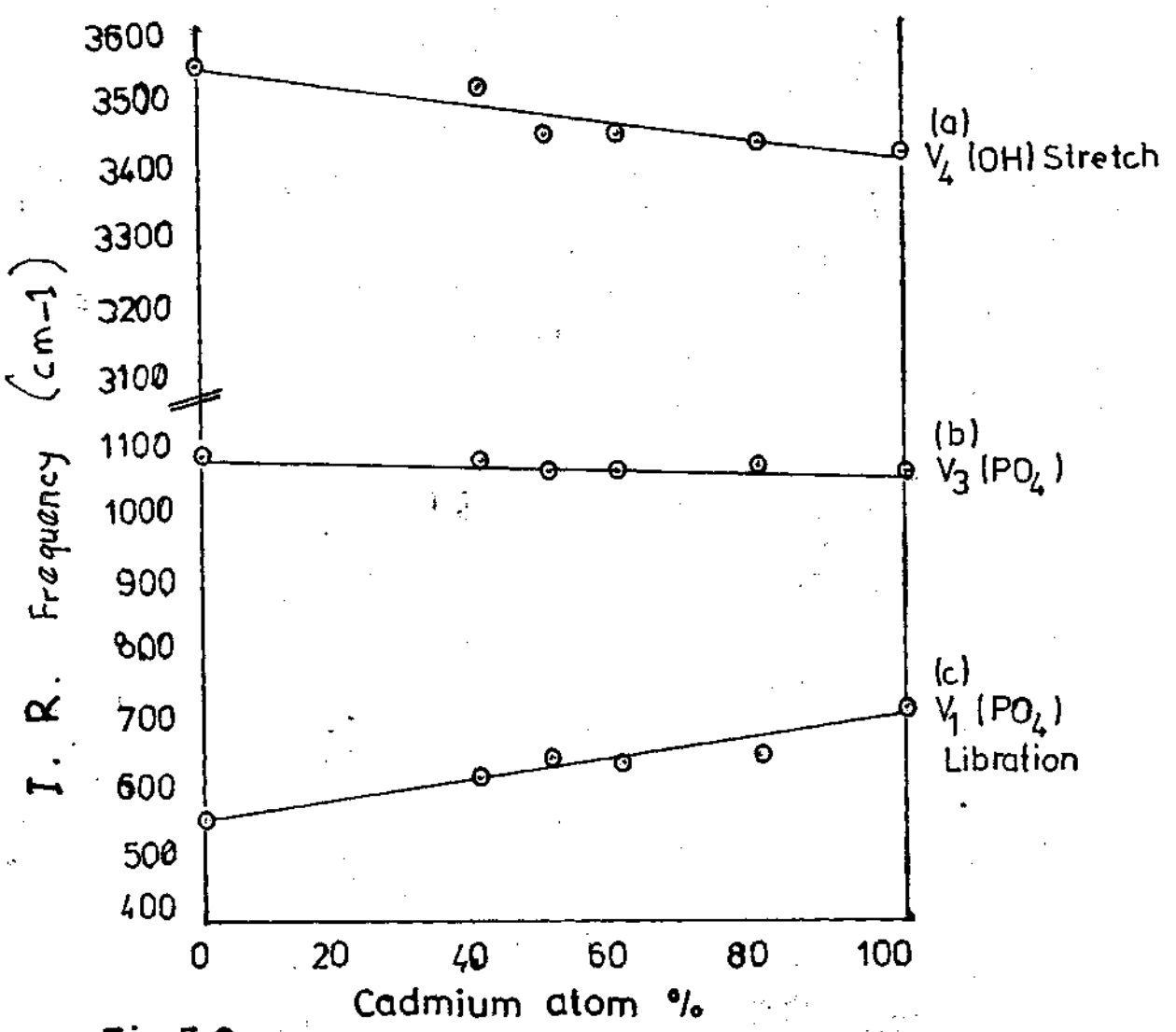


Fig 5.2

Infra-red frequencies for Sr-Cd hydroxyapatite solid solutions against atom % cadmium.(PH 5-6)

Equations for the lines:

(a) $y=3587.30-1.35x$ ($n=6$; $\sigma=11.40$)

(b) $y=1087.30-0.44x$ ($n=6$; $\sigma=5.01$)

(c) $y=548.50+1.46x$ ($n=6$; $\sigma=12.67$)

(y = infra-red frequency; x = atom % cadmium; σ = standard deviation)

TABLE 5.5

Lead, strontium and Phosphorus contents (weight percent) of Strontium-lead hydroxyapatite solid solutions precipitated from Aqueous Ammonia Solution (pH 10.5) and their infra-red frequencies.

Pb Content (Atom %)	Weight (%) Sr	Pb	P	Molecular formula	Mole-Atom Ratio Sr+Pb/p	I.R Frequencies (cm^{-1}) (PO_4)	(OH)	(OH)
0	58.60	-	12.60	$Sr_{9.9}(PO_4)_6(OH)_2$	1.65	1090	540	3585
40	26.49	42.20	9.55	$Sr_{6.93}Pb_{3.99}(PO_4)_6(OH)_2$	1.62	1075	635	3560
50	20.80	50.10	8.47	$Sr_{4.93}Pb_{5.02}(PO_4)_6(OH)_2$	1.66	1070	630	3555
60	15.88	56.10	7.94	$Sr_{3.98}Pb_{5.95}(PO_4)_6(OH)_2$	1.66	1045	630	3540
80	6.22	70.35	7.43	$Sr_{1.7}Pb_{8.27}(PO_4)_6(OH)_2$	1.66	1045	630	3490
100	-		77.35	6.60 $Pb_{9.9}(PO_4)_6(OH)_2$			1.67	1030 630 3460

TABLE 5.6

Expected [e] and Observed [o] contents (weight percent) of lead, strontium and phosphorus in strontium-lead hydroxyapatite solid solutions precipitated from Aqueous Ammonia Solution (pH 10.5) based on the molecular formula, $Sr_{10-x}Cd_x(PO_4)_6(OH)_2$.

Pb content (atom %)	*Sr[o]*	*Sr[e]*	*Pb[o]*	*Pb[e]*	*P[o]*	*P[e]*
0	*58.60*	*59.20*	-	-	*12.60*	*12.56*
40	*26.49*	*26.85*	*42.20*	*42.32*	*9.55*	*9.49*
50	*20.80*	*21.08*	*50.10*	*49.86*	*8.47*	*8.94*
60	*15.88*	*15.95*	*56.10*	*56.57*	*7.94*	*8.46*
80	*6.20*	*7.19*	*70.35*	*68.03*	*7.43*	*7.63*
100	-	-	*77.35*	*77.43*	*6.60*	*6.94*

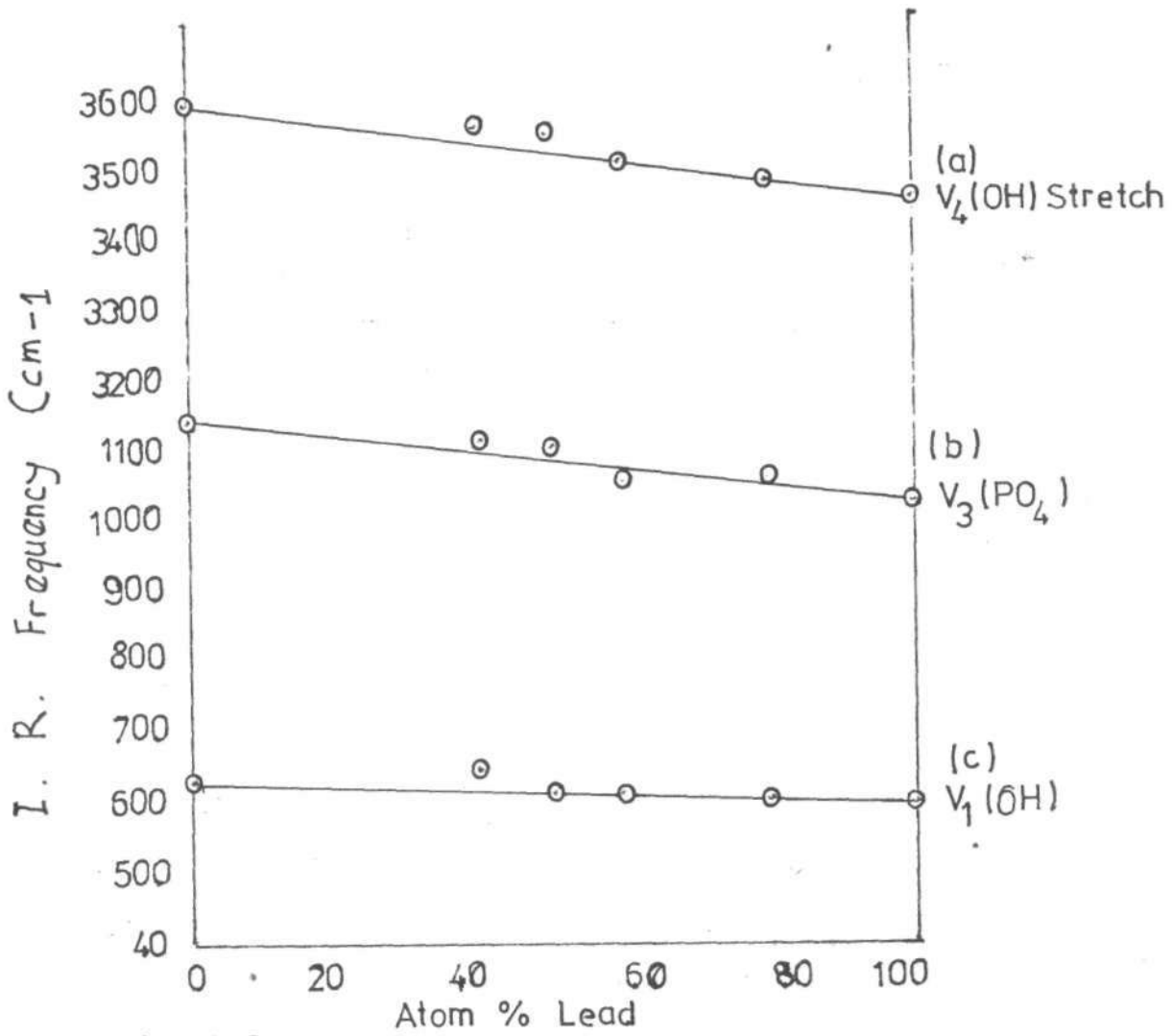


Fig 5.3

Infra red frequencies for Sr-Pb hydroxyapatite solid solutions against atom % Lead. (PH = 10.5)

Equations for the lines:

(a) $y = 3602.80 - 1.29x$ ($n=6, \sigma=14.04$)

(b) $y = 1093 - 0.63x$ ($n=6, \sigma=6.34$)

(c) $y = 634.70 - 0.06x$ ($n=6, \sigma=2.99$)

(y=infra red frequency; x= atom % Lead; σ=standard deviation)

TABLE 5.7
Lead, strontium and Phosphorus contents (weight percent) of strontium-lead hydroxyapatite solid solutions precipitated from Acidic medium (pH 5-6) and their infra-red frequencies.

Pb Content Atom %)	Weight (%) Sr	Pb	P	Molecular formula	Mole-Atom Ratio Sr+Pb/p	I.R. Frequencies (cm^{-1}) (PO_4)	(OH)	(OH)
0	58.75	0	12.24	$Sr_{9.92}(PO_4)_6(OH)_2$	1.65	950	540	3590
40	26.30	41.40	8.74	$Sr_{5.88}Pb_{3.91}(PO_4)_6(OH)_2$	1.63	945	635	3530
50	20.50	49.80	8.67	$Sr_{4.86}Pb_{4.99}(PO_4)_6(OH)_2$	1.64	938	635	3500
60	15.01	57.00	9.34	$Sr_{3.76}Pb_{6.05}(PO_4)_6(OH)_2$	1.64	935	630	3590
80	6.64	67.92	7.01	$Sr_{1.85}Pb_{7.99}(PO_4)_6(OH)_2$	1.64	930	630	3450
100	-	77.04	6.45	$Pb_{9.97}(PO_4)_6(OH)_2$	1.66	930	630	3440

TABLE 5.8
Expected [e] and Observed [o] contents (weight percent) of lead, strontium and phosphorus in strontium-lead hydroxyapatite solid solutions precipitated from mild Acidic medium based on the molecular formula, $Sr_{10-x}Cd_x(PO_4)_6(OH)_2$.

Pb content (atom %)	Pb[o]	Pb[e]	Sr[o]	Sr[e]	P[o]	P[e]
0	77.04	77.43	-	-	6.45	6.94
40	67.92	78.03	6.64	17.19	7.01	7.63
50	57.00	56.57	15.93	15.95	8.34	8.46
60	49.80	49.86	20.50	21.08	8.67	8.94
80	41.40	42.32	26.80	26.85	8.74	9.49
100	-	-	58.75	59.20	12.24	12.56

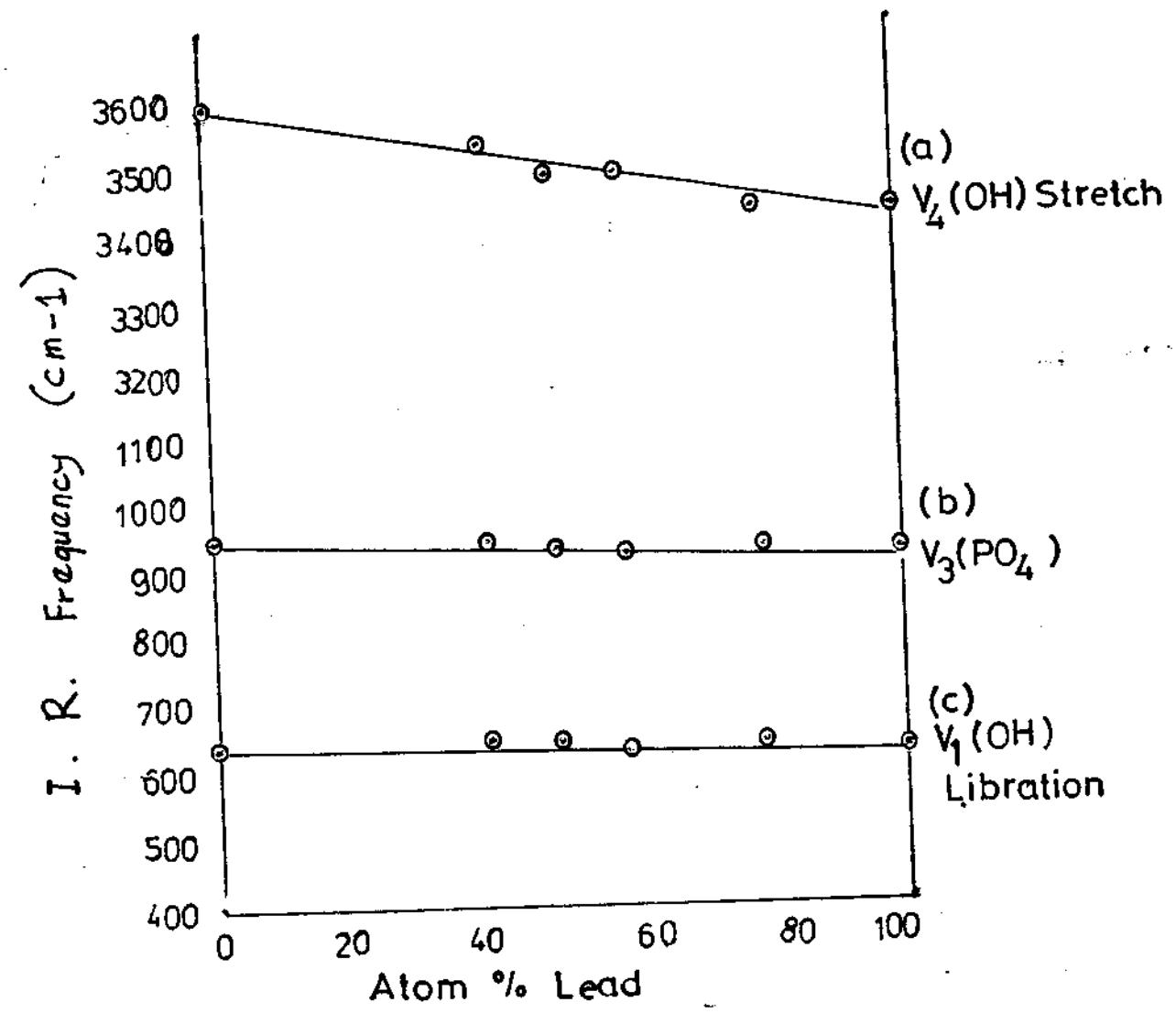


Fig 5.4

Infra-red frequencies for Sr-Pb hydroxyapatite solid solutions against atom % lead (PH 5~6)

Equations for the lines:

(a) $y = 3586.90 - 1.58x$ ($n=6$, $\sigma = 7.6$)

(b) $y = 950.39 - 0.23x$ ($n=6$, $\sigma = 2.22$

(c) $y = 637.97 - 0.09x$ ($n=6$, $\sigma = 2.36$

(y = infra-red frequency; x = atom % lead; σ = standard deviation)

TABLE 5.9
Strontium, zinc and Phosphorus contents (weight percent) of Strontium-zinc hydroxyapatite solid solutions precipitated from Aqueous Ammonia Solution (pH 10.5) and their infra-red frequencies.

Zn Content (Atom %)	Weight (%) Sr	Zn	P	Molecular formula	Mole-Atom Ratio Sr+Zn/p	I.R. Frequencies (cm^{-1}) (PO_4)	(OH)	(OH)
0	57.80	-	12.06	$Sr_{9.96}(PO_4)_6(OH)_2$	1.66	1090	540	3590
40	36.87	18.40	12.98	$Sr_{5.86}Zn_{3.92}(PO_4)_6(OH)_2$	1.63	1090	580	3580
50	31.03	23.75	13.08	$Sr_{4.86}Zn_{4.97}(PO_4)_6(OH)_2$	1.64	1075	620	3565
60	24.80	30.06	13.62	$Sr_{3.81}Zn_{6.19}(PO_4)_6(OH)_2$	1.67	1080	630	3560
80	13.20	39.63	13.93	$Sr_{1.96}Zn_{7.89}(PO_4)_6(OH)_2$	1.64	1080	630	3540
100	-	51.86	14.40	$Zn_{9.6}(PO_4)_6(OH)_2$	1.66	1080	640	3500

TABLE 5.10
Expected [e] and Observed [o] contents (weight percent) of strontium, zinc and phosphorus in strontium-zinc hydroxyapatite solid solutions precipitated from Aqueous Ammonia Solution (pH = 10.5) based on the molecular formula, $Sr_{10-x}Zn_x(PO_4)_6(OH)_2$.

Zn content (atom %)	Sr[o]	Sr[e]	Zn[o]	Zn[e]	P[o]	P[e]
0	57.8	59.20	0	0	12.06	12.56
40	36.87	37.79	18.40	18.80	12.36	13.36
50	31.03	32.01	23.75	23.88	13.08	13.58
60	24.80	26.03	30.06	29.13	13.62	13.80
80	13.20	13.46	39.63	40.17	13.93	14.28
100	0	0	51.86	59.98	14.40	14.78

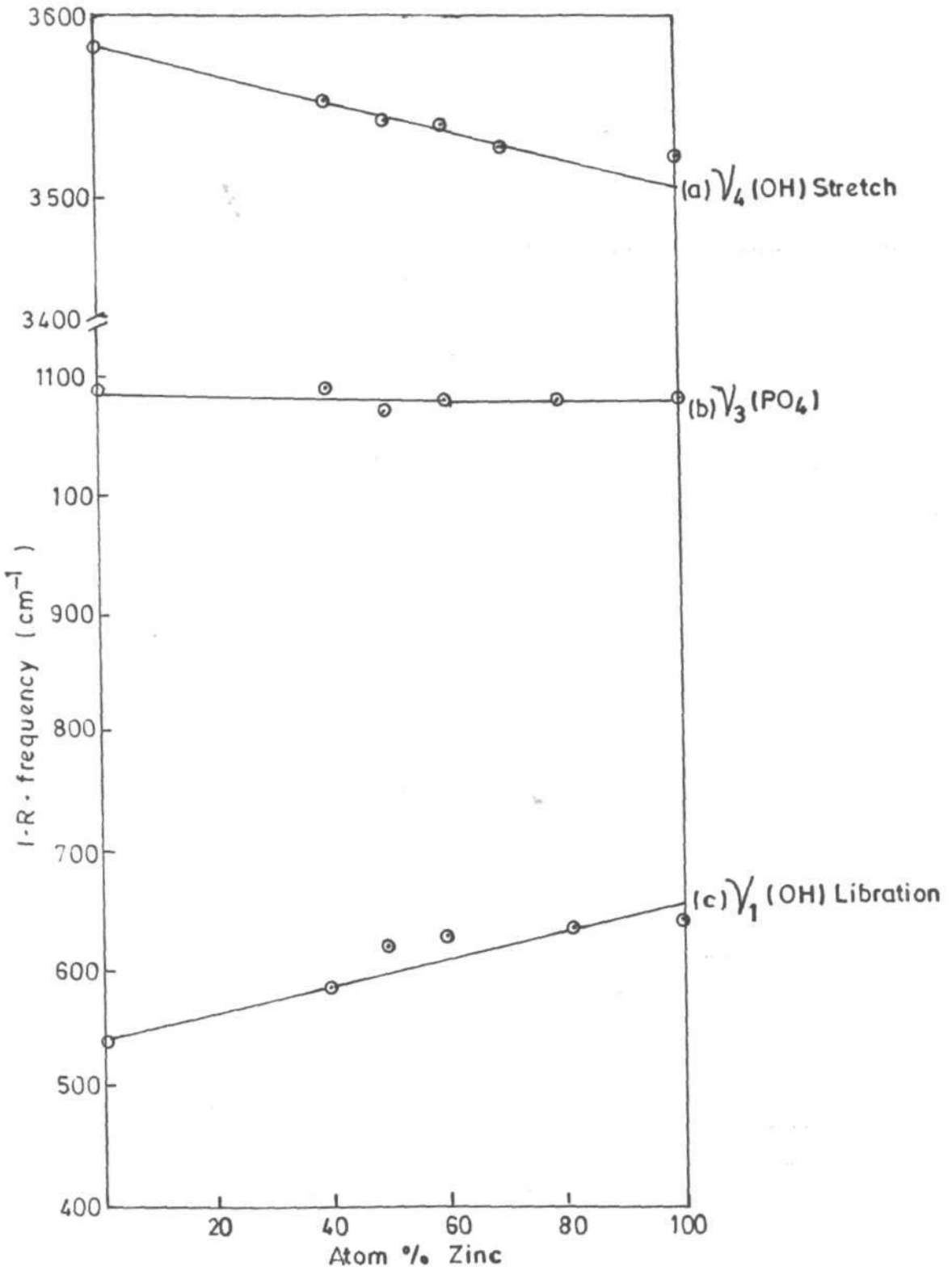


Figure 5.5: Infra-red frequencies for strontium-zinc hydroxyaptite solid solutions against atom % zinc (Basic medium, PH = 10·5)

Equations for the Lines:–

(a) $y = 3603{\cdot}7 - 0{\cdot}87x$ ($n = 6, \sigma = 10{\cdot}7$)

(b) $y = 1088 - 0{\cdot}1x$ ($n = 6, \sigma = 4{\cdot}44$)

(c) $y = 548 + 1{\cdot}06x$ ($n = 6, \sigma = 13{\cdot}9$)

(y = infra-red frequency; x = atom %; σ = standard deviation)

TABLE 5.11
Strontium, zinc and Phosphorus contents (weight percent) of Strontium-zinc hydroxyapatite solid solutions precipitated from Acidic Medium and their their infra-red frequencies.

Zn Content (Atom %)	Weight (%) Sr	Zn	P	Molecular formula	Mole-Atom Ratio Sr+Zn/p	I.R Frequencies (cm^{-1}) (PO_4	(OH)	(OH)
0	58.75	0	12.24	$Sr_{9.92}(PO_4)_6(OH)_2$	1.65	1100	540	3590
40	37.37	17.88	13.20	$Sr_{5.93}Zn_{3.59}(PO_4)_6(OH)_2$	1.62	1105	620	3580
50	31.50	23.42	13.51	$Sr_{4.92}Zn_{4.90}(PO_4)_6(OH)_2$	1.64	1080	630	3565
60	25.50	29.20	13.91	$Sr_{3.92}Zn_{6.01}(PO_4)_6(OH)_2$	1.66	1075	640	3560
80	12.99	38.92	13.69	$Sr_{1.93}Zn_{8.06}(PO_4)_6(OH)_2$	1.67	1080	640	3560
100	0	49.85	13.83	$Zn_{9.98}(PO_4)_6(OH)_2$	1.66	1080	640	3560

TABLE 5.12
Expected [e] and Observed [o] strontium, zinc and phosphorus contents (weight percent) of strontium-zinc hydroxyapatite solid solutions precipitated from Acidic medium (pH ≃ 5-6) based on the molecular formula, $Sr_{10-x}Zn_x(PO_4)_6(OH)_2$.

Zn content (atom %)	Sr[o]	Sr[e]	Zn[o]	Zn[e]	P[o]	P[e]
0	58.78	59.20	0	0	12.24	12.56
40	37.37	37.79	17.88	18.80	13.20	13.36
50	31.50	32.01	23.42	23.88	13.51	13.58
60	25.50	26.03	29.20	29.13	13.91	13.80
80	12.99	13.46	38.92	40.17	13.69	14.27
100	0	0	49.85	51.98	13.83	14.78

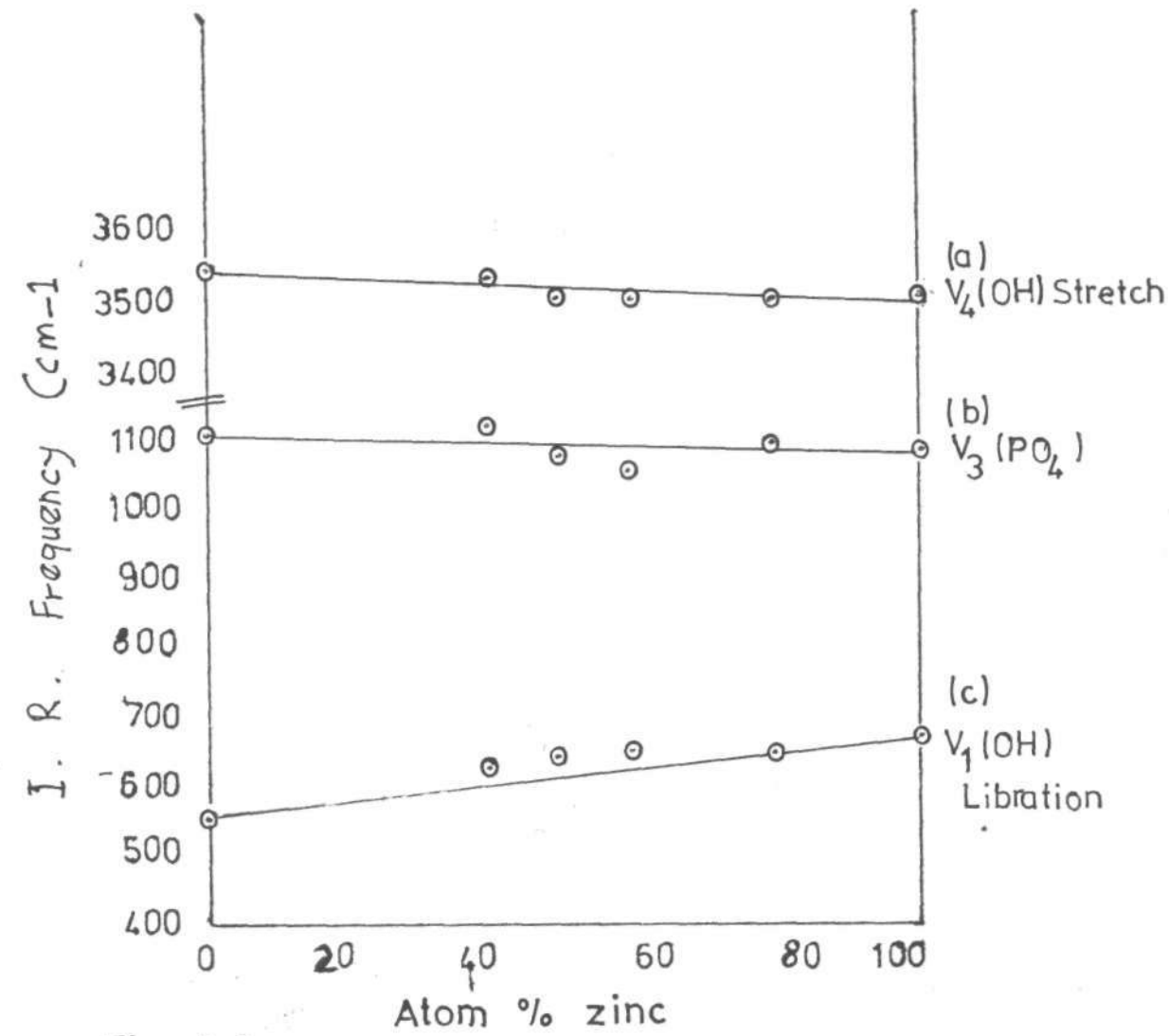


Fig 5.6

Infra-red frequencies for Sr-Zn hydroxyapatite solid solutions against atom % zinc (PH = 5~6)

Equations for the lines:

(a) $y = 3588 - 0.33x$ ($n = 6$; $\sigma = 4.30$)

(b) $y = 1100.25 - 0.25x$ ($n = 6$; $\sigma = 8.27$)

(c) $y = 564.26 + 0.98x$ ($n = 6$; $\sigma = 18.06$)

(y = infra-red frequency; x = atom % zinc; σ = standard deviation)

5.4 Discussion

The analytical results (tables 5.1, 5.3, 5.5 and 5.9) show that the concentrations of cadmium and zinc in the strontium-cadmium and strontium-zinc hydroxyapatites respectively are slightly less than concentrations in the mediating solutions. Similar results have been observed for calcium-magnesium and calcium-zinc hydroxyapatite solid solutions which are also in agreement with that reported by Bigi et al (1984) for the calcium-barium hydroxyapatite system. A comparison of tables 5.1, 5.3, 5.5 and 5.9 shows that higher concentrations of the substituting cations are incorporated in the hydroxyapatite structure in the basic medium than in the acidic medium. This again, may be attributed to a possible loss of the substituting cation as the acid phosphate, the formation of which is probably enhanced in an acidic medium (Rathje, 1941, as quoted by Narasaraju et al, 1972). The amount of the substituting cation rejected is however quite small. For example, the amount of cadmium rejected is about 0.10-1.35%; while the amount of zinc rejected in the strontium-zinc hydroxyapatite system ranges from 0.5-1.3%. Similarly, the amount of lead rejected in the strontium-lead hydroxyapatite (about 0.5-2.1%) is negligible (tables 5.6, 5.8, 5.10 & 5.12).

The infra-red absorption patterns for the cadmium substituted strontium hydroxyapatite and for the zinc substituted strontium hydroxyapatite systems are quite

similar. The frequencies attributable to the PO_4 vibrational mode and the OH stretching mode are shifted to lower values in both cases with increasing cation substitution for the strontium. Another area of similarity is the increase in the OH librational frequencies with increasing replacement of strontium by either cadmium or zinc (figures 5.1, 5.2, 5.5 and 5.6).

The observed similarity in the behaviour of cadmium and zinc towards strontium hydroxyapatite may be attributed to the similarities in the chemistries of zinc and cadmium. For instance, cadmium and zinc have completed d-shells and there is no ligand field stabilization in Cd^{2+} and Zn^{2+} ions. They also have large polarizing power (Cotton and Wilkinson, 1972). Cd^{2+} and Zn^{2+} ions may consequently cause similar binding effects arising from M-OH interactions which will be in agreement with predominant role of M-OH (M = cation) interaction with respect to the $OH-\overset{?}{-}-O(PO_3)$ hydrogen bond (Fowler, 1974; Bigi et al, 1991).

The intermediate internal PO_4 frequencies for cadmium, lead and zinc substituted strontium hydroxyapatite which shift to lower values with increasing replacement of strontium may be explained as being due primarily to the effects of decreased anion-anion repulsion concomitant with increased cation mass and weaker cation-anion bonding (Fowler, 1974). This is in agreement with the report of Klee and Engel (1970) which indicated that the mass of the cation has the greatest influence on the mean frequencies

of the internal PO_4 vibrational modes. They reported that decreasing trends in mean vibrational frequencies of the PO_4 group occurs as the mass of the cation increases.

The observed shift of PO_4 absorption bands to lower values may also be explained on the basis of binding energy effects whereby under the reaction conditions, these cations, Cd^{2+}, Zn^{2+} and Pb^{2+} form stronger coordination bonds with the PO_4 group which in turn weakens the P-O bond. This then causes an increase in the bond length of the P-O bond which lowers the frequency.

The observed decrease in OH-stretching frequencies with increasing concentrations of the substituting cation for the strontium-cadmium, strontium-zinc and strontium-lead hydroxy-apatite solid solutions (figures 5.1, 5.2, 5.3, 5.4, 5.5 and 5,6) and the marked increase in the OH-librational frequencies with increasing concentration of the substituting cation for strontium-cadmium and strontium-zinc hydroxyapatites (figures 5.1, 5.2, 5.3 and 5.4) are in agreement with those reported by Bigi et al (1984) for calcium-barium hydroxyapatite system. These results are also similar to those reported by Fowler (1974) for calcium, strontium and barium hydroxyapatites. He attributed the shift in OH frequencies to differences in OH-bonding between the cations. The shift in OH librational mode to higher frequencies is however not continuous for the strontium-zinc system in the non-basic medium. For example, with greater than 60 zinc atom percent, the

frequencies remained practically constant (figure 5.5). This observation is similar to that made by Bigi et al, (1991) for the OH vibrational modes for lead-calcium hydroxyapatite system. It may be due to inhomogeneous distribution of zinc in the two non-equivalent cation sites of the apatite structure.

On the whole, the near linearity of the plot of infra-red absorption frequencies against atom percent of each substituting cation and the mole-atom ratios for the preparations which ranged from 1.62 - 1.67 (theoretical value = 1.67) are indications that solid solutions have been obtained in all proportions when zinc, cadmium, or lead substitutes for strontium in strontium hydroxyapatite both in basic and acidic media. The formation of apatitic samples in both basic and acidic media indicates that the mode of interaction is such that allows the incorporation of the substituting cation (Pb^{2+}, Cd^{2+} and Zn^{2+}) into the apatite lattice.

CHAPTER SIX

A MODIFIED METHOD OF PREPARATION OF LEAD HYDROXYAPATITE FROM AQUEOUS SOLUTION

6.1 Introduction

While the preparation of calcium hydroxyapatite has been investigated in great detail, that of lead hydroxyapatite has not and therefore needs further investigation. Most available methods for the preparation of lead hydroxyapatite are of limited utility especially for a rapid preparation of appreciable quantities of the apatite (Narasaraju et al, 1972; Bigi et al, 1989 and 1991; Legeros et al, 1980; Merker and Wondratschek, 1959; Klee and Engel, 1970). Lead hydroxyapatite (PbHA) has been used in ion-exchange column by some Japanese workers (Thomas, 1992). For this and similar large-scale use of the apatite, a method for its high yield production is required. An attempt by Bigi et al (1991) to device a method of high yield preparation of lead hydroxyapatite gave both the required apatite and a contaminating Lead(II)oxide, PbO, as by product.

In this chapter, an attempt has been made to modify the method of Bigi et al (1991) in order to obtain pure lead hydroxyapatite free from contamination by lead (II) oxide, PbO. The products obtained have been characterised by atomic absorption, infra-red, colorimetry and X-ray powder diffraction analyses.

6.2 Experimental.

6.2.1 Preparation of the basic salt, $Pb_6O_5(NO_3)_2$.

The basic salt, $Pb_6O_5(NO_3)_2$ is often erroneously referred to as lead (II) hydroxide. The uncertain status of lead (II) hydroxide was first pointed out by Robin and Theolier (Kirk and Hughes, 1970) who claimed to have made it by the thermal decomposition at 280 - 300°C of a basic salt precipitated by ammonium hydroxide from a solution of lead (II) nitrate. This "lead hydroxide" of Robin and Theolier was later identified as $Pb_6O_5(NO_3)_2$.

The basic salt, $Pb_6O_5(NO_3)_2$, was prepared by using the Robin and Theolier method (Kirk and Hughes, 1970). 70g of lead (II) nitrate was dissolved in 2.10dm^3 of doubly distilled water and precipitated with 175 cm^3 concentrated ammonia solution. The supernatant liquid was filtered off and the resulting precipitate heated in an oven at 285°C for 15hours. This gave the basic salt, $Pb_6O_5(NO_3)_2$ which is a yellow solid and commonly referred to as "lead (II) hydroxide."

6.2.2 Preparation of Lead hydroxyapatite from the basic salt, $Pb_6O_5(NO_3)_2$.

500 cm^3 solution of 0.5M $Pb_6O_5(NO_3)_2$ was prepared by dissolving stoichiometric amount of the basic salt in water. The solution was heated to boil in a flask with continuous stirring. 500 cm^3 of 0.3M Orthophosphoric acid solution was then added drop-wise with constant stirring

and the temperature maintained at about 100°C.

The product was brought to pH 12 with concentrated ammonia solution and refluxed for about 2hours. Such basic medium has been reported by Narasaraju et al, (1972) to be favourable for the formation of lead hydroxyapatite. Since the addition of ammonia solution to lead nitrate results in the precipitation of "lead (II) hydroxide", care was taken to see that the mixing was done in such a way as to ensure total conversion of all lead (II) oxide along with the lead (II) nitrate in the basic salt, $Pb_6O_5(NO_3)_2$ into the hydroxy-orthophosphate groups characteristic of the desired apatite.

The resulting precipitate after refluxing was dissolved in concentrated nitric acid to give a brown solution. Ammonia solution was subsequently added to the brown solution to raise its pH to 12, when lead hydroxyapatite was precipitated as a white solid. Using a suction pump and sodalime towers, carbon dioxide-free air was bubbled through the medium of precipitation to eliminate the formation of carbonate apatite and to keep it, in addition, well stirred. The precipitate and mother liquor were again aged by boiling under reflux for about 30 minutes to improve the homogeneity and crystallinity of the precipitate. Maintenance of the desired pH during precipitation was ensured by checking the pH of the filtrate after separation of the precipitate. The precipitate was left overnight in contact with mother

liquor and later filtered, washed with doubly distilled water till washings were neutral and dried at 105°C for 6 hours.

6.2.3 Chemical Analyses of Lead Hydroxyapatite.

6.2.3.1 Colorimetric Determination of Phosphorus Content of lead Hydroxyapatite.

The phosphorus content of the prepared lead hydroxyapatite samples were determined colorimetrically using the molybdenum blue method as described for calcium-magnesium hydroxyapatite in section 3.2.8.1 using a Unicam SP 1750 B for absorbance measurements.

6.2.3.3 Infra-red Absorption Analysis.

Infra-red absorptions of the prepared lead hydroxyapatite samples were taken using the same instrumental conditions and procedure as stated in section 3.2.8.3.

6.2.4 X-ray Powder Diffraction Analysis.

X-ray Powder Diffraction Measurements for the prepared lead hydroxyapatite were carried as described for calcium-magnesium hydroxyapatite in section 3.1.9.

6.2.5 Results and Discussion.

The results of the chemical analyses of the lead hydroxyapatite prepared by the modified method are shown in

table 6.1. The atomic absorption data for lead and the colorimetric data for phosphorus contents are in excellent agreement with those based on stoichiometry (expected values). The infra-red frequencies shown in table 6.1, reveal the presence of three major bands in each sample which are characteristic of apatitic samples. These include 933 to 930cm^{-1} and 1030cm^{-1} corresponding to the PO_4 vibrational modes and the 3560 to 3550cm^{-1} attributable to the OH stretching mode (Klee and Engel, 1970, 1974; Bigi et al, 1991).

Based on the fact that a mole of each sample has a total of 10 moles of lead atoms, the molecular formulae of the samples were calculated from the atomic absorption results in table 6.1. The mole-atom ratio for each sample was obtained from the calculated molecular formulae. The values obtained are in agreement with that based on stoichiometry (Narasaraju et al, 1972) as shown in table 6.2. They are also in agreement with those reported by Bigi et al (1989) for lead hydroxyapatite samples.

The X-ray powder diffraction patterns obtained have been compared with that reported by Bigi et al (1991). The results show that reflections due to the contamination of the lead hydroxyapatite by lead (II) oxide, PbO as reported by Bigi et al (1991) are absent in the powder patterns obtained for lead hydroxyapatite prepared by the modified method (figure 6.1). This indicates that the modified method has a dual advantage of being suitable for high

yield preparation of lead hydroxyapatite and gives pure apatitic samples. Furthermore, the d-spacing and relative intensities obtained from the powder diffraction patterns of the lead hydroxyapatite samples prepared by the modified method were compared with standard X-ray powder diffraction patterns of lead hydroxyapatite provided by the Joint Committee on Powder Diffraction Standards (JCPDS). The highest peak (relative intensity = 100) observed for three samples of the prepared lead hydroxyapatite had 2θ values of 30.30° and 30.00°; corresponding to d-spacing of 2.95 and 2.98Å respectively (Appendix IV). These are in good agreement with values contained in the JCPDS cards for lead hydroxyapatite where the highest peak (relative intensity = 100) had d-spacing of 2.965 and 2.974Å. The d-spacing and relative intensities for other peaks are also closely matched. This level of correspondence in d-spacing and relative intensities provide additional evidence that the samples prepared by this modified method are pure lead hydroxyapatite (Thomas, 1989).

TABLE 6.1
Expected [e] and Observed [o] Lead and Phosphorus contents of Lead hydroxyapatite prepared by the Modified method and its infra-red frequencies.

	Weight %				Infra-red Frequency		
Sample	Pb[e]	Pb[o]	P[e]	P[o]	$V_1(PO_4)$	$V_3(PO_4)$	$V_4(OH_4)$
1.	77.43	77.38	6.94	6.85	935	1030	3560
2.	77.43	77.35	6.94	6.88	935	1030	3550
3.	77.43	77.36	6.94	6.80	930	1030	3560
4.	77.43	77.38	6.94	6.85	930	1030	3560

TABLE 6.2
Observed Molecular Formula and Mole-Atom Ratio of Lead Hydroxyapatite prepared by the Modified Method.

Sample	Observed Molecular Formula	Mole-Atom Ratio (Pb/p)
1.	$Pb_{9.99}(PO_4)_6(OH)_2$	1.67
2.	$Pb_{9.98}(PO_4)_6(OH)_2$	1.67
3.	$Pb_{9.99}(PO_4)_6(OH)_2$	1.67
4.	$Pb_{9.99}(PO_4)_6(OH)_2$	1.67

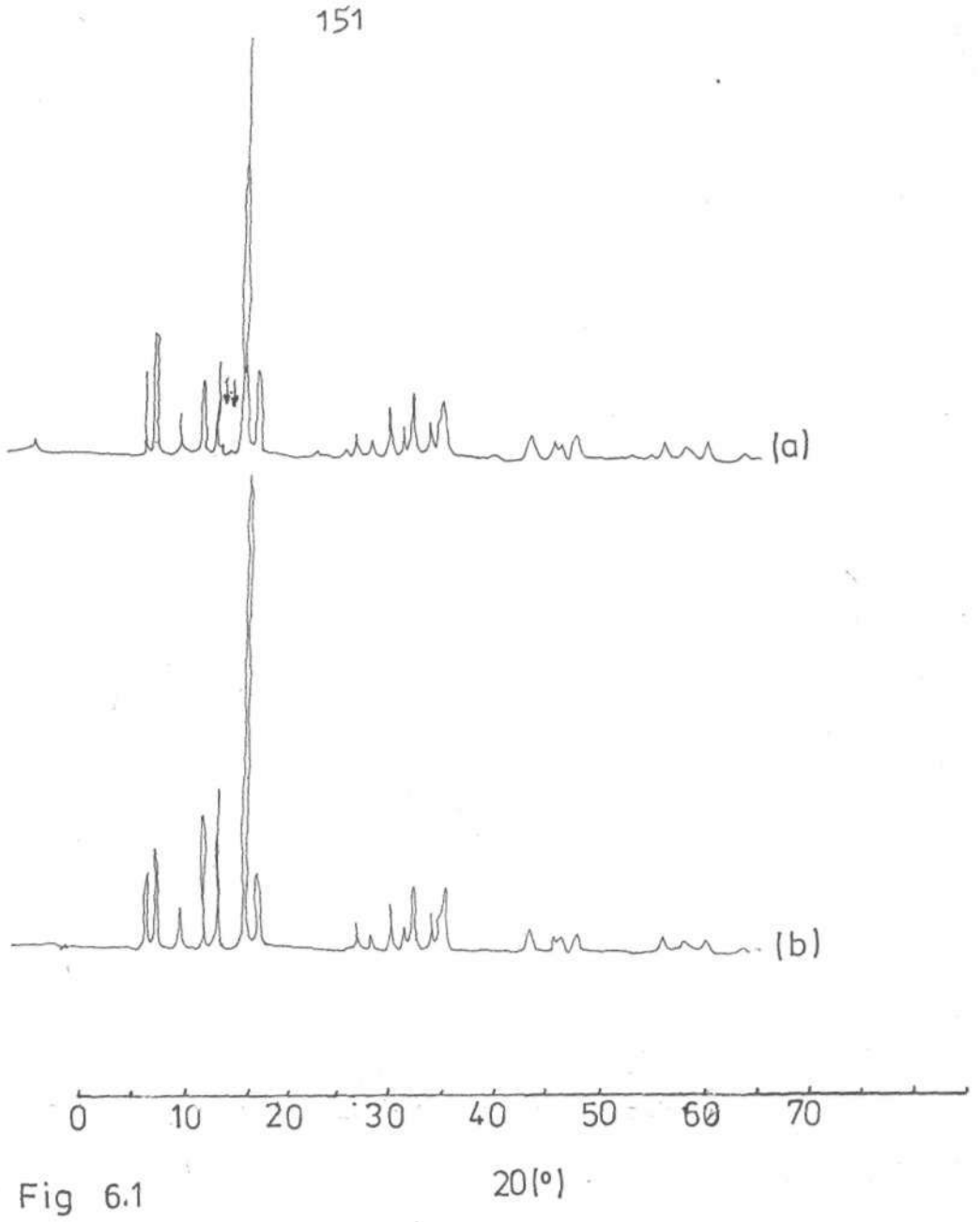


Fig 6.1

A comparison of x-ray powder diffraction patterns for Lead hydroxyapatite curve (a) is the powder diffraction patterns of Lead hydroxyapatite contaminated with PbO_2; the arrows indicate the reflections due to the PbO phase. curve (b) is the powder patterns for pure Lead hydroxyapatite.

CHAPTER SEVEN

SUMMARY, CONCLUSION AND RECOMMENDATIONS.

7.1 Summary.

In this study, cation exchange reactions in calcium hydroxyapatite and other metal hydroxyapatites have being carried out by the method of co-precipitation in aqueous ammonia and acidic media. Solid state synthesis have also been carried out in some cases. Products of the substitution reactions were characterized by atomic absorption, infra-red, ultraviolet/ visible and in some cases, X-ray powder diffraction analyses. The study was undertaken as part of an on-going attempt at clarifying the nature of interaction of cations with hydroxyapatite.

Solid solutions of calcium-magnesium hydroxyapatite were prepared by the method of co-precipitation (Legeros et al, 1980, Bigi et al, 1984, Patel, 1979) from aqueous solution at pH 12. Preparation of calcium-zinc hydroxyapatite solid solutions were attempted using the co-precipitation method in basic and acidic media. While solid solutions were formed between Mg^{2+} and Ca^{2+} at a high pH, solid solutions of calcium-zinc hydrodyapatite were not obtained in both acidic and basic media. Magnesium formed solid solutions of calcium-magnesium hydroxyapatite in the entire range at a high pH of 12 in agreement with the report of Patel (1979) which stated that Mg^{2+} is able to form solid solutions of calcium-magnesium hydroxyapatite at

pH9 and above. However, zinc did not form solid solutions of calcium-zinc hydroxyapatite in both basic and acidic media as reveald by the x-ray powder diffraction results. The products were mainly zinc and calcium pyrophosphates. Substitution reactions between lead and calcium hydroxyapatite were also carried out by solid state process at 900°C. It gave solid solutions in the whole range.

The solid solutions of calcium-magnesium and calcium-lead hydroxyapatite obtained were characterized by spectroscopic and crystallographic analysis (calcium-zinc hydroxyapatites were characterized by spectroscopic method only). Their infra-red absorption frequencies gave values which varied essentially linearly with the atom % of each substituting cation in the whole composition range. This suggests that solid solutions have been formed in the whole series (Patel, 1979; Bigi et al, 1984 and 1991; Collin, 1959; Partington, 1957). The X-ray powder diffraction patterns for the calcium-magnesium hydroxyapatite samples show that the incorporation of Mg^{2+} in the hydroxyapatite lattice produces a sharpening of the X-ray peaks and the enhancement of peak intensity. Also, the replacement of calcium by lead in the hydroxyapatite structure caused expansion of lattice parameters which is consistent with the larger ionic radius of lead (Pb^{2+} = 1.21A°; Ca^{2+} = 0.99A°). Such dilation with increasing proportion of lead content is in agreement with that reported by Narasaraju et al, (1972), Bigi et al (1984 and 1991) and Collin, (1959).

Isomorphous substitution in lead hydroxyapatite (PbHA) by Cd^{2+} and Ba^{2+} has been carried out. While calcium formed solid solutions of lead - calcium hydroxyapatite in the entire range in both basic and acidic media, barium did not. Precipitates obtained at 100°C through co-precipitation by drop-wise addition of lead and barium acetate solutions to a stirring ammonium dihydrogen phosphate in both basic and acidic media gave solid solutions only in the range of barium concentration in solution from 0 - 40%. This is evidenced from the infra-red absorption spectra of the samples in which the bands characteristic of the OH group are absent for samples beyond 40 atom % barium. However, the products obtained from the solid state reaction between lead hydroxyapatite and barium hydroxyapatite are solid solutions in the whole composition range. Infra-red frequencies of the products are characteristic of apatitic samples. While the OH stretching and librational frequencies for lead - cadmium hydroxyapatite samples increase with increase in cadmium atom concentration, the V_1. (PO_4) and V_3 (PO_4) internal vibrational modes decrease with increase in cadmium atom %. The plots of the infra-red absorption frequencies of lead-cadmium hydroxyapatite prepared in basic and acidic media show that the frequencies vary linearly with increasing cadmium concentration. The same variation is observed for lead-barium hydroxyapatite samples prepared by solid state reaction as the barium atom concentration increases.

Substitution of strontium in strontium hydroxyapatite by cadmium, zinc and lead have been studied in basic and acidic media by the method of co-precipitation. Solid solutions of strontium - cadmium, strontium-lead and strontium-zinc in the complete series were obtained in each case. Results obtained show that cadmium and zinc behave in a similar manner towards strontium hydroxyapatite. This similarity in the behaviour of zinc and cadmium has been attributed to the similarities in the chemistries of both elements. For instance, cadmium and zinc have completed d-shells and there is no ligand field stabilization in Zn^{2+} and Cd^{2+} ions. They also have large polarizing power (Cotton and Wilkinson, 1972). These results are similar to those observed for substitution reactions between Mg^{2+} and calcium hydroxyapatite and that between Zn^{2+} and calcium hydroxyapatite. The concentrations of cadmium and zinc in the strontium - cadmium and strontium-zinc hydroxyapatite solid solutions respectively, are only slightly less than those in the mediating solutions. Higher concentrations of the substituting cation are incorporated into the apatite lattice in the basic than acidic medium.

The infra-red absorption patterns for strontium - cadmium and strontium-zinc hydroxyapatite solid solutions are similar but differ from that of strontium-lead hydroxyapatite in certain respect. The frequencies due to PO_4 vibrational mode and the OH stretching mode are shifted to lower values in the strontium-cadmium, strontium-zinc

and strontium-lead hydroxyapatites with increasing cation substitution. However, while the OH librational mode increases with increasing replacement of Sr^{2+} by either Cd^{2+} or Zn^{2+}, it decreases with increasing replacement of Sr^{2+} by Pb^{2+}. The similarity in the infra-red patterns for strontium-cadmium and strontium-zinc hydroxyapatites has been attributed to the similarities in the chemistries of cadmium and zinc. The PO_4 frequencies are shifted to lower values with increasing replacement of strontium. Vibrational frequencies of the PO_4 group have been reported to decrease as the mass of the cation increases. (Fowler, 1974; Klee and Engel, 1970). The mole-atom ratios for the preparations range from 1.62 to 1.67. These suggest that solid solutions are formed in the whole composition range in each case when Cd^{2+}, Zn^{2+} or Pb^{2+} substitutes for strontium in strontium hydroxyapatite.

Also in this study, a modified method has been evolved for a high yield preparation of lead hydroxyapatite. This involves the initial synthesis of the basic salt, $Pb_6O_6(NO_3)_2$ using the Robin and Theolier method as described by Newkirk and Hughes (1970). A stoichiometric amount of the salt is then dissolved in doubly distilled water and titrated with phosphoric acid with constant stirring at about 100°C. Products obtained are brought to pH 12 with concentrated ammonia solution and refluxed for about 2 hours. The resulting precipitate is dissolved in concentrated nitric acid followed by another addition of

concentrated ammonia solution to raise the pH back to 12. A white precipitate of lead hydroxyapatite obtained at this stage is refluxed with the mother liquor for about 30 minutes and left over-night. X-ray powder diffraction patterns of the prepared lead hydroxyapatite have similar d-spacing and relative intensities with standard powder patterns of lead hydroxyapatite provided by the Joint Committee on Powder Diffraction Standards. (JCPDS, 1974).

7.2 Conclusion.

It has been established that:

I. The pH of the medium from which solid solutions are precipitated may affect the nature of the products and extent of incorporation of cation in the apatite structure. Thus, Mg^{2+} substituted Ca^{2+} in hydroxy-apatite in the whole composition range at pH 12. By comparison with literature reports it would appear that at pH less than 9, tricalcium phosphate is the main product of the interaction of Mg^{2+} with hydroxyapatite. When Zn^{2+} substitutes Ca^{2+} in hydroxyapatite, in both basic and acidic media the major product is the pyrophosphate. Furthermore, higher concentrations of Cd^{2+} ions are accepted into the apatite lattice in a basic medium (pH = 10.5) than in acidic medium (pH = 5 - 6) when Cd^{2+} replaces Pb^{2+} in lead hydroxyapatite. Higher

concentrations of the substituting cation were also incorporated in the basic medium than in the acidic medium when Cd^{2+}, Zn^{2+} and Pb^{2+} substituted Sr^{2+} in strontium hydroxyapatite. These observations indicate that some cations may be lost to the mediating medium as the hydrogen phosphate. It may also be concluded that at acidic/ physiological pH, the interaction of Mg^{2+} with the apatite is a surface phenomenon. However, at alkaline pH, there is a possibility of the incorporation of the Mg^{2+} into the apatite lattice. This leads to only growth sites at the apatite lattice which are blocked, thus leading to the formation of other phases such as tricalcium phosphate and its derivatives. In the other cases, Pb - Cd, Pb - Sr, and Sr - Zn hydroxyapatites where apatitic samples are obtained in both acidic and alkaline media, the mode of interaction is such that allows their incorporation into the apatite lattice.

II. The method of preparation may also influence the extent of cationic substitution in the apatite structure. For example, only 0 to 40 atom % barium substituted for lead in hydroxyapatite in aqueous medium. However, by solid state reaction, barium replaced lead in hydroxyapatite in the whole composition range. Literature

reports also show that in aqueous medium, Ba^{2+} replaces Ca^{2+} in hydroxyapatite only in the range of barium concentration from 0 to 25%. In the solid state reaction however, Ba^{2+} is reported to have substituted Ca^{2+} in hydroxyapatite from 60 to 100 atom % barium.

III The size of the substituting cation appears to affect the extent of isomorphous substitution in apatite systems. Thus, Cd^{2+}, a smaller cation than Pb^{2+}, formed solid solutions of lead-cadmium hydroxyapatite in aqueous medium in the whole series. Ba^{2+}, a larger cation than Pb^{2+}, formed solid solutions of lead - barium hydroxyapatite in aqueous medium only in the range of about 0 to 40 atom % barium. Mg^{2+} which is smaller in size than Ca^{2+} replaced calcium in hydroxyapatite in the whole series in aqueous medium while Ba^{2+} does not. Similarly, Cd^{2+}, Zn^{2+} and Pb^{2+} which are smaller than Sr^{2+} replaced strontium in strontium hydroxyapatite in the entire composition range in aqueous medium.

IV The crystallinity of an apatite prepared under the conditions used in this study appears to increase with increasing replacement of a larger cation. Similarly, the crystallinity of an apatite seems to decrease with increasing substitution of a smaller cation with a larger

one. For example, the x-ray powder peaks for calcium-magnesium hydroxyapatite solid solutions are sharper with increasing concentration of Mg^{2+}. The same observation has been made for the lead - cadmium hydroxyapatite solid solutions as the Cd^{2+} concentration increases. The increased sharpening of the x-ray powder peaks is an indication of increase in crystallinity. However, the substitution of Pb^{2+} by a larger cation, Ba^{2+}, resulted in broader x-ray powder peaks as the Ba^{2+} concentration increases. Amorphous precipitates were obtained for reactions containing more than 40 atom % barium when Ba^{2+} interacted with lead hydroxyapatite in aqueous medium.

V Preparation of lead hydroxyapatite can be made from the basic salt, $Pb_3O_3(NO_3)_2$. Contamination by lead (II) oxide, PbO, is eliminated by fluctuating the pH of the reaction medium. The modified method gives a high yield of the lead hydroxyapatite (about 100%).

<u>Recommendations</u>

I. Isomorphous substitution in synthetic hydroxyapatite should be carried out in an atmosphere free of carbon dioxide. In the form of a carbonate, CO_3^{2-}, carbon dioxide causes changes

in morphology of apatite from needle - like rods to equi-axial crystals and reduction in crystallite size.

II. Since the present study is limited to synthetic systems, its extension to biological systems should be worthwhile. The role of strontium for example, in biological apatite needs further investigation. This becomes apparent from the fact that experiments have shown that lack of strontium in rats is thought to cause a high incidence of dental caries.

III Further investigation of strontium-zinc hydroxyapatite solid solutions for a possible inhomogeneous distribution of zinc in non-equivalent cation sites is recommended.

REFERENCES

AASENDEN, R. and Peebles, T.C. (1978). Effects of Fluoride Supplementation from Birth on Dental Caries and Fluorisis in Teenaged children. Arch. Oral Biol. 23 (2), 111 - 115.

AMLER, M. H. and Legeros, R. Z (1979) Infra-red absorption analysis of enameloma. N.Y Sc. Jour. 45 , 502 - 503

ANDRES - VERGES, M., Higes - Rolando, F. J, Valenzuela - Calahorro, C. and Gonzales - Diaz, P. F. (1983), Spectrochim Acta part A, 39, 1077.

BARAVELLI, S., Bigi, A., Ripamonti, A., Roveri, N. and Foresti E. (1984). Thermal Behaviour of Bone and Synthetic Hydroxyapatites Submitted to magnesium Interaction in Aqueous medium. Journal of Inorganic Biochemistry, 20, 1-12.

BARNES, R. R., Gore, R. C., Liddel, V. and Williams, V.Z (1944). "Infra - red spectroscopy," Reinhold, New york.

BARONE, J. P., Nancollas, G. H. and Tomson, M. (1976). The Seeded Growth of Calcium Phosphate; the kinetics of Growth of dicalcium Phosphate Dihydrate on Hydroxyapatite. Calcif Tissue Res 21, 171 - 182.

BASSETT, J., Denny, R.C., Jeffery, G.A. and Mendham, J. (1982). Vogels Textbook of Quantitative Inorganic Analysis (Including Elementary Instrumental Analysis) 4th Ed. English Language Book Society and Longman, London.

Appendix II: X-ray Powder Diffraction Data for Lead-cadmium Hydroxyapatite Solid Solutions

$Pb_{100}Cd_0$			$Pb_{80}Cd_{20}$		
2θ	I/I_1	d(Å)	2θ	I/I_1	d(Å)
20.60	15.00	4.31	21.40	14.96	4.15
21.60	18.95	4.11	22.20	18.82	4.00
26.20	16.84	3.40	26.80	20.40	3.33
28.00	26.32	3.19	28.20	22.60	3.16
30.00	100	2.98	30.80	100.00	2.90
31.40	36.80	2.85	32.00	36.40	2.80
43.80	22.11	2.07	44.80	40.26	2.02
45.00	28.42	2.01	47.00	42.20	1.93
48.80	36.80	1.87	49.80	50.00	1.83

$Pb_{60}Cd_{40}$			$Pb_{60}Cd_{40}$		
2θ	I/I_1	d(Å)	2θ	I/I_1	d(Å)
21.00	10.80	4.23	20.20	12.00	4.40
22.00	15.63	4.04	21.60	20.20	4.11
26.60	20.30	3.35	26.2	18.00	3.40
27.80	28.13	3.21	27.40	20.40	3.26
30.40	100.00	2.94	30.00	100.00	2.98
31.80	29.69	2.81	31.40	32.36	2.85
41.40	12.50	2.18	42.20	18.00	2.14
44.60	26.80	2.03	44.60	27.60	2.03
46.8	39.06	1.94	45.80	40.80	1.98
49.8	40.60	1.83	49.60	60.40	1.84

Appendix III

X-ray Powder diffraction data for Barium Substituted lead hydroxyapatite (Basic Medium pH = 10.5)

Pb_{100} Bao			Pb_{80} Ba_{20}		
2θ	I/I_1	d(Å)	2θ	I/I_1	d(Å)
20.60	15.00	4.31	20.60	27.28	4.31
21.60	18.95	4.11	21.50	29.88	4.13
26.20	16.84	3.40	26.20	33.77	3.40
28.00	26.32	3.19	27.60	33.77	3.23
30.00	100.00	2.98	30.00	100.00	2.98
31.40	36.80	2.85	31.20	38.97	2.87
43.80	22.11	2.07	43.80	36.37	2.07
45.00	28.42	2.01	45.20	29.88	2.00
48.80	36.80	1.87	46.00	37.67	1.97
			47.80	62.09	1.90
			49.0	63.64	1.86

Pb_{60} Ba_{40}			Pb_{50} Ba_{50}		
2θ	I/I_1	d(Å)	2θ	I/I_1	d(Å)
20.30	30.14	4.37	20.20	30.00	4.40
21.20	33.70	4.19	21.0	32.50	4.23
25.00	68.48	3.56	24.2	32.50	3.68
28.00	64.13	3.19	25.6	32.50	3.48
29.60	100.00	3.02	27.0	37.50	3.30
31.00	42.39	2.88	29.60	100.00	3.02
31.60	39.13	2.83	30.80	60.00	2.90
35.40	21.14	2.54	35.20	22.50	2.55
38.00	26.43	2.37	38.60	20.00	2.33
43.50	30.65	2.08	40.00	25.00	2.25
44.80	32.25	2.02	43.40	32.50	2.08
45.69	33.70	1.99	44.60	30.00	2.30
47.40	32.61	1.92	45.60	35.00	1.99
48.60	36.96	1.87	47.20	27.50	1.93
			48.40	42.50	1.88

$Pb_{40}Ba_{60}$			$Pb_{0}Ba_{100}$		
2θ	I/I_1	d(Å)	2θ	I/I_1	d(Å)
18.80	17.42	4.72	20.00	35.00	4.44
20.00	19.28	4.44	23.00	21.25	3.87
20.40	16.51	4.35	25.00	100.00	3.55
21.60	16.51	4.11	25.40	42.50	3.51
25.20	100.00	3.53	28.80	30.00	3.10
26.50	61.44	3.53	31.40	32.50	2.84
30.00	46.77	2.98	35.60	56.25	2.52
31.40	25.68	2.85	39.00	37.50	2.31
32.00	32.10	2.80	40.60	19.49	2.22
35.80	26.59	2.51	41.40	11.69	2.18
38.20	31.18	2.36	45.20	21.25	2.01
39.20	29.34	2.30	46.00	10.39	1.97
43.20	19.26	2.09			
43.80	15.59	2.07			
45.30	16.51	2.00			
46.10	18.34	1.97			
47.80	22.93	1.90			

APPENDIX IV
X-ray Powder Diffraction Data for Lead Hydroxyapatite, $Pb_{10}(PO_4)_6(OH)_2$, prepared by the modified method.

Sample I			Sample II			Sample III		
2θ	I/I_1	d(A)	2θ	I/I_1	d(A)	2θ	I/I_1	d(A)
10.2	6	8.67	11.6	5	7.63	11.60	5	7.63
20.4	35	4.35	14.8	10	5.99	12.20	10	7.25
21.4	45	4.15	19.80	10	4.48	20.20	15	4.40
23.8	15	3.74	20.60	40	4.31	20.60	40	4.31
25.8	20	3.45	21.40	45	4.15	21.40	35	4.15
26.4	30	3.38	23.80	10	3.74	23.80	10	3.75
28.2	36	3.16	25.00	30	3.56	25.00	30	3.56
28.8	25	3.10	25.8	45	3.45	26.40	30	3.38
30.00	100	2.98	26.40	40	3.38	26.60	25	3.12
31.00	45	2.88	27.20	30	3.28	29.80	30	3.00
32.60	40	2.75	28.20	28	3.16	30.30	100	2.95
33.80	10	2.65	30.20	100	2.96	31.00	50	2.88
36.10	8	2.49	31.00	50	2.88	33.00	10	2.71
38.00	3	2.37	32.60	40	2.75	33.80	20	2.65
41.00	12	2.20	33.50	10	2.67	36.00	5	2.49
44.2	15	2.05	36.20	8	2.48	38.00	5	2.37
45.8	20	1.98	37.8	6	2.38	41.00	8	2.20
47.90	25	1.90	41.00	10	2.20	44.20	20	2.05
51.4	28	1.78	44.20	25	2.05	45.80	15	1.98
52.2	10	1.75	45.80	30	1.98	47.80	20	1.90
54.2	5	1.69	47.60	20	1.91	48.60	15	1.87
55.0	8	1.67	48.60	15	1.87	51.40	5	1.78
			50.40	15	1.81	54.20	6	1.69
			52.20	10	1.75	55.00	8	1.67
			54.20	5	1.69			

Appendix V

Joint Committee on Powder Diffraction Standards (1974)

for Lead Hydroxyapatite, $Pb_5(PO_4)_3OH$.

d(A)	I/I1	d(A)	I/I1
8.63	2	1.966	20
4.93	6	1.963	10
4.28	40	1.896	20
4.11	40	1.866	20
3.71	6	1.860	10
3.41	40	1.852	20
3.24	40	1.815	2
2.974	100	1.739	4
2.85	45	1.737	2
2.803	4	1.704	4
2.660	2	1.668	4
2.469	4	1.646	2
2.442	2	1.616	2
2.373	4	1.612	6
2.343	2	1.608	6
2.263	6	1.557	6
2.214	10	1.556	6
2.139	8	1.538	4
2.056	30		
1.999	20		

BARTELS, t., Van Pett, A. W., De Jong, H. P. and Arends, J. (1982) Surface Characteristics of Hydroxyapatite and Enamel after Absorption of Fluoride - Containing Macromolecules. Caries Res, 16(1), 51 - 56.

BAUD, C. A. Bangs, S. and Very, J. M. (1977). Minor Elements in Bone Mineral and their Effects on its Solubility. J. Biol Buccale, 5, 105 - 202.

BAUD, C. A. and Very, J, M. (1973) Colloq. Int. C.N.R.S. No 230, 405, In Emeleus, H. J. and Sowerby, D. B. (1975). International Review of Science. Inorganic Chemistry, Series Two, Volume 2, Butterworths University Park Press.

BERRY, E.E. (1967). The Structure and Composition of some Calcium Deficient Apatite. J. Inorg. nucl. Chem. 29, 317 -327.

BERRY, E.E., (1967). The Structure and Composition of Calcium Deficient Apatite II. J. Inorg. nucl. Chem. 29, 1585 - 1590.

BIGI, A., Foresti, E., Marchetti, F., Ripamonti A. and Roveri, N. (1984). Barium-Calcium Hydroxyapatite Solid Solutions. J. Chem. Soc. Dalton Trans., 1091-1094.

BIGI, A., Foresti, E., Incerti, A., Roveri, N., Borea, P. A. and Zavagli, G. (1980). Chemical and Structural Study of Mineral Phase Association with a Human Subcutaneous Ectopic Calcification Inorganica Chimica Acta, 46, 271 - 274.

BIGI, A., Foresti, E., Marchetti, F., Ripamonti, A., Roveri, N. and Thomas, S. A. (1991). Structural Modifications of Hydroxyapatite induced lead Substitution

for Calcium. J. Chem. Soc. Dalton Trans. 2883 - 2886.

BIGI, A., Ripamonti, A., Bruckner, S., Gazzano, M., Roveri, N. and Thomas, S. A. (1989). Structure Refinements of Lead Substituted Calcium Hydroxyapatite by x-ray Powder Fitting. Acta Cryst. B. 45, 247 - 251.

BROWN, W.E. and Chow, L. C. (1981). Thermodynamics of Apatite Crystal Growth and Dissolution. J. Cryst. Growth. 53 (1), 31 - 41.

BROWN, W. E., Smith, J. P., Lehr, J. R.[4] and Frazler, A. W. (1962). Crystallographic and Chemical Relation Between Octacalcium Phosphate and Hydroxyapatite. Nature. 196, 1048-1055.

BROWN, W. E., Schroeder, L. W. and Ferris, J. S. (1979). Interlayering of Crystalline Octacalcium Phosphate and Hydroxyapatite. J. Phys. Chem., 83, 1385 - 1388.

BOSKEY, A. L. and Posner, A. S. (1974). Magnesium Stabilization of Amorphous Calcium Phosphate. A Kinetic Study. Mat. Res. Bull., 9, 907 - 916.

BOYD, W. (1962). A Text Book of Pathology. Lea and Febiger, Philadelphia, P. 428.

CASONOVAS, A. M., Fauran - Clavel, M. J. and Oustrin, J. (1980) Influence of Cadmium on Calcium Metabolism: Effect on Cytochrome. P. 450. Experietia 36 (12), 1342 - 1343.

CHICKERUR, N.S., Tung, M. S. and Brown, W. E. (1980). A Mechanism for Incorporation of Carbonate into Apatite. Calcif. Tissue Int., 32, 55 - 62.

CHIRANJEEVIRAO, S. V., Hemmerce, J., Voegel, J. C. and Frank, R. M. (1982). A Method of Preparation and Characterization of Magnesium Apatite. Inorganica Chimica Acta. 67, 183 - 187.

COLLIN, R. L. (1959). Strontium- Calcium Hydroxyapatite Solid solutions: Preparation and Lattice Constant Measurements. J. Amer. Chem. Soc., 81, 5275 - 5278.

COLLIN, R. L. (1960). Strontium - Calcium Hydroxyapatite Solid Solutions Precipitated from Basic Aqueous Solutions. J. Amer. Chem. Soc., 82, 5067 - 5069.

COTTON, F. A. and Wilkinson, G (1972). Advanced Inorganic Chemistry: A comprehensive Text. 3rd Ed. Interscience Publishers, New York.

CURZON, M. E. J., Atkins B. L., Bibby, B. G. and Losee, F. L. (1970). J. Dent. Res. 49, 526: In: Legeros, R. Z., Tahere, M. H., Quirolgoco, G. B. and Legeros, J. P. (1980). Formation and Stability of Apatite: Effects of some Cationic Substituents. Proc. 2nd International Congress on Phosphorus Compounds, Boston.

DOI, Y., Moriwaki, Y., Aoba, T., Takahashi, J. and Joshin, K. (1982). ESR and I.R Studies of Carbonate Containing Hydroxyapatites. Calcif . Tissue Int. 34, 178 - 181.

EANES, E.D. (1979). Enamel Apatite: Chemistry, Structure and Properties. J. Dent. Res. 58, 829 - 834.

EANES, E.D. and Posner, A. S. (1970). Matter Res. Bull. 5, 377. In: Sowerby and Emeleus, (1975). International Review of Science. Inorganic Chemistry Series Two Volume 2. Butterworths, University Park Press.

ELLIOT, J.C. (1973) The problem of the composition and structure of the mineral components of Hard Tissues. Clin. Orthop., 93,313-333.

ELLIOTT, J.C. (1971). Nature. Phy. Sci., 230,72. In: Emeleus, H.J. and Sowenby (1975). International Review of Science, Inorganic Chemistry Series Two, Vol.2, Butherworths, University Park Press.

ENGEL, G, Krieg, F. and Rief, G (1975). J. Solid State Chem., 15,117. In: Bigi A., Gandolfi, M., Gazzano, M., Ripamonti, A., Roveri, N. and Thomas, S.A. (1991). Structural Modifications of Hydroxyapatite induced Lead Substitution for Calcium. J. Chem. Soc., Dalton Trans., 2883-2886

ENGSTROM, A (1972). The Biochemistry and physiology of Bone., Academic Press, New York, p.237.

FOWLER, B.O. (1974). Infra-red studies of Apatites I: Vibrational Assignments for Calcium, Strontium and Barium Hydroxyapatites Utilizing Isotopic Substitution. Inorg. Chem., 13(1), 194-207.

FOWLER, B.O. (1974). Infra-red Studies of Apatites II: preparation of Normal and Isotopically substituted calcium Strontium and Barium Hydroxyapatite and Spectra Structure - composition - correlations. Inorg. Chem 13(1), 207-214.

FRANCIS, M.D. (1969). Calcif. Tissue Res., 3, 151: In: Sowerby and Emeleus (1975). International Review of Science, Inorganic University, Series Two, volume 2. Butterworths University Park Press. London.

GADSDEN, J.A. (1975). Infra-red spectra of minerals and related Inorganic Compounds. Butterworths, London.

GRISAFE, D.A. and Hummel, F.A. (1970). J. Solid State Chem. 2, 160, In: Legeros, R.Z. Tahari, M.H., Quiorolgico, G.B. and Legeros, J.P. (1980)). Formation and Stability of Apatites: Effects of some cationic substituents. Proc. 2nd. International Congress on Phosphorus Compounds, Boston.

HANUSA, T.P. (1987). Re-Examining the Diagonal Relationships. J. Chem. Educ. 64, 686.

HEIJLIGERS, H.J.M., Driessens, F.C.M. and Verberck, R.M.H. (1979). Calcif. Tissue Int., 29, 127-131. In: Bigi, A. Ripamonti, A., Bruckner, S., Gazzano, M., Roveri, N. and Thomas, S.A. (1989). Structure Refinements of Lead Substituted calcium Hydroxyapatite by X-ray Powder Fitting. Acta Cryst. B 45, 247-251.

HERZBERG, G. (1945). Infra-red and Roman Spectra of Polyatomic molecules. Vol.2., Nostrand, New York.

INIKORI, G.O., Thomas, S.A. and Ayoko, G.A. (1991). Solid solutions of Ca-Mg Hydroxyapatite. Nig. Journ. of Science Vol.25 (Accepted for Publication).

JENKINGS, G.N. (1978). The Physiology and Biochemistry of the mouth. 4th ed. Blackwell, Oxford, p.80.

JOINT Committee on Power Diffraction Standards for Lead Hydroxyapatite (1974).

KIELY, M.L. and Domm, L.V. (1977). The effect of magnesium Deficient Diet and Cortison on the Growth of the Rat Incisor. J. Dent. Res. 56(12), 1577-1585.

KLEE, W.E. and Engel, G. (1970). I.R. Spectra of the Phosphate Ions in Various Apatites. J. Inorg. Nucl. Chem. 32, 1837-1843.

KLUG, H.P. and Alexander, L.E. (1974). X-ray Diffraction Procedures for Polycrystalline and Amorphous Materials 2nd ed. Wiley and Sons, New York.

KOUTSOUKOS, P.G. and Nancollas, G.H. (1981). Influence of Strontium Ion on the Crystallization of Hydroxyapatite from Aqueous Solution. J. Phys. Chem. 85, 2403-2408.

KRAJEWSKI, A. and Ravagliolie, A. (1981). A physico-chemical study of crystal Growth of Hydroxyapatite Bioceramic. Biomaterials, 2(2), 105-115.

LEGEROS, R.Z., Tahari, M.H. Quirolgico, G.B. and Legeros, J.P. (1980). Formation and stability of Apatites: Effects of some cationic substituents. In: Proc. 2nd International Congress on Phosphorus Compounds, Boston.

LEGEROS, R.Z., Shirra, W.P., Miravite, M.A. and Legeros, J.P. (1975). Amorphous Calcium Phosphates: Synthetic and Biological. Colloques Internationaux C.N.R.S. 230, 105-111.

LEGEROS, R.Z. (1981). Prog. Crystal Growth Charact., 4, 1. In: Bigi, A., Gandolfi, M., Ripamonti, A., Roveri, N. and Thomas S.A. (1991). Structural Modifications of Hydroxyapatite Induced by Lead Substitution for Calcium. J. Chem. Soc. Dalton Trans. 2883-2886.

LEGEROS, R.Z. and Legeros, J.P. (1980). Phosphate Minerals in Human Tissues. Proc. 2nd Int. Congr. Phosph Compd., Inst Mond Phos. Paris.

LEGEROS, R.Z. (1977). 1st International Congress on Phosphorus Compounds. Rabat, p.347.

LUDWIG, A., Dave, S.C., Higuchi, W.I. and Fox, J.L. (1982). Influence of Fluoride on the Dissolution and Kinetics of Apatite Powders. Bull. Soc. Chim. Belges, 90(4) 482-486.

McCONNEL, D. (1973). Applied Mineralogy vol.5, Springer-Verlang, Wien, In: Baravelli, S., Bigi, A., Ripamonti, A. and Roveri, N. (1984). Thermal Behaviour of Bone and Synthetic Hydroxyapatites Submitted to Magnesium Interaction in Aqueous Medium. Journ. Inorg. Biochem. 20, 1-12.

MERKER, L., and Wondratschek, H. (1959). Z. anorg. allg chem., 300, 41.

MEYER, J.I. and Fowler, B.O. (1982). Lattice Defects in Nonstoichiometric Calcium hydroxyapatites: A Chemical Approach. Inorg. Chem., 21, 3029-3035.

MISSON, G. (1908). Chem. Ztg, 32, 633. In: Quinlan, P.K. and Dessessa, A.M, (1955). Spectrophotometric Determination of Phosphorus as Molybdovanadophosphoric Acid. Anal. Chem. 27(10), 1626-1629.

MOONEY, R.W. and Aia, M.A. (1961). Alkaline Earth Phosphates. Chem Rev., 61, 433-462.

MORENO, E.C. and Varughese, K. (1981). Crystal Growth of Calcium Apatites from Dilute Solutions. J. Cryst. Growth., 53(1), 20-30.

NARASARAJU, T.S.B., Singh, R.P. and Rao, V.I.N. (1972). A New Method of Preparation of Solid Solutions of Calcium and

Lead Hydroxyapatite. J. Inorg. Nucl. Chem., 34, 2072-2074.

NELSON, D.G., (1981). The Influence of Carbonate on the Atomic Structure and Reactivity of Hydroxyapatite. J. Dent. Res. 60, 1621-1629.

NEUMAN, W.F. and Neuman, M.F. (1969). The Chemical Dynamics of Bone Mineral. University of Chicago Press, Chicago.

NEWKIRK, E.A. and Hughes, B.V. (1970). Identification of the Lead (II) Hydroxide of Robin and Theolier. Inorg. Chem., 9(2), 401-403.

PATEL, P.N. (1979). Magnesium calcium Hydroxyapatite Solid Solutions: Preparation, IR and Lattice Constant Measurements. J. Inorg. Nucl. Chem., 42, 1129-1132.

PARTINGTON, J.R. (1957), Advanced Treatise on Physical Chemistry, Vol.3. Longman, London, p.121.

PEARCE, E.I. (1981). Ion Displacement Following the Adsorption of Anion Macromolecule on Hydroxyapatite. Calcif. Tissue Int., 33(4), 395-402.

PEASE, B.F. (1980). Basic Instrument Analysis. D. Van Nostrand Company, New York.

POSNER, A.S. (1958). Phosphorus and its Compounds (Edited by Van Wazer, J.R.). Vol.II, Interscience, New York.

QUINLAN, P.K. and Desesa, A.M. (1955). Spectrophotometric Determination of Phosphorus and Molybdovanadophosphoric Acid. Analytical Chemistry, 27(10), 1626-1629.

RATHJE, W. (1941). Ber. 74B., 347. In: Narasaraju, T.S.B., Singh, R.P., and Rao, V.I.N. (1972). A New Method of Preparation of Solid Solutions of Calcium and Lead Hydroxyapatite. J. Inorg. Nucl. Chem., 34, 2072-2074.

ROSKEY, A.L. and Posner, A.S. (1976). Formation of Hydroxyapatite at Low Supersaturation. J. Phys. Chem., 80, 40-45.

SOWERBY, D.B. and Emeleus, H.J. (1975). International Review of Science. Inorganic Chemistry Series Two, Vol.2, Butterworths University Park Press, London.

TANAKA, G., Kawamura, H. and Nomura, E. (1981)., Distribution of Strontium in the Skeleton and in the mass of Mineralized Bone. Health Phys., 40(5), 601-614.

TERMINE, J.D. Peckauskas, R.A. and Posner A.A. (1970). Calcium Phosphate Formation in Vitro II. Effects of Environment on Amorphous Crystalline Transformation. Archives of Biochem. and Biophys., 140, 318-325.

THOMAS, S.A. (1988). Studies on Some Calcium Phosphate Systems. A report Submitted to the 3rd World Academy of Sciences Trieste, Italy.

THOMAS, S.A. (1989). Isomorphous Substitution in Calcium Hydroxyapatite. An Introductory note. Department of Chemistry, Ahmadu Bello University, Zaria, Nigeria.

THOMAS, S.A., Ajibola, V. and Olayemi, J.Y. (1989). Tin-Calcium Hydroxyapatite Solid Solutions. A Research Paper Presented at the XIVth Annual National Conference of the Chemical Society of Nigeria, Effurun, Delta State.

THOMAS, S.A. (1992). Personal Communications. Department of Chemistry, Ahmadu Bello University, Zaria, Nigeria.

TRAUTZ, O.R. (1955). X-ray Diffraction of Biological and Synthetic Apatite. Ann. N.Y. Acad. Sci., 60, 696-712.

VAN WAZER, J.R (1961). Phosphorus and its Compounds. Inter Science Publishers, New York, Vol.2, 1429-1459.

VERBEECK, R.M.H., Driessens, F.C.M. Ihun, H.P. and Verbeeck, F. (1981). Stability of Calcium-Strontium Hydroxyapatite Solid Solutions in Aqueous Solutions at 25°C. Bull. Soc. Chim. Beges. 90(4), 409-417.

VOGEL, A.I. (1961). A Textbook of Quantitative Inorganic Analysis. 3rd ed. The English Lang. Book Society and Longmans. Green and Co., Ltd., London.

WALSH, A (1955). Spectrochemica Acta 7: 100 In: Veillon, C. (1976). Trace Analysis Spectroscopic Methods for Elements. Chemistry Analysis Series, Vol.46 (Winefordner, J.D., ed), John Wiley and Sons, New York, pp.123-181.

WHITEHEAD, P.J. (1975). Pye Unicam Atomic Absorption Data Book. 1st ed. Pye Unicam Ltd., New York Street, Cambridge, CBI, 2PX, England.

WILLIS, J.B. (1965). Nitrous Oxide-Acetylene Flame in Atomic Absorption Spectroscopy. Nature, 207, 4998-715-716.

YOUNG, R.A. K (1975). Biological Apatite Vs Hydroxyapatite at the Atomic Level. Clin. Orthop., 113. 240-262.

YOUNG, R.A. (1980). Large Effects from Small Structural Differences in Apatites. Proc. 2nd Int. Congress on Phosphorus Compounds. Mond. Phos., Paris, 73-88.

Appendix I: X-ray Powder Diffraction Data for Calcium-Lead Hydroxyapatite Solid Solutions

$Pb_{20}Ca_{80}$			$Pb_{45}Ca_{55}$		
2θ	I/I_1	d(Å)	2θ	I/I_1	d(Å)
10.76	4	8.19	10.63	15	8.35
16.70	1	5.31	16.44	0.50	5.40
18.70	10	4.75	18.47	6	4.80
21.62	10	4.13	21.35	9	4.15
22.69	9	3.92	22.36	29	3.97
25.63	22	3.48	25.17	27	3.53
27.86	10	3.20	25.39	14	3.51
28.74	24	3.01	28.37	19	3.14
31.54	100	2.84	31.12	100	2.88
31.91	20	2.81	31.40	21	2.85
32.68	30	2.74	32.27	15	2.77
33.77	1	2.65	33.24	10	2705
37.92	0.5	2.37	37.44	1	2.40
38.88	3	2.32	38.29	7	2.35
39.53	11	2.28	39.00	5	2.31
40.14	2	2.24	39.60	1.5	2.23
43.45	7	2.08	42.70	12	2.12
44.07	7	2.05	43.50	9	2.08
46.33	13	1.96	45.60	10	1.99
47.70	9	1.91	47.63	3	1.91
48.26	4	1.88	48.22	28	1.89
49.04	24	1.86	49.45	17	1.84

$Pb_{80}Ca_{20}(PO_4)_6(OH)_2$

2θ	I/I_1	d(Å)
10.50	1	8.43
18.20	0.50	4.87
21.00	16	4.23
21.90	24	4.06
24.30	9	3.66
26.50	16	3.35
27.90	21	3.20
30.50	100	2.93
31.70	20	2.82
37.30	2	2.41
38.40	1.50	2.34
38.90	0.50	2.32
41.40	8	2.18
42.80	5	2.11
44.60	15	2.03
45.90	9	1.94
46.80	22	1.94
48.50	13	1.88
49.40	11	1.84
49.80	22	1.83